NASA SCIENTIFIC AND TECHNICAL INFORMATION FACILITY

LIMITED DISTRIBUTION
Copy Number 49

NASA CR 174959

NASA

EXPERIMENTAL AND ANALYTICAL EVALUATION OF THE EFFECTS OF SIMULATED ENGINE INLETS ON THE BLADE VIBRATORY STRESSES OF THE SR-3 MODEL PROP-FAN

Prem N. Bansal

Hamilton Standard Division
United Technologies Corporation
Windsor Locks, Connecticut 06096

September, 1985

National Aeronautics and Space Administration
Lewis Research Center
Cleveland, Ohio 44135
Contract NAS3-24222
Task Order Number 4

LIMITED DISTRIBUTION
This Document will remain
under distribution limitation
until September 30, 1988

NASA CR 174959

NASA

EXPERIMENTAL AND ANALYTICAL EVALUATION OF THE EFFECTS OF SIMULATED ENGINE INLETS ON THE BLADE VIBRATORY STRESSES OF THE SR-3 MODEL PROP-FAN

Prem N. Bansal

Hamilton Standard Division
United Technologies Corporation
Windsor Locks, Connecticut 06096

September, 1985

National Aeronautics and Space Administration
Lewis Research Center
Cleveland, Ohio 44135
Contract NAS3-24222
Task Order Number 4

1. Report No.	2. Government Accession No.	3. Recipient's Catalog No.
NASA - CR 174959		

4. Title and Subtitle
Experimental and Analytical Evaluation of the Effects of Simulated Engine Inlets on the Blade Vibratory Stress of the SR-3 Model Prop-Fan

5. Report Date
September, 1985

6. Performing Organization Code

7. Author(s)
Prem N. Bansal

8. Performing Organization Report No.

10. Work Unit No.

9. Performing Organization Name and Address
Hamilton Standard Division
United Technologies Corporation
Windsor Locks, CT 06096

11. Contract or Grant No.
NAS3 - 24222 Task Order #4

13. Type of Report and Period Covered
Contractor Report

12. Sponsoring Agency Name and Address
National Aeronautics and Space Administration
Washington, D.C. 20546

14. Sponsoring Agency Code

15. Supplementary Notes
Final Report.
Project Technical Monitor, I. Sumner, NASA - Lewis Research Center, Cleveland, Ohio 44135

16. Abstract

Experimental and predicted results showing the effects of simulated engine inlets on the blade vibratory stresses of an SR-3, solid titanium, 8-bladed, model Prop-Fan are presented. The test program was conducted in the high-speed wind tunnel of the United Technologies Research Center. Three inlet configurations were tested. These were: (1) single scoop, (2) twin scoop, and (3) annular. Tests were also performed without the inlet. The effects of Prop-Fan rotational speed, blade angle, tunnel speed, shaft power, rotor to inlet spacing, and inlet flow were evaluated.

Using finite element modeling techniques, blade stresses and rotational natural frequencies were calculated and compared with corresponding test data. Correlation between test and predicted blade natural frequencies was good, however, the test 1p and 2p stress components were under predicted. Results of data analysis show that the blade vibratory stresses were significantly increased by the presence of the inlets. Hence, the inlet has been identified as an important source of dynamic excitation for Prop-Fans.

17. Key Words (Suggested by Author(s))	18. Distribution Statement
Advanced Turboprop, Engine Inlet, Prop-Fan, Energy Efficient, Structural Response	[redacted] Until September 30, 1988

19. Security Classif. (of this report)	20. Security Classif. (of this page)	21. No. of Pages	22. Price*
Unclassified	Unclassified	109	

[redacted]

NASA-C-168 (Rev. 10-75)

PRECEDING PAGE BLANK NOT FILMED

FOREWORD

The experimental effort described in this report was conducted by the United Technologies Research Center in cooperation with the NASA-Lewis Research Center, the Lockheed-Georgia Company, and the Hamilton Standard and Pratt and Whitney Aircraft Divisions of the United Technologies Corporation, under NASA contract NAS3-23710, known as the GUN3 test series.

The vibratory blade stress evaluation portion of the overall effort was conducted by Hamilton Standard under NASA contract NAS3-24222, task order number 4. Mr. Irving E. Sumner of the NASA-Lewis Research Center was the technical monitor for the contract.

The data reduction was performed by Mr. Donald J. Marshall and the analysis and reporting was conducted by Mr. Prem N. Bansal, under the direction of Mr. Bennett M. Brooks, Hamilton Standard Project Manager.

CONTENTS

SUMMARY

A cooperative wind tunnel test program, referred to as GUN-3, had been conducted previously at the United Technologies Research Center to assess the effect of inlet configuration and location on the inlet face pressure recovery and inlet drag in the presence of a high-speed advanced turboprop. These tests were conducted with the inlets located just downstream of the SR-3 model Prop-Fan, a moderately swept, eight-bladed 62.2 cm (24.5 inch) diameter advanced, high-speed turboprop model fabricated from titanium. The participants in this test program, conducted from November 1983 to January 1984, were the Lockheed-Georgia Company, Hamilton Standard, Pratt & Whitney Aircraft, and the NASA-Lewis Research Center. During these tests, two blades of the SR-3 model Prop-Fan were strain gaged to measure the vibratory blade stresses occurring during the inlet aerodynamic test program. The purpose of the effort reported herein was to reduce and analyze the test results related to the vibratory strain gage measurements obtained.

Three inlet configurations had been tested. These were: 1) single scoop, 2) twin scoop, and 3) annular. Each of the three inlets was tested at a position just behind the rotor. The single scoop inlet was also tested at a position further aft. Tests were also done without an inlet.

During testing, several parameters such as tunnel speed, rotational speed, shaft power, and inlet flow had been varied to determine their effects on blade stresses. All tests were conducted with uniform inflow to the rotor, that is, without angular inflow. Two blades were gaged with four strain gages on the camber side of each blade. Bending and torsional vibratory stresses were measured and recorded.

In this effort, the test data were analyzed to determine total blade vibratory stresses and the harmonic vibratory stress components. The blade modal frequencies were determined from the spectral plots, and the blade responses found within the test range were examined. Specifically, the 2P blade response was significantly affected by the first mode 2P critical speed.

The inlet has been identified as an important source of dynamic excitation for Prop-Fans. Results of the data analysis show that the blade vibratory stresses were significantly affected by the presence of an inlet. The measured blade stresses were a function of the inlet type, the inlet/rotor spacing, and the inlet flow rate.

The annular inlet produced a blade response that was only slightly higher than the no inlet response. The single scoop and twin scoop inlets produced a very significant 2P response near the 2P critical speed, as expected. In comparison to the twin scoop inlet, the maximum 2P responses due to the single scoop mid and forward inlets were only one-third and two-thirds as high, respectively. Still, these results emphasize the importance of avoiding critical speeds in the continuous operating range.

Near the design cruise condition, the forward single scoop inlet produced significant 1P response, which was reduced by about 50% when the inlet was moved further away from the rotor, that is from the forward position to the mid position. The 1P response due to the twin scoop inlet was very low and always lower than the 2P response. This indicates that the twin scoop may be promising from an excitation factor (EF) standpoint, if the critical speed response can be controlled. For all inlets, the effect of increased inlet flow was to reduce the 1P and 2P blade response.

At the 0.8 cruise Mach number, 0.81 design mass flow ratio, and at an operating speed of 8204 rpm (near 100% rpm), the single scoop mid-inlet produced an equivalent 1P excitation factor (EF) of about 2.3. The EF is based on the blade inboard bending vibratory stresses, which were the highest measured stresses compared to the other strain gage locations of the blade.

Using finite element modeling techniques, blade stresses and frequencies were calculated for three test points. Correlation between test and predicted blade natural frequencies was good. However, the test 1P and 2P vibratory stresses were underpredicted.

In order to improve correlation between the tested and predicted blade vibratory stresses, several areas for further investigation have been identified.

1.0 INTRODUCTION

During the last decade, Hamilton Standard, in a joint effort with NASA, has successfully developed and demonstrated new concepts for advancing the state-of-the-art of high-speed Prop-Fan propulsion systems. As a part of this development effort, the structural integrity of model Prop-Fans has been demonstrated in wind-tunnel testing. The results of some of these investigations have been published in references 1-3.

Several paper studies [4] have shown that at cruising speeds of Mach 0.7 to 0.8, both military and civil transport aircrafts using Prop-Fan propulsive systems would produce significant savings in fuel cost (20 to 35 percent) relative to equivalent technology turbofans. Furthermore, for tactical transports there is also the potential for up to 30-percent reductions in field length for the same payload and range. However, to attain these objectives, the design of engine installations requires special considerations so that the beneficial effects of these installations are enhanced and the adverse effects are minimized.

An important part of the installation is the engine inlet, which has a large effect on the integrated engine/Prop-fan performance for tractor configurations. Recently, concerns have been expressed that the inlet may also be an important source of excitation of blade vibratory stress. This traditionally has not been a concern for conventional propellers. However, the smaller diameters and larger hub-to-tip ratios of the Prop-fan concept cause the inlet to encompass a larger percentage of the disk area and to be closer to the blade tips than for conventional propellers. This causes more blockage on the Prop-fan, which is exaggerated by the Prop-fan's higher disk loadings.

Aspects of inlet design, and potential inlet candidates for Prop-Fan applications are discussed in references 5 and 6. Inlet/Prop-Fan interaction effects on the overall performance of the propulsive system are discussed in reference 7.

A cooperative wind tunnel test program, referred to as GUN-3, had been conducted at the United Technologies Research Center to assess the effect of inlet configuration and location on the inlet face pressure recovery and inlet drag in the presence of a high-speed advanced turboprop (Reference 8). The tests were conducted with the inlets located just downstream of the SR-3 model Prop-Fan, a moderately swept, eight-bladed 62.2 cm (24.5 inch) diameter advanced, high-speed turboprop model fabricated from titanium. The participants in this test program, conducted from November 1983 to January 1984, were the Lockheed-Georgia Company, Hamilton Standard, Pratt & Whitney Aircraft, and the NASA-Lewis Research Center. During these tests, two blades of the SR-3 Model Prop-Fan were strain-gaged to measure vibratory blade stresses occurring the inlet aerodynamic test program. The purpose of the effort reported herein was to reduce and analyze the test results related to the vibratory strain gage measurements obtained.

1.0 (Continued)

Three inlet configurations had been tested. These were: 1) single scoop, 2) twin scoop, and 3) annular. All three inlets were tested at a forward (FWD) location, which was 6.86 cm (2.7 in) behind the pitch change axis of the propeller. In addition, the single scoop inlet was also tested at a location further aft, known as the mid-position, which was 12.45 cm (4.9 in) behind the pitch change axis. The mid-position tests were done in an attempt to investigate a means to minimize the Prop-Fan swirl effect on the pressure recovery at the face of the inlet and to reduce the blade vibratory stresses due to the presence of the inlet.

Tests were performed at Mach numbers up to 0.80 simulating both design cruise and off-design flight conditions. Other important test parameters varied during the testing included rotational speed (windmill to 8550 rpm) and inlet mass flow ratio (0.0 to 1.0). The Prop-Fan blades were set at or near the nominal blade angle (approximately 58-59°) for a Mach 0.80 cruise condition. Due to time constraints, the blade angles were not reset to lower values representing the appropriate design conditions for lower tunnel Mach numbers. This limited the rotational speed range which could be obtained, within the test rig limitations, for tunnel Mach numbers less than 0.8. Lower rpm's were set by Prop-Fan windmilling speeds and upper rpm's by rig power limits.

Two blades were gaged, with four strain gages installed on the camber side of each blade. Both, bending and torsional vibratory stresses were measured and recorded. The test data were analyzed to determine total stress and the p-order (harmonic) vibratory stress components.

Blade vibratory stresses, for three known test conditions, were predicted using finite element modeling techniques. The predicted stresses were compared with experimental results. Also the blade natural frequencies were calculated and compared with test values.

This report provides a description of the test model, test facility, instrumentation, data acquisition, data reduction, and analytic technique, and also provides a discussion of the results.

2.0 TEST PROGRAM

The United Technologies research facilities had been used to conduct the test program in a cooperative effort by the Lockheed-Georgia Company, Hamilton Standard, Pratt & Whitney Aircraft, and NASA-Lewis. The tests known as the GUN-3 series, were performed from November 1983 to January 1984 under separate NASA contract (NAS3-23710) and are described, in detail, in Reference 8. The test installation, model instrumentation, and test conditions are described in the following sections.

2.1 Test Installation

Testing had been conducted in the United Technology Research Center (UTRC) 8-foot high-speed wind-tunnel. The SR-3 Prop-Fan assembly was provided by NASA-Lewis, and is shown mounted on the test rig in Figure 1. The SR-3 model consisted of eight solid titanium, moderately swept blades. The blade diameter was 62.2 cm (24.5 in). It is an approximately 1/8 scale, variable pitch (ground adjustable) configuration.

The SR-3 Prop-Fan was designed for cruise conditions at an altitude of 10.7 km (35,000 ft) at a flight speed of 0.8 Mach number, with a tip rotational speed of 244 m/s (800 FPS). In the model scale, this yields a design rpm of about 7500 to 8500, depending on wind tunnel operating conditions. The Prop-Fan model assembly consisted of a unique hub, blades, spinner, and nacelle afterbody. The blades, hub, and spinner were designed and fabricated by Hamilton Standard and are owned by NASA-Lewis. The nacelle afterbody was fabricated by UTRC per Hamilton Standard design. The inlets were designed and fabricated by Lockheed-Georgia (references 4 and 5). The test model was designed for counter clockwise rotation (viewing upstream). Figure 2 shows an inlet installation.

A more detailed description of the test model, wind-tunnel facility, and propeller dynamometer can be found in references 2, 6 and 8.

2.2 Model Instrumentation

Two blades (#1 and #3) were equipped with strain gages. As shown in Figure 3, four strain gages were installed on the camber side of each of the two blades. The gages are labeled 1, 3, 4 and 6. Gage #1, the inboard gage, measured the bending stress. The mid-blade bending stress was measured by gage #3. The torsional stresses were measured by the VEE-gage (Gage #4). Tip bending stresses were measured by gage #6.

The data tables, which are discussed later, refer to the blade and strain gages using two types of identification. For example, BG3-1, refers to the inboard gage on blade #3. That is, the first numeral refers to the blade number, and the second numeral refers to the gage number. The second type of identification which has been used for the same gage is 3-1.

A detailed description of how the strain gage wiring was routed and connected can be found in reference 2.

2.3 Test Conditions

Tests had been conducted using three inlet configurations. As discussed before, these were: single scoop, twin scoop, and annular. The no-inlet configuration tests were used as a baseline reference. A series of nozzles attached to the downstream exit of each inlet was used to restrict the flow, and thus control the mass flow ratio variations. The mass flow ratio (MFR), as used in this report, is defined as the ratio of the area required to pass inlet air at freestream conditions (A_0), to the inlet throat area (A_T), that is MFR = A_0/A_T (see reference 6).

Tests had been conducted over a wide range of conditions to provide data at cruise design and off-design conditions. Variables included Prop-Fan rotational speed (4244 rpm to 8550 rpm), tunnel Mach numbers (0.6, 0.7, and 0.8), mass flow ratio (0 to 1.0), and shaft power 0 to 458 SHP (342 kW). Also, limited data were acquired at 0.4 Mach number. The blade angle was set at or near the nominal design blade angle (approximately 58-59°) for a Mach 0.80 cruise condition. This limited the upper rotational speeds that could be obtained at lower tunnel Mach numbers, due to power limitations of the test rig. Lower rpm limits were set by Prop-Fan windmilling speeds. A complete listing of the operating conditions, including free stream parameters, is given in Table A-I of the Appendix. A brief summary of the tested parameters can be found in Table I.

3.0 TEST DATA

Hamilton Standard and United Technologies Research Center personnel had been responsible for the stress test data monitoring and recording. The data reduction was done at Hamilton Standard. These topics are discussed in the following sections.

3.1 Test Data Acquisition

During wind tunnel testing, blade vibratory stress data had been displayed and monitored, on-line, on a multichannel oscilloscope. For each test point, a written record of the operating conditions was made, and the stress data were recorded using an FM magnetic tape system. The Prop-Fan speed/phase pipper signal was also recorded.

3.2 Test Data Reduction

Initially, the analog tapes were analyzed to obtain total vibratory stresses by using electronic peak detectors and recording the resulting signals on a strip chart (Brush chart). The peak detector outputs were also digitized using an analog to digital conversion system. Based on the digitized data, the system then produced a tabulation of the total vibratory stress amplitude for every strain gage at all of the test points. Data from over 200 test points were tabulated. Each test point contained data for 8 strain gages, from two blades with 4 strain gages each.

The total stresses are expressed as $\bar{X} + 2\sigma$, where $\bar{X}$ is the data-sample average of the peak vibratory stress amplitude, and σ is the standard deviation. The instantaneous stress will be below this level 97.72 percent of the time during the sampling period. That is, only 2.28 percent of the vibratory stresses are above this value. It was found that the $\bar{X} + 2\sigma$ value is a good representation of total stress, which is mathematically rigorous. It replaces the previously used "infrequently repeating peak" method, which involves the subjective reading of strip charts. The $\bar{X} + 2\sigma$ stress values are listed in Table A-II of the Appendix.

As a second step in the data reduction process data samples, of 24 seconds in length from the analog tape, were processed to produce spectral analyses for selected strain gages and test conditions. This spectral information was then stored on a computer disc for later retrieval. A Hamilton Standard written computer program was then used to pick out the stress peaks and their associated frequencies. These were then tabulated according to the test point and related strain gages.

Harmonic (p-order) stress component tables were prepared for each of the inlet conditions. In addition to the stress components (1P to 6P), for each of the strain gages, the tables also include the operating conditions for each of the test points.

The p-order stresses for the single scoop forward inlet, single scoop mid-inlet, twin scoop forward inlet, annular forward inlet, and no-inlet (bare) tests are given in the Appendix, respectively, in Tables A-III, A-IV, A-V, A-VI, and A-VII.

4.0 TEST DATA ANALYSIS

All data points described above were analyzed. In addition, six test points were selected for more detailed data analysis. Test runs 35.2 and 37.2 are from the single scoop mid-inlet tests, and test run 10.2 represents the single scoop forward inlet condition. Test runs 22.2, 24.2, and 22.3 represent the corresponding no-inlet tests at about similar operating conditions. For all the six data points, strip charts, spectral plots, and oscillograms were generated. Samples of a strip chart, spectral plot, and an oscillogram for test run 35.2 are shown in Figures 4, 5, and 6, respectively.

Spectral plots provided the blade rotational frequencies and the P-order stresses. These correspond to the measured periodic, coherent time domain signals. In order to compare the P-order test stresses with the predicted stresses, it was necessary to determine whether a stress component (1P or 2P) for an inlet condition was in-phase or out-of-phase with the corresponding stress component of the appropriate no-inlet condition. If the two values were in phase, then the no-inlet stress could be subtracted from the inlet stress component giving the net effective stress induced by the inlet. However, if the two values were out-of-phase, the resultant was determined by vector addition/subtraction. Oscillograms were used to calculate these phase relationships.

For each of the six test points, the phase angle of the stress peak with respect to the Prop-Fan speed/phase pip was determined. Also, the resultant phase between the inlet and no-inlet signals was calculated. This procedure was repeated for both 1P and 2P components. The resulting effective test stress components, along with the phase angles, are listed in Table II.

Automated plotting routines developed by Hamilton Standard, along with traditional plotting techniques, were used to generate curves which show trends of total and 1P/2P vibratory stresses with operating conditions.

5.0 DISCUSSION OF TEST RESULTS

The test data analysis, which was discussed in the previous section, characterized the blade vibratory stresses and rotating natural frequencies under various operating conditions. This section contains a detailed discussion of blade response frequencies, total vibratory stresses, and P-order vibratory stresses.

5.1 Blade Response Frequencies

The experimental rotating natural frequencies of the blade were obtained via spectral plots. Test frequencies are plotted as a function of the Prop-Fan rotational speed in Figure 7. Also superimposed on this figure are the predicted blade frequencies. The prediction procedure is described in Section 6.0, and the prediction results, with correlation to test data, are discussed in Section 7.0. Examination of Figure 7 shows that the 2P excitation frequency intersected the blade first mode response, resulting in a critical speed, around 5800 rpm. When the model was operating near the critical speed, high blade stresses were produced, as discussed in the next section.

5.2 Total Vibratory Stresses

Measured vibratory stresses for all the test points are listed in the Appendix. Table A-II lists total vibratory stresses, the parameter most significant for comparison with material fatigue strength. Harmonic components of the vibratory stress, useful in studying the sources of the stressing, are discussed in the following section.

Table A-II lists data for eight strain gages, four each from blades 1 and 3. Gages on blade 1 are labeled (1-1, 1-3, 1-4, and 1-6). Similarly, strain gages on blade 3 are identified as: 3-1, 3-3, 3-4, and 3-6. It should be noted that for some test runs (30.1 to 37.4, mid-inlet) the blade 1 stresses only were recorded. Similarly for other test runs (40.1 to 46.10, twin scoop inlet), the blade 3 stresses only were recorded.

Maximum Total Stresses - Listed in Table III are the maximum experimental vibratory stresses which were produced by each of the inlet configurations during the entire test program. These stresses are from blade 3, and were measured at the inboard bending station. The associated operating conditions for each of the test points are also included in Table III.

Analysis of the data has shown that the measured inboard blade bending stresses, as compared to the other stresses, were the highest. Also, blade 3 stresses were slightly higher than the blade 1 stresses. However, the differences between the blades, except near the first mode critical speed, were less than 10-percent, showing the consistency of the test data.

5.2 (Continued)

During the entire test program, the highest measured inboard bending total vibratory stress of $\pm$188 MPa ($\pm$27,200 Psi) was produced by the twin scoop inlet, for test run 42.1 at 0.8 Mach number and 58.3 degrees blade angle. This stress is considered to be extremely high, and unacceptable on a continuous basis. A significant portion of this stress is the 2P harmonic component, which was magnified by operation of the Prop-Fan at 6127 rpm, near the first mode/2P critical speed. During normal turboprop operations, critical speed conditions such as this are avoided, by increasing the rpm to the design point rapidly, to pass through the critical speed as quickly as possible.

As shown in Table III, the single scoop mid inlet produced about 40% lower inboard bending total vibratory stresses than the single scoop forward-inlet, showing that the increased rotor/inlet distance decreased the resulting blade vibratory stresses. For the single scoop forward inlet, the highest inboard bending stress on blade 3 was $\pm$130 MPa ($\pm$18,800 psi). The corresponding stress on blade 1 was $\pm$127 MPa ($\pm$18,400 psi) showing the consistency of the test data. Again, this maximum stress test run case (11.5) was very near critical speed operation, which would not normally be run on a continuous basis. The operating conditions for this run were: 0.8 Mach number, 6221 rpm, 57.8 degree blade angle, and 0.81 mass flow ratio.

The maximum total vibratory inboard bending stress for the single scoop mid-inlet was $\pm$76.5 MPa ($\pm$11,100 psi). Again, the operating conditions of 0.8 Mach number, 6110 rpm, 58.0 degree blade angle, and 0.97 mass flow ratio represent a 2P/first mode critical speed case, not normally run continuously.

The stresses produced by the annular inlet were only slightly higher than the no-inlet stresses, which were generally low. There is some residual stress for the no-inlet case, possibly due to a small amount of tunnel turbulence present. Also, a small angular error in the physical rotor shaft alignment to the tunnel centerline, or the presence of the nacelle/pylon may introduce a small degree of non-uniformity to the rotor inflow.

In reviewing the vibratory stress data of Table III, it should be noted that the test conditions listed here are not identical for all the inlets which were tested. However, the operating conditions being "qualitatively" similar, do allow comparisons of the resulting blade stresses.

Total Stress Trends - A graphic comparison of the inboard bending total vibratory stresses, for all the inlets, is shown in Figure 8. The stresses are plotted as a function of the Prop-Fan rotational speed. Only the test data for which the influence of the 2P/first mode critical speed is relatively small have been included. The mass flow ratio (MFR) was 0.81 and the blade angle was 58.5 ($\pm$0.5) degrees. For each case this blade angle represents the design cruise blade angle, and 0.8 MFR was determined (reference 5) to be the optimum design point for a currently available technology engine application.

5.2 (Continued)

The data trends shown in Figure 8 clearly demonstrate that each inlet configuration and location produced blade vibratory stresses which were higher by varying degrees than the no-inlet configuration. Thus the inlet was identified as an important source of excitation for Prop-Fans. Furthermore, the most severe stress environment was produced by the single scoop forward inlet. The annular inlet stresses were the lowest, that is equal to or only slightly higher than the no-inlet stresses.

The total vibratory inboard bending stresses produced by the single scoop forward and mid-inlets are compared in Figure 9. Clearly, the blade stresses for the mid inlet were about 40% lower than the forward-inlet, showing that an increased blade/inlet gap decreases the blade vibratory stresses. Also plotted on Figure 9 are the no-inlet stresses. Again, the blade stresses due to either of the inlets are significantly higher than the no-inlet configuration. The test conditions for the data shown include a mass flow ratio of 0.81 and blade angle of 58.5 ±0.5 degrees, approximating the cruise design values at 0.8 Mach number.

A comparison of the single scoop forward and twin scoop forward inlets is shown in figure 10. The plotted stresses are the inboard bending total vibratory stresses. No data were available to make comparisons at exact operating conditions. However, the plotted test data represent nearly similar operating conditions. The single scoop forward inlet data are for a 57.8 degree blade angle, and 0.81 mass flow ratio. The twin scoop data are for 58.3 degree blade angle and 0.75 mass flow ratio. The twin scoop stresses were slightly lower than the single scoop stresses away from the influence of the first mode critical speed.

It is also observed from Figures 8 to 10 that the Prop-Fan rotational speed has a strong effect on the blade stresses. The stresses were lower as the speed was increased. This trend is due to the fact that, as the model was operated at higher speeds, the influence of the 2P/first mode critical speed on the model response decreased. The 2P/first mode critical speed is at about 5800 rpm.

Data measured for all of the blade 1 strain gages during mid-inlet testing are shown in Figures 11 through 14. The mid-inlet data were acquired at flight Mach numbers of 0.6, 0.7, and 0.8, over a speed range of 4244 to 8550 rpm, for a blade angle of 58.5 degrees and mass flow ratio of 0.81. Figure 11 is a plot of the blade 1 inboard bending stresses. The stress trends are very clear, and the maximum stresses occurred near the 2P/first mode critical speed, at about 5900 rpm. At off-critical speeds, the stresses were considerably lower, less than ±30 MPa (±4350 psi).

Figure 12 shows mid-blade bending stresses, which are only slightly lower than the inboard bending stresses. The torsional stresses, seen in Figure 13, show little modal response, and show little effect of rpm. They were less than ±10 MPa (±1450 psi). The tip bending stresses away from the critical speed, shown in Figure 14, were less than ±16 MPa (±2320 psi).

5.2 (Continued)

A comparison of the blade 1 and blade 3 inboard bending total vibratory stresses, at 0.8 Mach for the mid-inlet, is shown in Figure 15. Blade 3 stresses are about 7% higher than blade 1 stresses. These differences are small and may be due to blade manufacturing variations, or to non-identical location of the strain gages.

5.3 P-order Stresses

Spectral analyses were performed for the strain gage data in order to determine the P-order harmonic stress components for each test case. This diagnostic tool allowed a more accurate interpretation of the blade responses. The P-order stresses (1P to 6P) are listed in Tables A-III to A-VII in the Appendix. The single scoop forward inlet results are given in Table A-III, the single scoop mid-inlet in Table A-IV, the twin scoop forward inlet in Table A-V, the annular forward inlet in Table A-VI, and the no-inlet (bare nacelle) results in Table A-VII. As per availability of the data, the tabulated results include data for blades 1 and 3 from all the four strain gages, except in the case of the twin scoop inlet for which data from blade 3 only were recorded.

From data Tables A-III to A-VII, it is observed that stress components higher than the third harmonic are quite small. Also, the 1P and 2P components are much higher than the 3P components. As would be expected, the 2P components were the highest when operating near the 2P critical speed. In the cruise design rpm range, the 1P components generally dominated. Table III lists the maximum 1P and 2P vibratory stress components for each of the tested inlet configurations at the inboard station of the blade.

Single Scoop Inlets - The 1P experimental stresses for the single scoop mid-inlet are shown in the form of a composite plot in Figure 16. Stresses are plotted against the Prop-Fan rotational speed. The data plotted are at 58.0 and 59.2 degree blade angle, 0.6, 0.7 and 0.8 Mach number, and 0.81 and 0.97 mass flow ratio.

Review of Figure 16 shows that the blade 1P stresses tended to decrease with increased mass flow ratio. That is, stresses were lowered by the increased inlet flow which reduced the blockage on the rotor disk. Generally, 1P stresses increased with rpm, although at 0.8 Mach number the stresses stabilized around 8000 rpm and slightly decreased with further increase in rpm. This is an indication of compressibility effects, and was also seen in earlier tests reported in reference 1.

The highest experimental 1P vibratory stress at the inboard bending station, during mid-inlet testing, was ± 9 MPa (± 1300 psi) at 0.8 Mach number and 8204 rpm. This case approximates the design cruise operating condition.

The 1P stresses for the single scoop forward inlet are plotted in Figure 17. The stresses are plotted as a function of Prop-Fan rotational speed. The data trends are similar to those observed from the mid-inlet tests. However,

5.3 (Continued)

the maximum measured 1P stress of ± 12 MPa (± 1,800 psi) for the forward inlet was significantly higher than for the mid-inlet. The maximum 1P stress case again approximates the design cruise operating condition. Note that, as expected, 1P vibratory stresses were not affected by the first mode critical speed at the 2P crossover.

Figures 18 and 19, respectively, show the 2P stress variations as a function of the Prop-Fan rotational speed, for the single scoop mid and forward inlets. Near the first mode 2P critical speed, the dynamic magnification effect on the 2P stress response is apparent. Hence, compared to the 1P stress response, the 2P stress response is very high.

For the forward inlet, the maximum 2P stress component of ± 109 MPa (±15,800 psi) was measured at 0.8 Mach number and 6221 rpm. For the mid-inlet, the maximum 2P stress of ± 61 MPa (±8,900 psi) was lower than the forward inlet case. The mid-inlet stress was measured at 0.8 Mach number and 6110 rpm condition. At higher rpm's also, the mid-inlet induced lower blade stresses than the forward inlet. For both inlets, the 2P stresses decreased significantly with increased rpm, as the influence of the critical speed decreased.

<u>Twin Scoop Forward Inlet</u> - The 2P stress data for the twin scoop inlet are plotted in Figure 20. The data are for 0.6, 0.7, and 0.8 Mach numbers, 58.3 and 59.1 degree blade angles, and 1.0 mass flow ratio. For this configuration, the maximum 2P stress was ± 174 MPa (±25,200 psi), which is considered to be very high. This stress is listed in Table III but is not shown on Figure 20. The stress trend with rpm is similar to that for the single scoop case. The stress decreased rapidly as rpm was increased, reducing the effect of the critical speed. In the design cruise rpm range, the stress values are about the same as those for the forward single scoop, roughly ±12 MPa (±1,700 psi). Since the blade angles for the data differ only by 0.8 degree, the effect of the blade angle variations on the resulting blade stresses was small. Note from Table III that the 1P stress levels for the twin scoop are low, approaching those for the no-inlet cases. This indicates that the twin scoop way be promising from a blade stress standpoint, if the influence of any 2P critical speeds can be controlled in the blade design.

Figure 21 shows the effect of the inlet flow on the blade stresses due to the twin scoop inlet. The 2P stresses are plotted at 58.3 degree blade angle, 0.57 and 1.0 mass flow ratio, and 0.6, 0.7, and 0.8 Mach numbers. The blade stresses were reduced by as much as 20% when the mass flow ratio was increased from 0.57 to 1.0, at the Mach 0.8 cruise condition. As for the single scoop, increased inlet flow (reduced blockage) produced lower blade stresses.

<u>Annular Forward Inlet</u> - The 1P and 2P bending vibratory stress component plots for the inboard station of blade 1 are shown in Figures 22 and 23, respectively. These plots represent data for the annular inlet at 59.0 degree blade angle, 0.70 mass flow ratio, and 0.6, 0.7, and 0.8 Mach numbers. Also

5.3 (Continued)

shown are comparable stress data for no-inlet test cases. The annular inlet stresses are only slightly higher than the no-inlet stresses.

Blade to Blade Comparisons - The single scoop forward inlet configuration was selected to present blade to blade comparisons of the 1P and 2P components at each of the four gage locations. Figures 24 to 27 show the results for 1P stresses and Figures 28 to 31 show 2P results. Blade to blade stress comparisons show excellent agreement, except for 2P stresses near the first mode critical speed.

Significance of Inlet Induced 1P Stress Response - The practical significance of the inlet induced 1P blade stress response, for blade design considerations, is explained by introducing the concept of an equivalent excitation factor (EF). The concept of EF has been in use for many years to provide guidance for propeller design. It is used to isolate the effects of pure angular inflow and dynamic pressure on 1P blade loads. Normalizing blade stress by EF allows different blade designs to be compared at a variety of operating conditions. A discussion of the importance of the EF concept to Prop-Fan design is given in Reference 3.

The stress sensitivity (σ/EF) for the SR-3 model blade, that is the level of stress produced by a given excitation factor, was established during previous testing. The inboard bending stress sensitivity (σ/EF) of the SR-3 model Prop-Fan as a function of the shaft power was reported in Figures 4-12 and 4-13 of reference 1. The tests were performed in the NASA-Lewis 8x6 foot wind tunnel and the blade stresses were produced by pure angular inflow. By relating the blade stress sensitivity to the 1P stress response due to various inlet configurations, the equivalent excitation factors were calculated for the inlet tests at design conditions (0.8 M, 0.81 MFR). The resulting equivalent excitation factors for the no-inlet (tare stress), single scoop mid inlet, and single scoop forward inlet configurations are listed in Table IV. Also listed in Table IV are the averaged values of the equivalent excitation factors for each of the three configurations.

The measured 1P excitation factor (EF) for the no-inlet case (tare stress) is about 0.4. The single scoop forward inlet EF is about 3.1 and the mid-inlet EF is about 2.3. Normally, an angular phase difference exists between the inlet induced stress signals and the tare stress signals at like operating conditions. This was determined from oscillograph time histories of these signals. Therefore, the tare EF cannot be directly subtracted from the inlet induced EF. However, the results of vectorially subtracting the tare EF indicate that the net EF values are close to the as-measured values.

The equivalent EF's due to the inlet excitation alone can be compared with the design EF for a typical Prop-Fan aircraft application. The design or maximum EF for these typical study aircraft usually is in the range of 3.5 to 5.0, which would be at a maximum gross weight climb condition. Typically, the EF at the cruise design condition would be somewhat lower. Comparing the

5.3 (Continued)

inlet EF's to design study aircraft EF's shows the inlet alone to represent a moderate stress environment for the Prop-Fan.

It should be emphasized that aircraft design EF's are currently formulated without regard for inlet-induced stressing, using only wing, nacelle and climb condition related stressing. Therefore, the inlet is seen to produce a significant portion of the total design EF. It should also be noted that, since the inlet tests were performed at zero-degree inflow angle, it can not be predicted if the effects of inflow angle, wing/nacelle upwash, and nacelle downtilt, among others, would be additive, or if these factors would have a moderating effect on the inlet induced 1P excitations. These influences can be evaluated only by further testing of the model Prop-Fan using a full aircraft simulation, including a fuselage, wing, nacelle and operating inlet. Further, this testing should be performed at the climb operating condition, which usually represents the most severe excitation environment, in addition to testing at the more moderate cruise condition.

6.0 PREDICTION METHODS

In order to calculate Prop-Fan blade stresses due to the presence of an inlet, three distinct analyses must be applied. First, the distortion to the uniform flow field which is induced by the inlet must be determined. Second, the airloads on the blade caused by the disturbed inflow are found. Finally, the structural response caused by the application of these airloads is calculated.

The analysis methodology used in this study included predictions of the flow field, the steady and vibratory airloads, the deflected position of the blade in space, the blade mode shapes and natural frequencies, and the 1P and 2P blade stress response. It is also described in References 1 and 2.

After a preliminary review of the stress test data, three test points were selected to proceed with the analysis work. Two test points (Runs 35.2 and 37.2) were for the single scoop mid-inlet condition, and test run 10.2 was for the single scoop forward inlet condition. The operating conditions for these runs are listed in Table V.

6.1 Flow Field Analysis

For each of the test points selected for the analysis, the Lockheed-Georgia Company (LGC) generated the flow field using the QUADPAN code, which accounts for the presence of the inlet on the nacelle and the inlet mass flow rate. The flow field data were produced in the form of axial velocity ratio (V_z/V_o) which was azimuthally distributed (0 to 360°). These distributions were produced at ten Gauss stations (radial distances) along the blade span. Figure 32 shows the flow field distributions at three Gauss stations for test run 37.2, which represents the single scoop mid-inlet configuration. The operating conditions are: 0.8 Mach number, 8415 rpm, and 0.81 flow ratio.

6.2 Calculation of Airloads

Spanwise Load Distributions - The flow fields supplied by LGC were used as inputs to the Hamilton Standard (HSD) Prop-Fan aerodynamic analysis, embodied in computer code H337. This program is a strip analysis which employs a skewed wake vortex theory and was used to calculate the steady airloads, and the 1P and 2P vibratory airloads. Out-of-plane and in-plane components of the airloads were output by the H337 program at each of the ten Gauss stations along the blade span. Results of predicted chordwise steady airloads showed that out-of-plane components were about 25 to 45 percent higher than the in-plane components. The load distributions were biased towards the tip section and the load peaks for both components occurred between 75 to 88 percent of the blade span.

6.2 (Continued)

For the calculated 1P airloads, the out-of-plane load peaks occurred at about the mid-span (45 to 55 percent radius). The in-plane load peaks were biased towards the tip section (60 to 80 percent radius). The calculations showed that the magnitudes of the 2P loads were about one-half to one-third of the corresponding 1P airloads. The 2P load distribution trends are similar to those for the 1P load distributions.

Chordwise Loads Distributions - The next step in the airloads analysis was to calculate the chordwise center of pressure along the blade span. Two types of center of pressure were needed, for both steady-state and cyclic airloads. The steady state center of pressure (CP_{SS}) is defined as the location at which, for an applied steady lift force (F), a quarter chord moment is produced. The cyclic (1P) center of pressure CP_{1P} is defined as the location at which, for an applied 1P lift force (ΔF) a 1P quarter chord moment is produced. Thus,

$$(CP)_{SS} = 0.25 - C_m/C_l \quad (1)$$

where: C_m = steady state component of 1/4 chord moment coefficient

C_l = steady state component of 1/4 chord lift coefficient

and

$$(CP)_{nP} = 0.25 - C_m'/C_l' \quad (2)$$

where: C_m' and C_l', respectively, represent the nP components of the 1/4 chord moment and lift coefficients.

The HSD strip analysis code HX45, in conjunction with LGC flow field, was used to determine the quarter chord moment and lift coefficients and hence the steady state and cyclic center of pressures from equations (1) and (2). The center of pressure was calculated at ten Gauss stations. The 1P and 2P center of pressure values were assumed to be identical.

6.3 Distribution of Airloads

The airloads which are calculated by the aerodynamic codes have to be distributed on to the finite element model of the blade so that the response due to the airloads may be evaluated. The finite element model is briefly described in the next section.

The HSD developed computer program F194 was used to distribute the airloads on to the finite element model shown in Figure 33. Basically, the input to the program includes the out-of-plane and in-plane aerodynamic loads (steady or vibratory) as discussed in the previous section, at the 10 Gauss stations. The program (F194) distributes the loads over the surface of the blade, determining the loads for the finite element nodes.

6.3 (Continued)

For the SR-3 model, as shown in Figure 33, 16 grid lines were selected at which the loads were distributed. The loads were in the form of pressure loading. From these pressure loads, concentrated nodal loads were calculated.

6.4 Calculation of Mode Shapes and Frequencies

A finite element model of the swept blade, applicable to the MSC/NASTRAN program, was developed. As shown in Figure 33, the blade geometry was described by 346 CTRIA3 elements, and there were 206 grid points.

The first step in the calculation procedure was to determine the blade stiffness. To accomplish this, the steady airloads, which were discussed in the previous section, and the centrifugal force field due to blade rotation, were applied at the nodes of the blade model. The blade stiffness was then calculated using the non-linear capability of NASTRAN via solution 64 (rigid format 64). The solution procedure involved a Newton-Raphson iteration, with a geometry update until the equilibrium was satisfied.

Upon completion of the iteration within rigid format 64 of MSC/NASTRAN, the incremental stiffness matrix was saved on magnetic tape. The incremental stiffness matrix was the stiffness matrix which is used to examine small (linear) perturbations about the steady-state deflected position. It included the basic elemental structural stiffness and the differential representing the additional stiffness due to the fact that the blade was in a centrifugal field. However, the matrix output from NASTRAN does not recognize that the magnitudes of the load vectors on the model's mass points change as the points vibrate about the steady-state position. This effect can be explained as follows. Consider an element of mass under the influence of a centrifugal field. There is a radial force acting on this mass equal to '$mr\omega^2$' where 'r' is the radius from the center of rotation. If the mass is allowed to deflect outward, then there will be an increase in the centrifugal force due to the increase in radius, i.e.:

$$\Delta F = m\omega^2 \Delta r \tag{3}$$

Since the increment in the force is in the same direction as the displacement (instead of a restoring force), it is equivalent to a negative stiffness, thus:

$$K_{radial} = -(\Delta F/\Delta r) = -m\omega^2 \tag{4}$$

It can also be shown that the same effect is present in the tangential direction, hence:

$$K_{tangential} = -m\omega^2 \tag{5}$$

6.4 (Continued)

The inclusion of these terms in the stiffness matrix was necessary to produce accurate results. Since the new terms are proportional to the mass matrix, just as the inertia terms are in a vibration problem, it is clear that their importance depends upon the relationship between the frequency of vibration and the rotational speed. The lower the frequency of vibration, the more important these terms are. At high frequencies the inertia terms dominate and the negative in-plane stiffness terms were less important. This negative in-plane stiffness matrix was added to the incremental stiffness matrix using a program modification (DMAP alter) in rigid format 64 of MSC/NASTRAN. The resulting stiffness matrix was then saved on magnetic tape.

The blade frequencies and mode shapes were calculated using the real Eigenvalue solution, NASTRAN rigid format 3. The resulting blade frequencies were plotted against the Prop-Fan speed to provide a Campbell diagram, shown in Figure 7.

6.5 P-order Stress Calculation

Both the 1P and 2P vibratory stresses were calculated. For the 1P stress calculation, the 1P airloads were distributed on to the grid points of the finite element model via computer code F194. Using the deflected shape of the blade, previously calculated by NASTRAN solution 64, input to the NASTRAN rigid format 26 was prepared. The 1P elemental stresses were then calculated using the frequency response capability of solution 26. To calculate the 2P elemental stresses, the foregoing 1P procedure was repeated with the 2P airloads applied to the model.

6.6 Gage Stresses

The NASTRAN calculation provided the elemental stresses for the blade finite element model. As discussed previously, the strain gages were installed on the camber side of the blade. Hence, the next step in the calculation procedure was to transform the elemental stresses into surface stresses so that the predicted stresses could be compared with the experimental stresses. This was accomplished by using a Hamilton Standard developed post-processor code. The predicted blade stresses are discussed in the next section.

7.0 DISCUSSION OF PREDICTED RESULTS AND COMPARISONS WITH TEST

Discussed in this section are the predicted blade modal frequencies/mode shapes, and the P-order vibratory stresses. The blade frequencies are presented in the form of a Campbell diagram. The 1P and 2P stress contours for each of the three test points, which were plotted by the MOVIEBYU computer program, are also shown. The predicted results are compared with the corresponding test results.

7.1 Modal Frequencies

The predicted Campbell diagram of the SR-3 model Prop-Fan is shown in Figure 7. The frequencies for six modes are plotted as a function of the Prop-Fan rotational speed. The three-quarter radius blade angle ($\beta_{3/4}$) used in the analysis was about 57 degrees with the effects of airloads and centrifugal loads included. The stiffening effect of the centrifugal loads on the blade natural frequencies is evident from the Campbell diagram.

Superimposed on Figure 7 are the blade test frequencies (at 6801, 7000, and 8454 rpm) which were obtained from the spectral plots. The NASTRAN calculated first mode natural frequencies at these three Prop-Fan speeds are about 5 percent lower than the corresponding measured modal frequencies. The agreement between the predicted and test frequencies for the second and third modes is very good. The 4th and 5th mode test frequencies are about 4 to 6 percent lower than the predicted frequencies, but this is considered to be of second order significance. This agreement indicates that the dynamic characteristics of the Prop-Fan blade are properly represented by the finite element model of the blade.

Also shown on Figure 7 are the p-order frequency lines. An examination of the blade Campbell diagram shows that within the test speed range of 4244 rpm to 8550 rpm, the 2P excitation frequency is in resonance with the predicted first mode frequency at about 5600 rpm. At 6100 rpm, the first mode response is primarily caused by the 2P excitation, with lesser contributions being made by the 1P excitation. That is, the dynamic magnification of the 2P response should be significantly higher than the 1P response. Note that at 6100 rpm, the second mode response is primarily due to the 4P excitation, and the third mode response due to the 6P excitation.

As the Prop-Fan rotational speed was increased, the contributions to the first mode response due to the 1P excitation began to increase and the 2P excitation contributions decreased. Based upon a single degree of freedom (SDOF) undamped-model analysis, the dynamic amplication factor ratios of 2P/1st mode response to the corresponding 1P response at 6100 rpm, 7015 rpm, and 8450 rpm were 4.9, 3.6, and 1.3, respectively. This simple illustration shows that at the upper end of the test speed (i.e., far-away from the first mode critical speed), the 2P response should be significantly lower than the response near the critical speed.

7.1 (Continued)

The six predicted mode shapes, showing contours of displacements normal to the plane of the paper (developed blade planform), are shown in Figure 34. The displacements are well defined, and the contours are smooth. These mode shapes correspond to test run 35.2 at 7015 rpm.

7.2 Stress Contours

The MOVIEBYU computer program was used to plot the predicted 1P and 2P stress contours. For each of the prediction points (runs 35.2, 37.2, and 10.2), stress contours are plotted. The stress contours represent the principal stresses at the camber side of the blade. The 1P stress contours for runs 35.2, 37.2, and 10.2 are shown respectively in Figures 35, 36, and 37. The corresponding 2P stress contours are shown in Figures 38, 39, and 40. In each case, the maximum predicted stresses occurred near the inboard region of the blade. This prediction was corroborated by experimental stress measurements, previously discussed.

7.3 P-Order Stress Comparisons

The predicted 1P and 2P stress components at the inboard position ($r/R = 0.36$), for each of the three prediction points (runs 35.2, 37.2, and 10.2), are shown in Table V. The operating conditions are also listed. For comparison, the measured test stresses are also included in Table V.

Reviewing the results of Table V, reveals that the predicted 1P stresses are 27 to 41 percent lower than the 1P experimental stresses. The 2P predicted stresses are 46 to 74 percent lower than the 2P test stresses. The comparisons are poorest near the first critical speed, as explained in the following paragraphs.

In order to understand the cause of the difference between the predicted and experimental stresses, dynamic magnification factors were calculated for each of the analysis points. Structural damping effects were not included in the NASTRAN model. The NASTRAN predicted dynamic magnification factors (MF) were obtained by the ratio of the P-order stress components at 1P or 2P frequencies to those stress components obtained at 0.1 Hz frequency, thus:

$$MF = (1P\ \text{stress response})/(0.1\ \text{Hz stress response}) \tag{6}$$

The tested magnification factors described in Section 7.1 were obtained using the single degree of freedom (SDOF) model, thus:

$$MF = 1/[1 - (\omega/\omega_n)^2] \tag{7}$$

where ω is the 1P or 2P frequency, and ω_n is the measured first mode frequency. The resulting MF are listed in Table VI. Also listed in Table VI are the calculated MF, which were also obtained from equation (7) with ω_n being the NASTRAN calculated first mode frequency.

7.3 (Continued)

Review of the contents of Table VI shows that for all three test points, the experimental dynamic magnification factors for the 1P response are about 0.97 times the values of the corresponding NASTRAN calculated dynamic magnification factors. This shows that even though the calculated first mode frequency was about 5 percent lower than the test frequency, its effect on the resulting test and calculated dynamic magnification factors for the 1P response was insignificant. However, the cause of the underprediction of the 1P stresses is not clear.

The experimental dynamic magnification of the 2P response, however, was significantly higher than the NASTRAN predicted values. The comparison deteriorates as the first mode/2P critical speed is approached. For example at 8415 rpm, the test MF was 1.57 times the NASTRAN calculated MF; at 7015 rpm the ratio was 1.83, and at 6808 rpm the ratio increased to 2.62. The foregoing results indicate that near the critical speed, the NASTRAN analysis had significantly underpredicted the dynamic magnification factor for the 2P response and hence, lower 2P stresses.

Comparisons of the predicted 1P and 2P stress components, at the three blade bending gage positions (inboard-blade, mid-blade, and tip), with the experimental stresses of test runs 35.2, 37.2, and 10.2, are shown in Figures 41, 42, and 43, respectively. Here again, the measured stresses were significantly higher than the calculated stresses, with the 1P comparisons better than the 2P comparisons.

Some of the differences between the measurements and the predictions may be due to small variations in the actual positioning of the strain gages on the blade and the corresponding position used for calculations with the NASTRAN model. The flow field calculation procedure and the subsequent airload calculation procedure may also require further investigation to improve the correlation between test and theory.

Comment on Underpredictions of P-order Stresses - Test run 37.2 (0.8 Mach number, 8417 rpm, 0.81 mass flow ratio) from Table V represents a data point for the single scoop mid-inlet at which the blade stresses were not influenced by the first mode critical speed. Also, this case approximately represented the design cruise condition.

For this case, the measured test 1P stress amplitude was 1.57 times larger than the predicted 1P stress, and the 2P test stress was 1.85 times larger than the predicted 2P stress. These two factors (1.57 and 1.85) are sufficiently close so that it can be argued that the tested and predicted stresses, at the design condition, differ by an average constant factor of about 1.7. For the other two prediction cases (runs 35.2 and 10.2) shown in Table V, which represent off-design 0.6 Mach number conditions for the single scoop mid and forward inlets, respectively, this factor also holds for the 1P response. The mid-inlet factor is 1.69 and the forward inlet factor is 1.36.

7.3 (Continued)

The rotational speeds for these cases were close to the 2P/first mode critical speed, so that the 2P predictions were not as good as discussed earlier. However, away from the influence of the 2P response, the correction factor of 1.7 is consistent with the design case, above. This empirical factor (1.7), therefore, could be used to estimate the blade vibratory stresses for other Prop-Fan design studies.

It should be noted that this factor is higher than the factor of 1.4, which was used in previous design studies, and was based on past 1P angular inflow tests and analyses. The reasons for this are not clear and require further study.

8.0 CONCLUSIONS

Based upon the analysis of an extensive wind tunnel test data bank and three prediction points, as discussed in this report, the following conclusions are drawn about the SR-3 model Prop-Fan with simulated engine inlets.

1. The inlet was identified as an important source of dynamic excitation for Prop-Fans. Measured blade vibratory stresses due to the inlet were significantly higher than the stresses without the inlet.

2. The single scoop forward inlet produced the highest 1P stress. Blade stresses due to the single scoop mid-inlet were lower than the forward inlet, establishing that an increased blade/inlet distance reduced blade excitation.

3. Increased inlet flow lowered the blade stresses for all inlets.

4. Due to resonances in the test operating range, Prop-Fan rotational speed was identified as an important test parameter. The tunnel speed and blade angle effects on the blade vibratory stresses were found to be small.

5. The single and twin scoop inlets excited considerable 2P stress response near the first mode critical speed. In this region, the 2P stress response was an order of magnitude or more higher than the 1P response. The 2P stresses for the twin scoop were the highest among all inlets. Away from the critical speed, 2P stresses were greatly reduced. This effect must be considered in the design of an integrated Prop-Fan airframe and powerplant.

6. The annular inlet stresses were only slightly higher than the no-inlet tests.

7. Predicted and experimental modal frequencies showed good correlation indicating that the structural model accurately represents the dynamic characteristics of the Prop-Fan blade.

8. The measured 1P and 2P blade stresses were underpredicted. Underprediction of 1P stresses was moderate and fairly consistent. The 2P predicted stresses were significantly lower than the experimental 2P stresses. The correlation was the poorest near the first critical speed and showed improvement when the model was operated farther away from the critical speed.

9. The tested 1P magnification factors were well predicted by NASTRAN. The tested dynamic magnification factors near the 2P/1st critical speed were higher than those obtained from NASTRAN calculations, probably due to small differences between the tested and calculated frequencies. Thus, small differences in frequency may cause greater differences between tested and predicted 2P stress values.

8.0 (Continued)

10. An empirical correction factor of 1.7 to the 1P and 2P predictions was found to provide consistently acceptable results, away from the influence of the 2P/first mode critical speed.

9.0 RECOMMENDATIONS

Future effort should be directed toward more completely characterizing the effects of the inlet on Prop-Fan blade stresses. This includes understanding isolated inlet effects, as well as the interaction of the inlet with the entire powerplant/airframe installation. Part of this effort should be to understand why the analysis underpredicted the blade vibratory stresses. Additionally, model wind tunnel tests will be required to investigate the complex issues involving the flowfield of an actual Prop-Fan installation.

Study of prediction methods in the following three areas is needed:

1) Flow field
2) Blade aerodynamic loads
3) Blade FEA model

This study should be conducted as follows:

- Flow Field - The currently applied method does not have transonic capability. Therefore, calculations should be performed using a full potential field equation method, such as the Euler Code or the Boppe Code (Grumman).

- Blade Aerodynamic Loads - Investigate the availability of a 3-dimensional lifting surface unsteady loads theory, and improved lifting line methods.

- Blade FEA Model - An experimental stress analysis (ESA) should be conducted for the SR-3 model blade, and the results compared to FEA calculations to validate the analysis.

Wind tunnel tests should be performed with both single rotation and counter rotation Prop-Fan models installed on a simulated fuselage/wing/nacelle/inlet model. Previous Prop-Fan/wing studies have neglected the operation of the inlet when investigating installed overall drag and performance, as well as blade structural response. A series of flexible tests should be conducted where a variety of wing, nacelle and inlet geometries can be studied in order to optimize the installed Prop-Fan performance and structural response.

SYMBOLS

A_0	Area required to pass inlet air at freestream conditions
A_T	Inlet throat area
C_P	Power Coefficient = $P/\rho n^3 D^5$
CP	Center of pressure
C_l	Steady state component of 1/4 chord lift coefficient
C_m	Steady state component of 1/4 chord moment coefficient
C_l'	Vibratory component of 1/4 chord lift coefficient
C_m'	Vibratory component of 1/4 chord moment coefficient
D	Rotor Diameter, m (ft)
EF	Excitation Factor = $\Psi(V_E/348)^2$
F	Blade elemental force, kg m/s^2
J	Advance ratio = V/nD
K	Blade elemental stiffness, kg/s^2
m	Blade elemental mass, kg
M	Mach Number
MF	Magnification factor
MFR	Mass Flow Ratio = A_0/A_T
n	Prop-Fan Rotational Speed, Revolutions Per Second
P	Shaft Power, kW
r	Blade Radial Station, m
R	Blade Tip Radius, m
rpm	Revolutions Per Minute
SHP	Shaft Horse Power

<u>SYMBOLS</u> (Continued)

V	True Air Speed, m/s (FPS)
V_E	Equivalent Air Speed = $V_T \sqrt{\rho/\rho_o}$, Knots
V_o	Free-stream Air Speed, m/s
V_T	True Air Speed, Knots
V_2	Axial Air Speed in Prop-Fan Plane, m/s
$\bar{X}$	Average of Peak Vibratory Stress Amplitudes, kPa
$\beta_{(3/4)}$	Blade Angle at 3/4 Radius, Degrees
ρ	Air Density, kg/m^3
ψ	Inflow angle, degrees
σ	Standard deviation of Peak Vibratory Stress Amplitudes, kPa
ω	Frequency, Hz Angular velocity, radians/second
ω_n	Natural Frequency, Hz
1P	Frequency = One Cycle Per Propeller Revolution
nP	Integer Multiples of 1P Frequency
#	Number

SI units of measurement used throughout, unless specified otherwise.

REFERENCES

1. Bansal, P.N., Arseneaux, P.J., Smith, A.F., Turnberg, J.E. and Brooks, B.M., "Evaluation of the Dynamic Response and Stability of Three Advanced Turboprop Models", NASA CR-174814, August, 1985.

2. Smith, A.F., "Analysis and Test Evaluation of the Dynamic Stability of Three Advanced Turboprop Models at Zero Forward Speed", NASA CR (To Be Published).

3. Smith, A.F., "Low Speed Blade Dynamic Response and Stall Flutter Tests on Three Advanced Turboprop Models", NASA CR (To Be Published).

4. Owens, R.E., and Ferguson, W.W., "Some Aspects of Prop-Fan Propulsion Systems Analysis", SAE Paper 821358, October, 1982.

5. Little, B.H. Jr., and Hinson, B.L., "Inlet Design for High-Speed Prop-Fans", SAE Paper 821359, October, 1982.

6. Hinson, B.L., "Design and Experimental Evaluation of Prop-Fan Inlets", SAE Paper 841477, October, 1984.

7. Tanner, D.D., and Wynosky, T.A., "Engine Inlet Interaction with a Prop-Fan Propulsion System", SAE Paper 841478, October, 1984.

8. Hancock, J.P., Lyman, V. and Pennock, A.P., "Analysis of Results from Wind Tunnel Tests of Inlets for an Advanced Turboprop Nacelle Installation", NASA CR 174937, June, 1985.

TABLE I. SUMMARY OF TESTED PARAMETERS

INLET TYPE	RANGE OF TEST PARAMETERS			
	M	β (DEG)	RPM	MFR
SS FWD	0.4, 0.6, 0.7, 0.8	57.8, 59.0	4295–8417	0.81, 0.97
SS MID	0.6, 0.7, 0.8	58.0, 59.2	4496–8410	0.81, 0.97
TS FWD	0.6, 0.7, 0.8	58.3, 59.1	4382–8505	0.0, 0.57, 0.75, 1.0
A FWD	0.6, 0.7, 0.8	58.1, 59.0	4212–8210	0.7, 0.86
NO INLET	0.6, 0.7, 0.8	58.0, 59.0	4244–8454	

NOTE:
SS FWD SINGLE SCOOP FORWARD INLET
SS MID SINGLE SCOOP MID INLET
TS FWD TWIN SCOOP FORWARD INLET
A FWD ANNULAR FORWARD INLET

TABLE II. PHASE RELATIONSHIP BETWEEN INLET AND NO-INLET STRESS

TEST NO.	INLET TYPE	MACH NO.	RPM	MASS FLOW RATIO (MFR)	KW (SHP)	1P TEST STRESS (BG1-1)					2P TEST STRESS (BG1-1)				
						± PSI	± kPa	PHASE ∡ BETWEEN INLET & NO-INLET	EFFECTIVE 1P		± PSI	±kPa	PHASE ∡ BETWEEN INLET & NO-INLET	EFFECTIVE 2P	
									± PSI	± kPa				± PSI	± kPa
*35.2	MID	0.6	7015	0.81	280 (376)	707	4875	-73°	676	4661	1388	9570	-21.3	1123	7743
22.2	NO-INLET	0.61	6970	0.0	283 (379)	231	1593				290	2000			
*37.2	MID	0.8	8415	0.81	266 (357)	1269	8750	42	1196	8246	633	4364	-10.0	342	2358
24.2	NO-INLET	0.81	8453	—	339 (454)	100	690				300	2068			
*10.2	FWD	0.6	6808	0.825	268 (360)	693	4778	79	689	4751	2910	20064	-12.0	2580	17789
22.3	NO-INLET	0.6	6774	—	248 (333)	293	2020				338	2330			

*USED FOR CORRELATION WITH PREDICTIONS

TABLE III. MAX. VIBRATORY INBOARD BENDING TEST STRESSES FOR VARIOUS INLETS

TYPE OF INLET	M	β¾ (DEG)	MFR	RPM	TEST NO.	TOTAL STRESS ±kPa (±PSI)	1P STRESS ±kPa (± PSI)	2P STRESS ±kPa (± PSI)	
SINGLE SCOOP FORWARD (SSFWD)	0.8	57.8	0.81	8392	11.7	22890 (3320)	12611 (1829)	7820 (1134)	1P MAX
	0.8	57.8	0.81	6221	11.5	126506 (18348)	8715 (1264)	108738 (15771)	2P MAX
SINGLE SCOOP MID (SSMID)	0.8	58.0	0.81	8204	37.3	14186 (2057)	8998 (1305)	4971 (721)	1P MAX
	0.8	58.0	0.97	6110	27.1	76511 (11097)	6509 (944)	61226 (8880)	2P MAX
TWIN SCOOP FORWARD (TSFWD)	0.6	58.3	0.75	6927	40.4	24710 (3584)	3413 (495)	17900 (2596)	1P MAX
	0.8	58.3	0.0	6127	42.1	187249 (27158)	1834 (266)	173487 (25162)	2P MAX
ANNULAR FORWARD (AFWD)	0.6	59.0	0.86	6432	215.3	13535 (1963)	3689 (535)	8715 (1264)	1P MAX
	0.6	59.0	0.86	6234	215.4	17209 (2496)	2840 (412)	12052 (1748)	2P MAX
NO-INLET	0.7	58.0		7655	23.2	6550 (950)	2524 (366)	1950 (283)	1P MAX
	0.8	59.0		5981	21.1	15472 (2244)	1393 (202)	9963 (1445)	2P MAX

TABLE IV. EQUIVALENT EXCITATION FACTORS SR-3 INBOARD BENDING STRESSES

(0.8M, 0.81 MFR)

Inlet Type	Test No.	$\beta_{3/4}$ (Deg)	RPM	SHP	σ/EF (from the Ref.)	1P Stress (± psi)	$(EF)_{eq}$	Averaged $(EF)_{eq}$
No inlet	21.4	59.0	7770	321	520	234	0.45	
↓	21.3	↓	7961	367	530	234	0.44	0.44
↓	21.2	↓	8165	429	545	237	0.43	
Single scoop (mid)	34.4	59.2	7764	325	520	1281	2.46	
↓	34.3	↓	7959	365	530	1317	2.48	
↓	34.2	↓	8153	430	546	1184	2.17	
↓	37.4	58.0	8009	273	512	1119	2.19	2.34
↓	37.3	↓	8204	389	537	1305	2.43	
↓	37.2	↓	8410	450	552	1269	2.30	
Single scoop forward	15.4	59.0	7674	316	520	1582	3.04	
↓	15.3	↓	7876	363	530	1574	2.97	
↓	15.2	↓	8066	411	541	1771	3.27	
↓	11.9	57.8	8007	337	525	1472	2.80	3.12
↓	11.8	↓	8208	392	537	1732	3.23	
↓	11.7	↓	8392	451	552	1829	3.31	
↓	11.6	↓	8417	424	545	1770	3.25	

TABLE V. COMPARISON OF PREDICTED AND TEST INBOARD BENDING STRESSES (1P AND 2P)

TEST NO.	LOCATION OF SINGLE SCOOP INLET	MACH NO.	RPM	MASS FLOW RATIO (MFR)	SHP	1P STRESS ± kPa		2P STRESS ± kPa	
						TEST	PREDICTION	TEST	PREDICTION
35.2	MID	0.6	7015	0.81	376	4661 (676 PSI)	2758 (400 PSI)	7743 (1123 PSI)	2275 (330 PSI)
37.2	MID	0.8	8415	0.81	357	8246 (1196 PSI)	5254 (762 PSI)	2358 (342 PSI)	1276 (185 PSI)
10.2	FWD	0.6	6808	0.825	360	4751 (689 PSI)	3482 (505 PSI)	17789 (2580 PSI)	4585 (665 PSI)

TABLE VI. COMPARISON OF TEST AND NASTRAN USED DYNAMIC RESPONSE MAGNIFICATION FACTORS

TEST POINT	PROP-FAN SPEED RPM	1P FREQ. (HZ)	2P FREQ. (HZ)	1ST MODE FREQ. (HZ)		MAGNIFICATION FACTOR (MF), 1P-RESPONSE			MF, 2P-RESPONSE		
				TEST	CALC	TEST (SDOF)	CALC (SDOF)	FROM NASTRAN	TEST (SDOF)	CALC. (SDOF)	FROM NASTRAN
35.2	7015	116.9	233.8	214.3	204.7	1.42	1.48	1.46	5.25	3.28	2.87
37.2	8410	140.2	280.4	228.6	215.0	1.60	1.74	1.67	1.98	1.43	1.26
10.2	6808	113.5	227.0	215.0	203.0	1.39	1.45	1.42	8.77	4.01	3.35

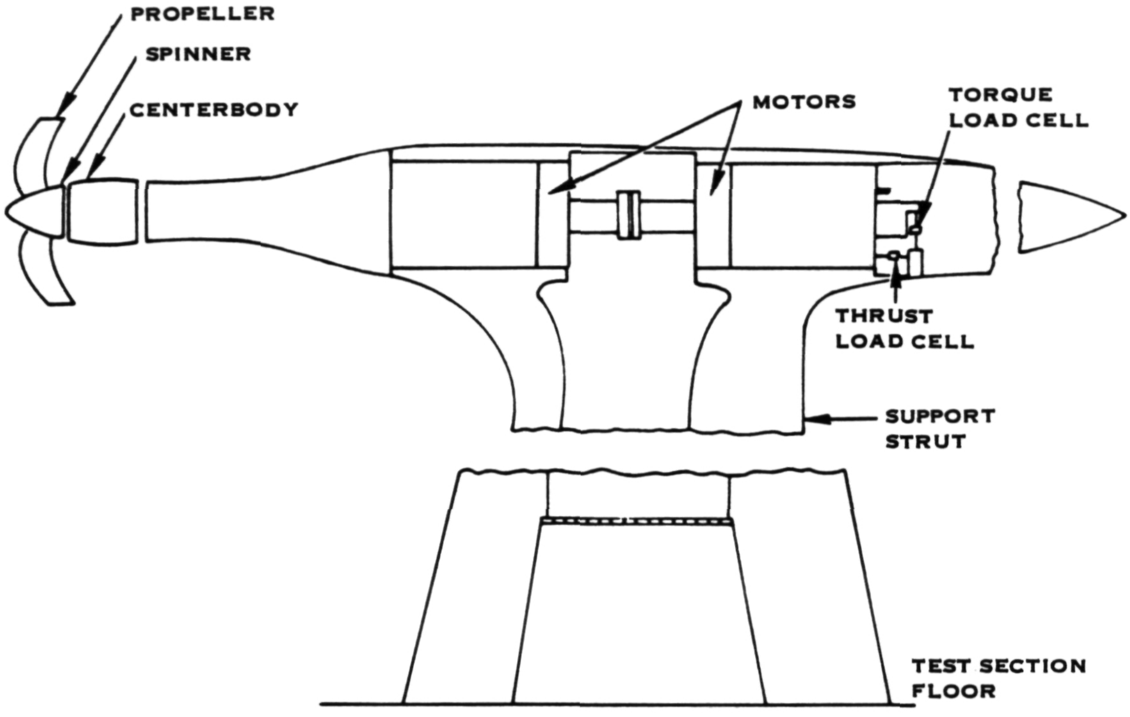

FIGURE 1. UTRC PROPELLER TEST RIG

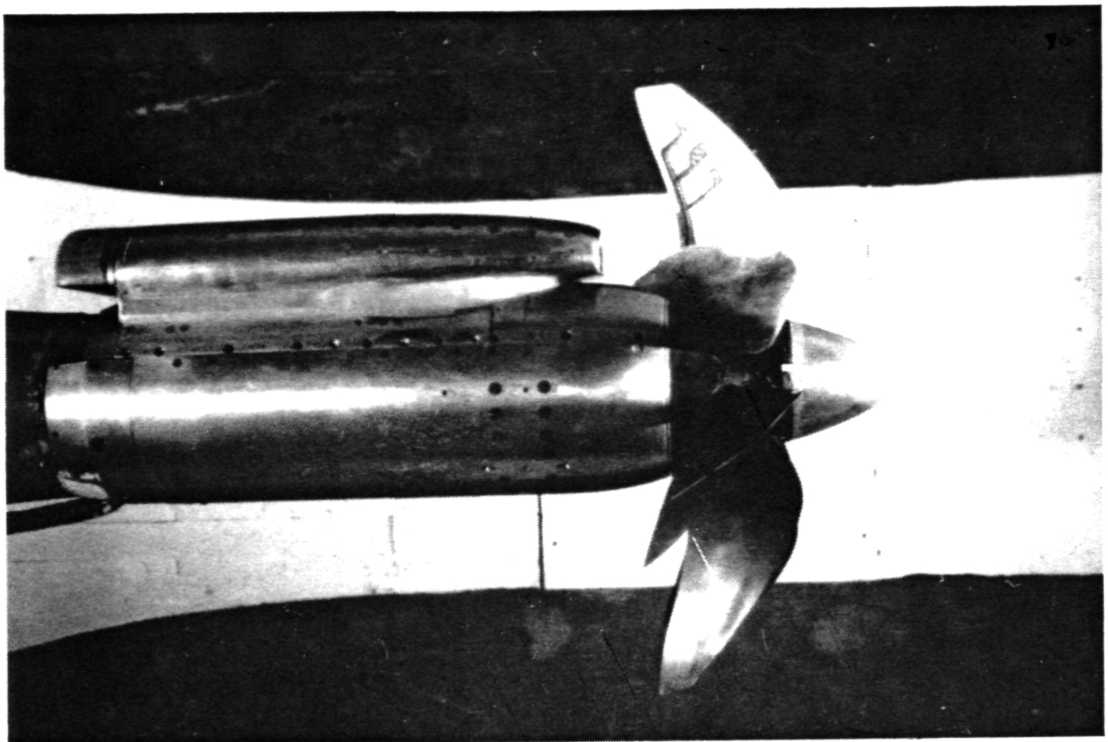

A) SINGLE SCOOP INLET INSTALLED IN THE MID-POSITION

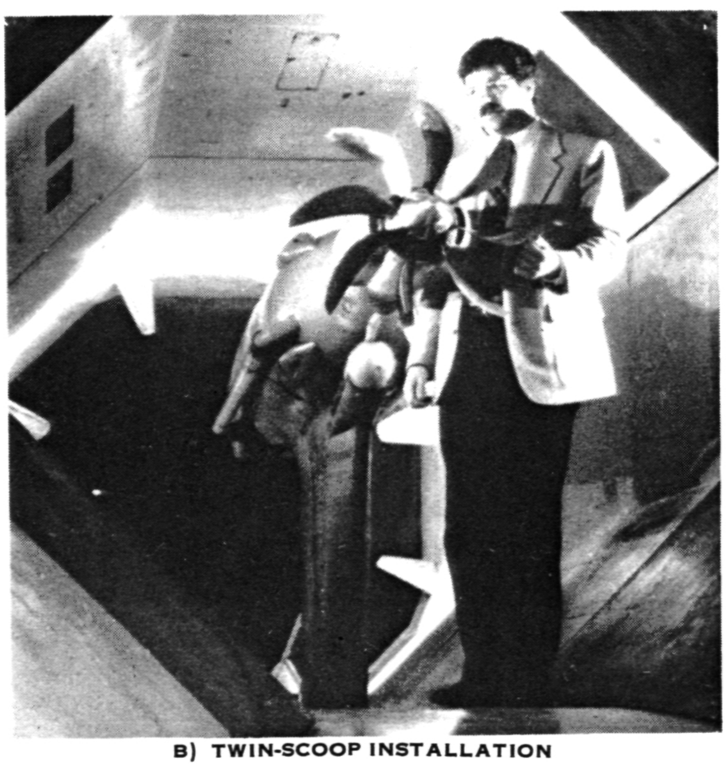

B) TWIN-SCOOP INSTALLATION

FIGURE 2. SR-3 PROP-FAN/INLET INSTALLATIONS IN THE UTRC WIND TUNNEL

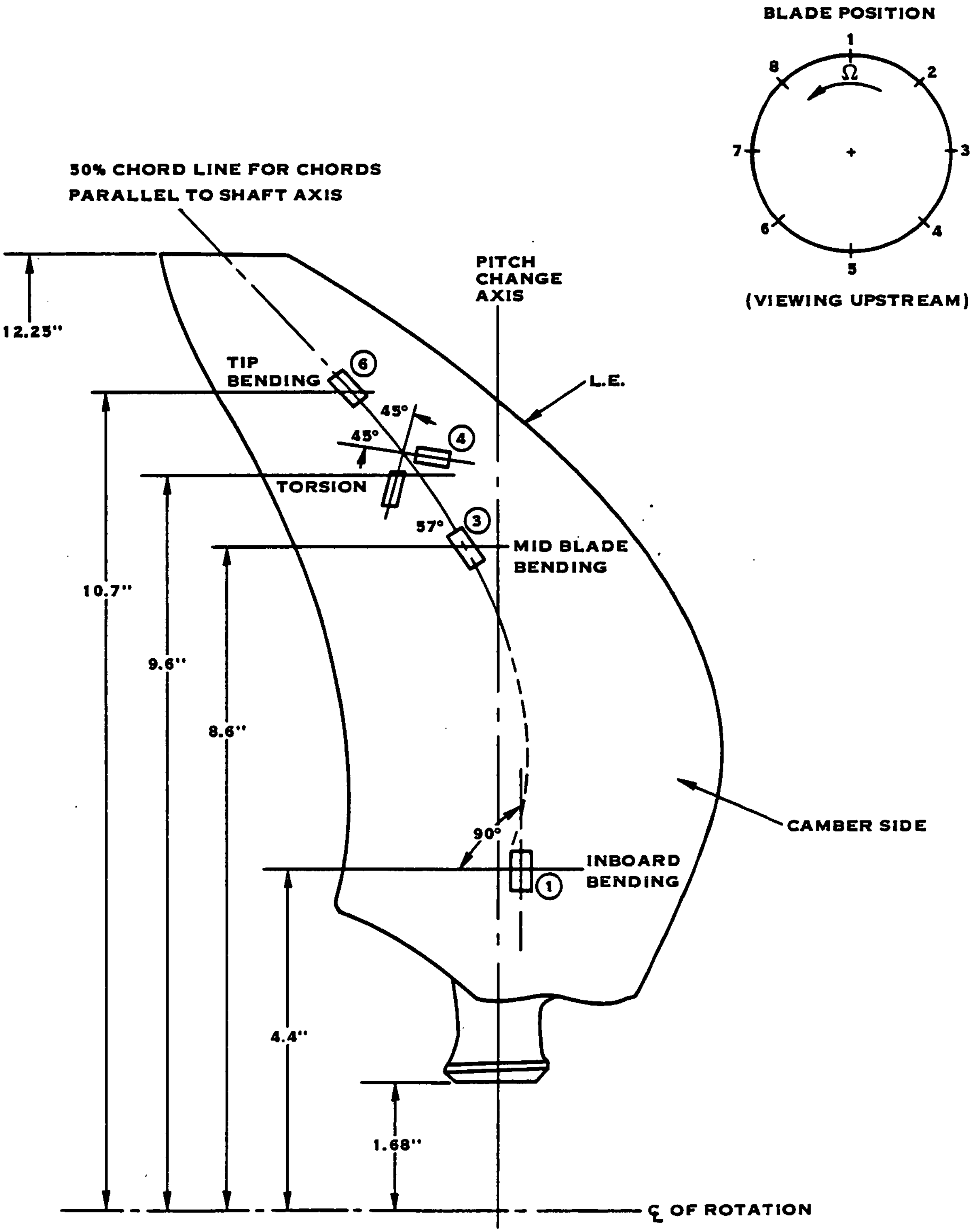

FIGURE 3. STRAIN GAGED SR-3 BLADE FOR INLET TESTS

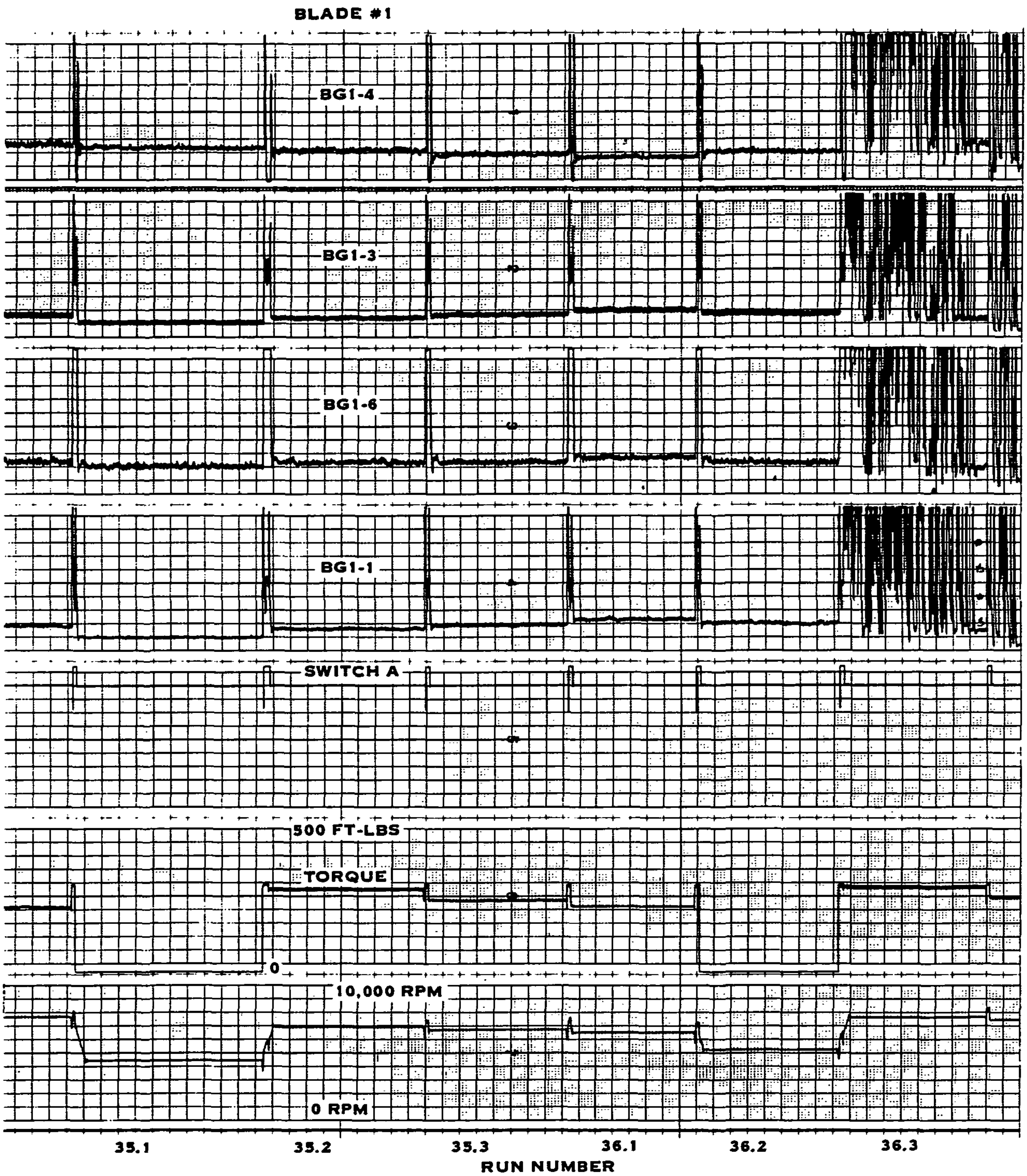

FIGURE 4. BRUSH CHART SAMPLE, TEST RUN 35.2(M=0.6, 7015 RPM, 0.81 MFR)
SINGLE SCOOP MID-INLET

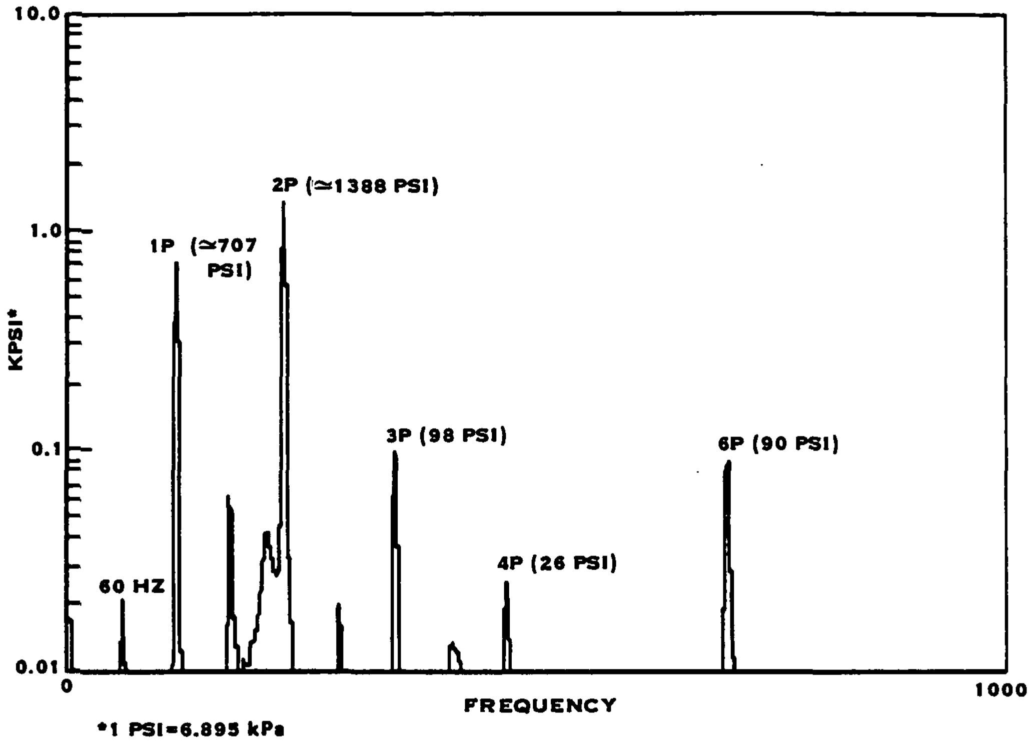

FIGURE 5. SPECTRAL PLOT OF INBOARD BENDING GAGE (BLADE 1), TEST RUN 35.2 (M=0.6, 7015 RPM, MFR=0.81, β=58°) SINGLE SCOOP MID-INLET

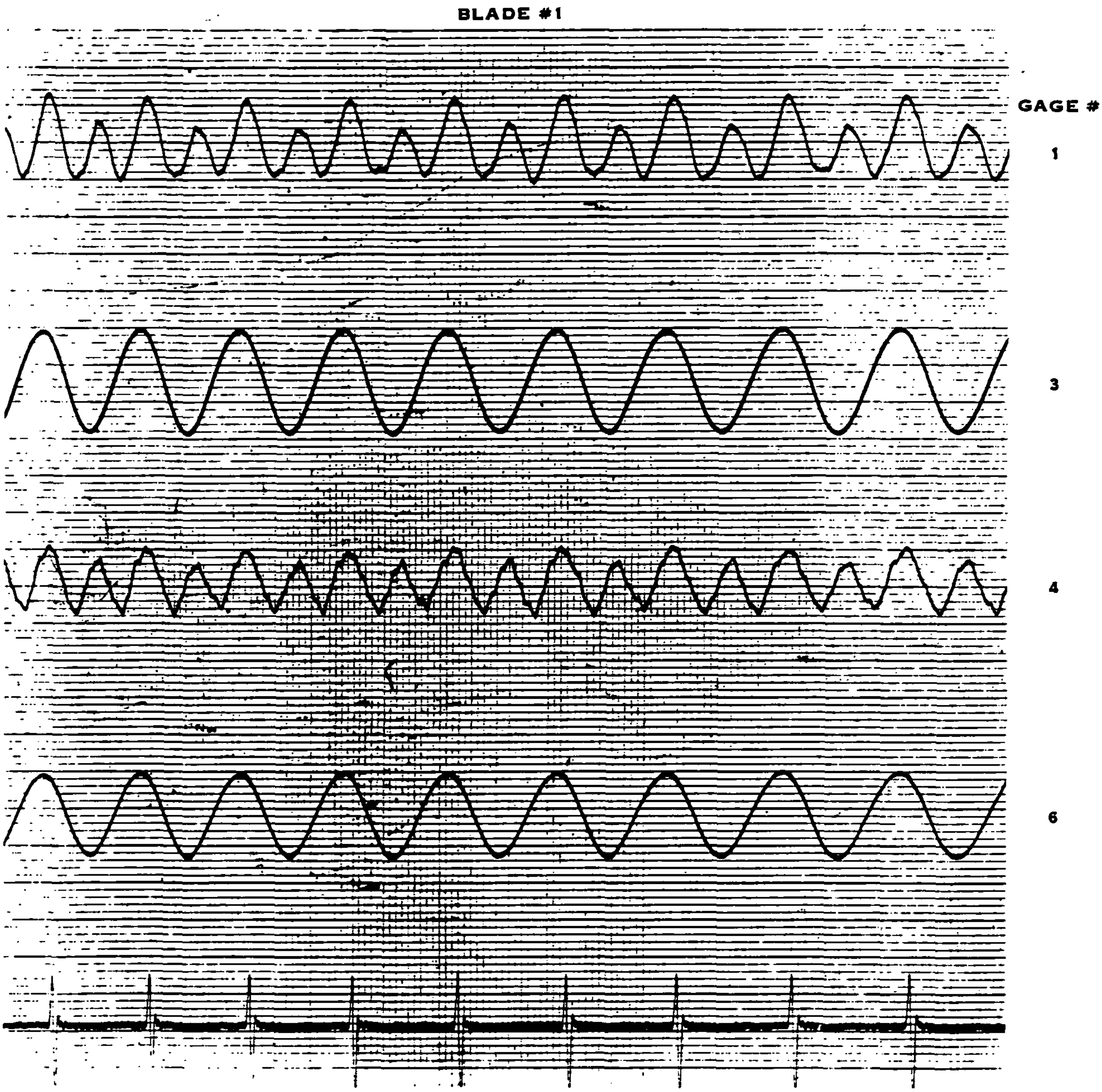

FIGURE 6. VISICORDER PLOT, TEST RUN 35.2
(M=0.6, 7015 RPM, 0.81 MFR) SINGLE SCOOP MID-INLET

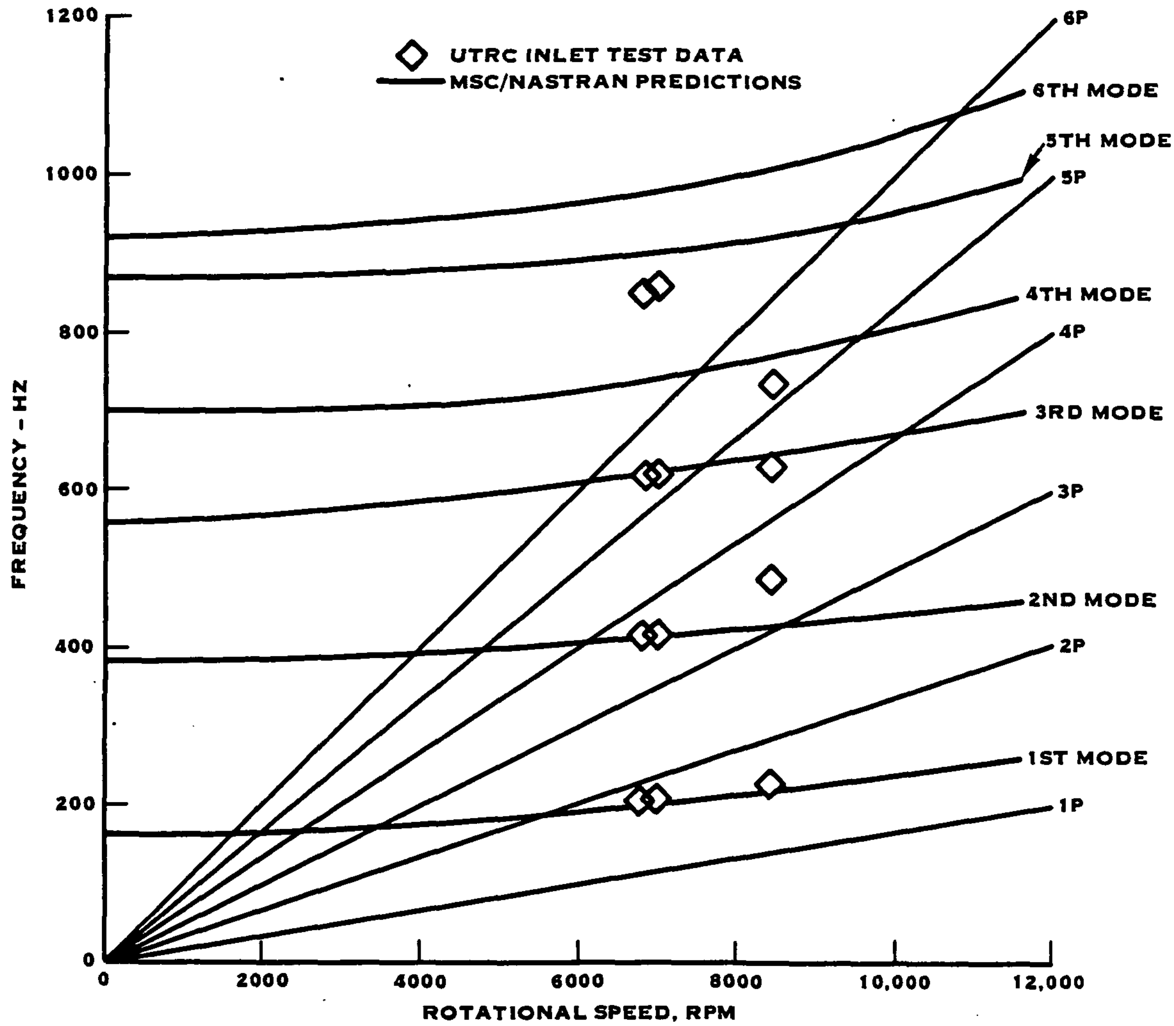

FIGURE 7. SR-3 PROP-FAN MODEL CAMPBELL DIAGRAM

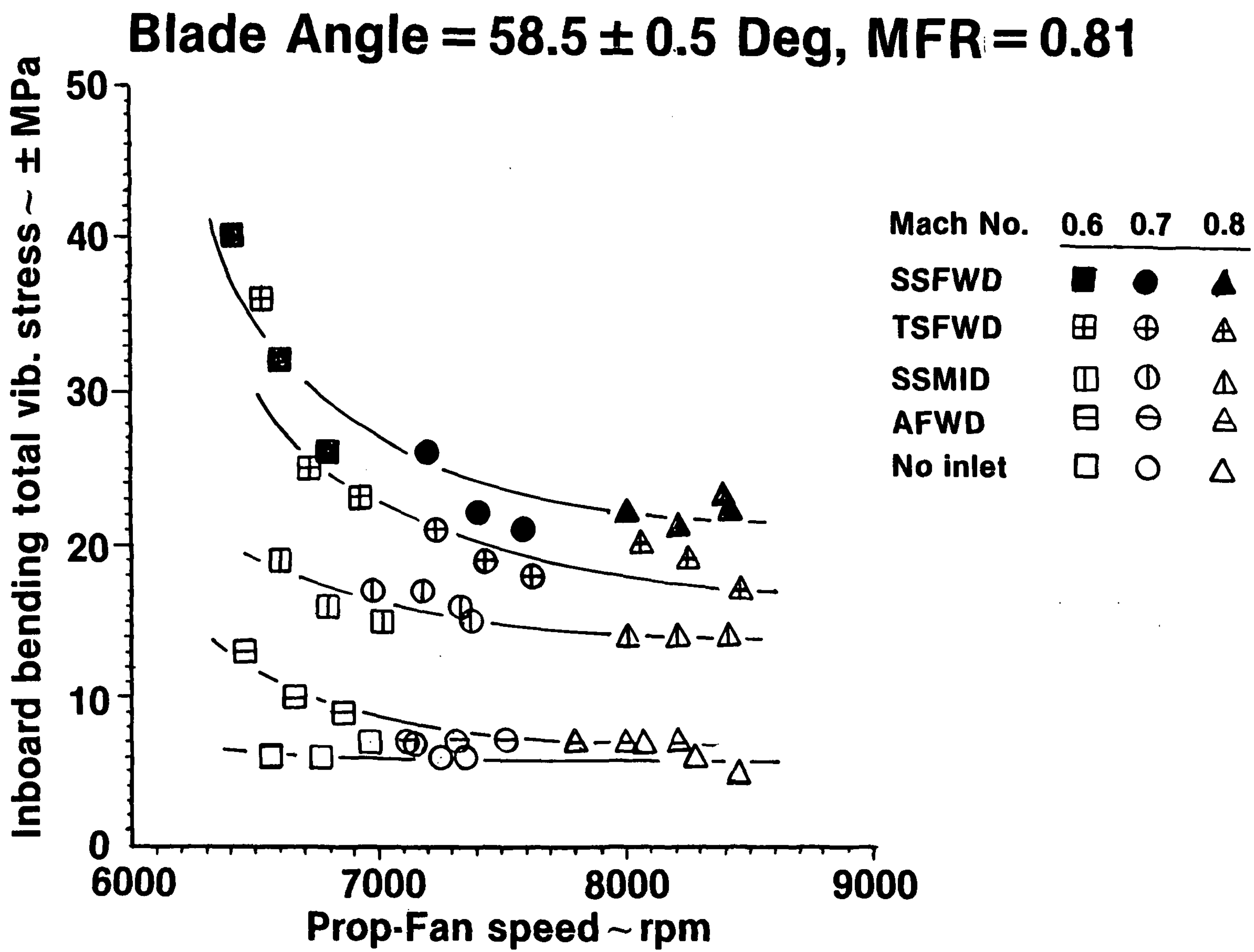

FIGURE 8. COMPARISON OF INLET TEST RESULTS - SINGLE FORWARD, TWIN FORWARD, SINGLE MID, ANNULAR AND NO-INLET CONFIGURATIONS.

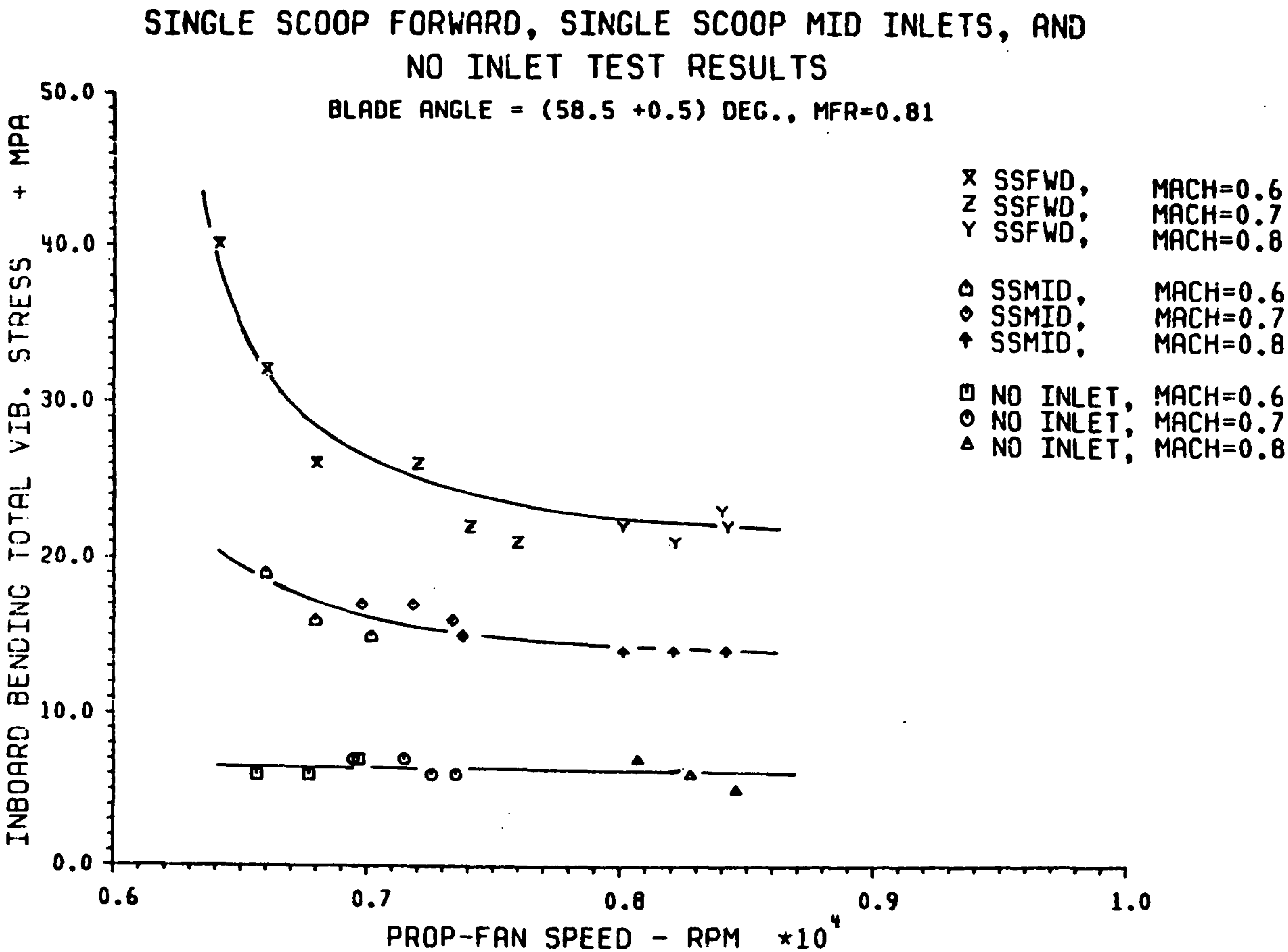

FIGURE 9 COMPARISON OF INLETS

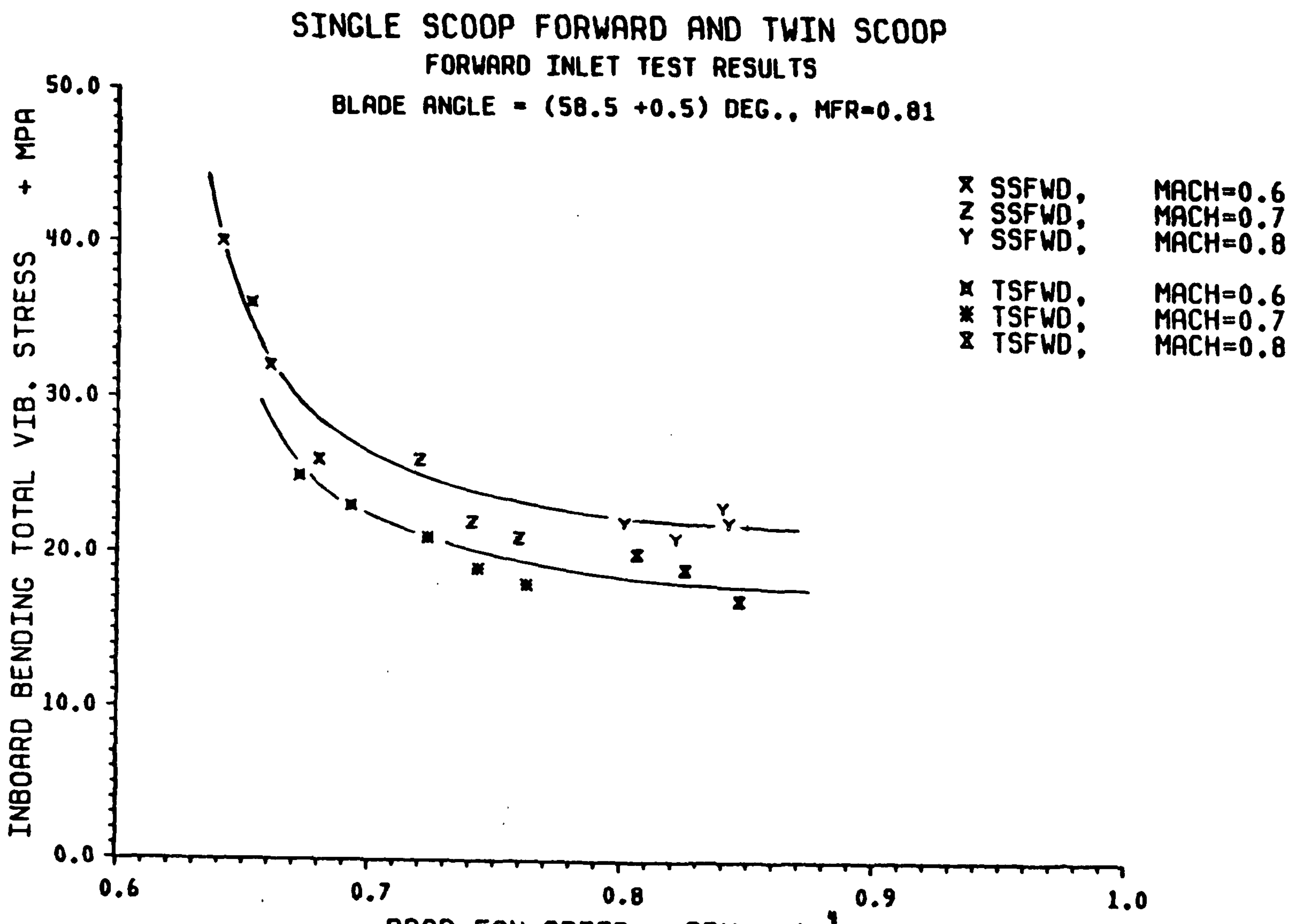

FIGURE 10 COMPARISON OF INLETS

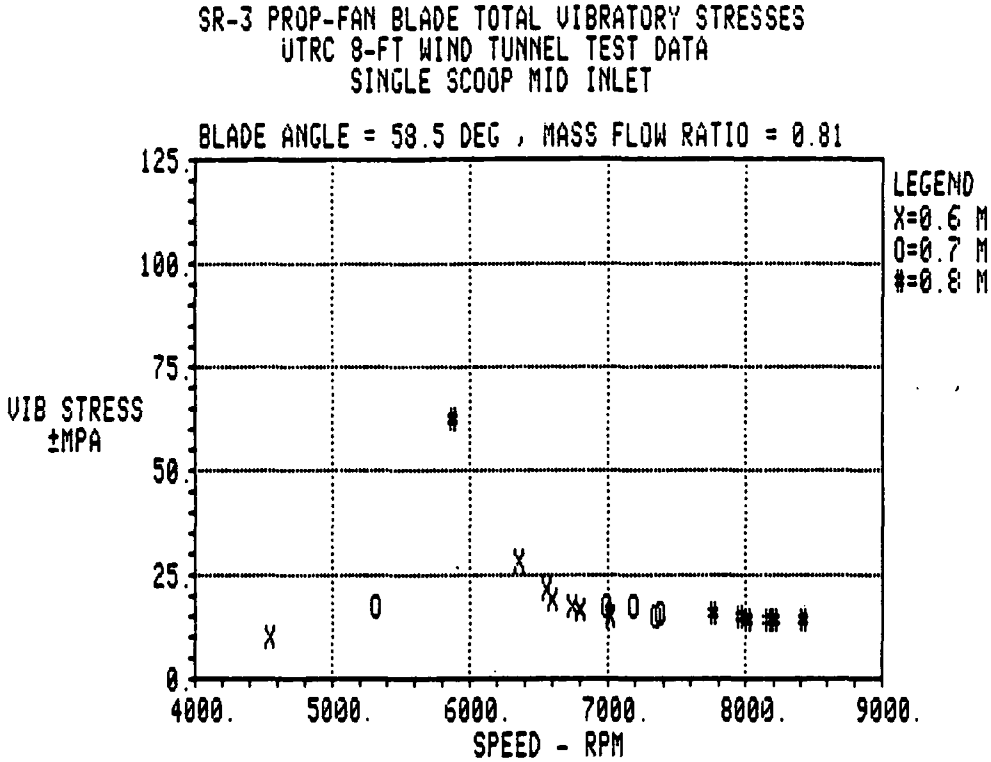

FIGURE 11. INBOARD BENDING (BG1-1) VS. PROP-FAN SPEED

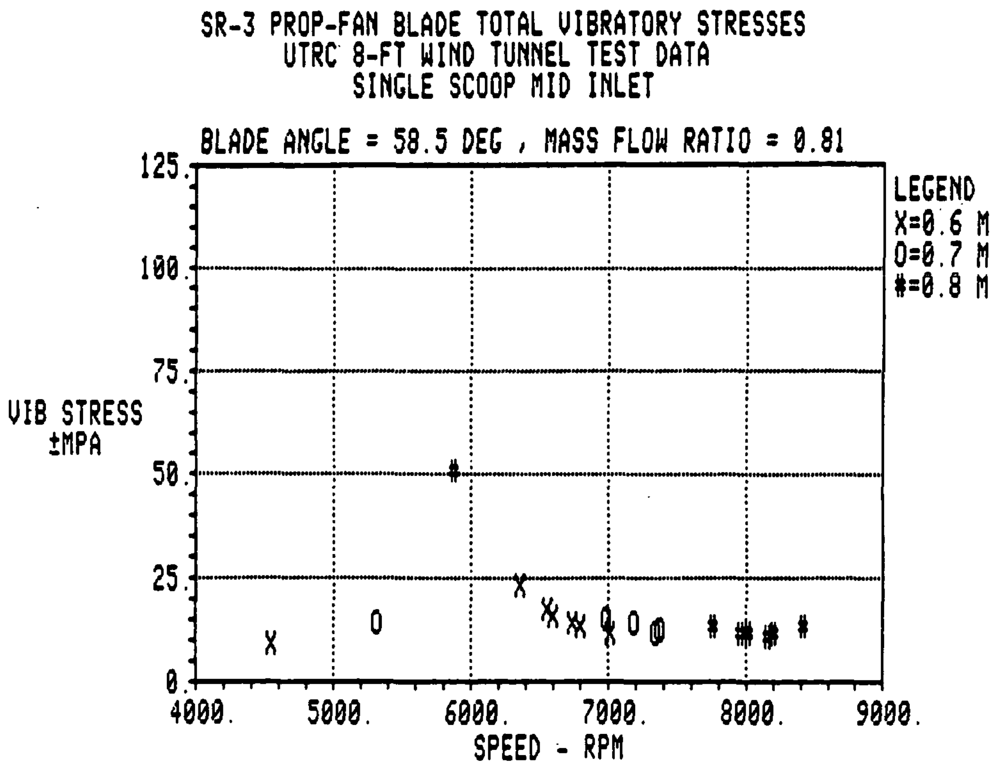

FIGURE 12. MID BLADE BENDING (BG1-3) VS. PROP-FAN SPEED

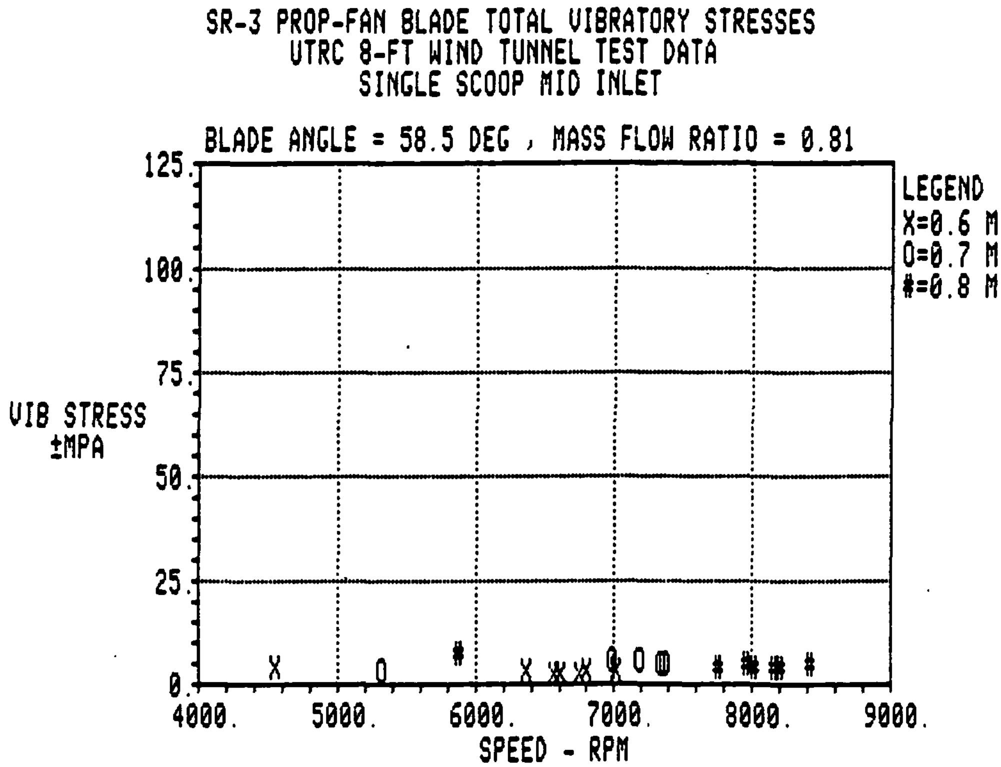

FIGURE 13. MID BLADE TORSION (BG1-4) VS. PROP-FAN SPEED

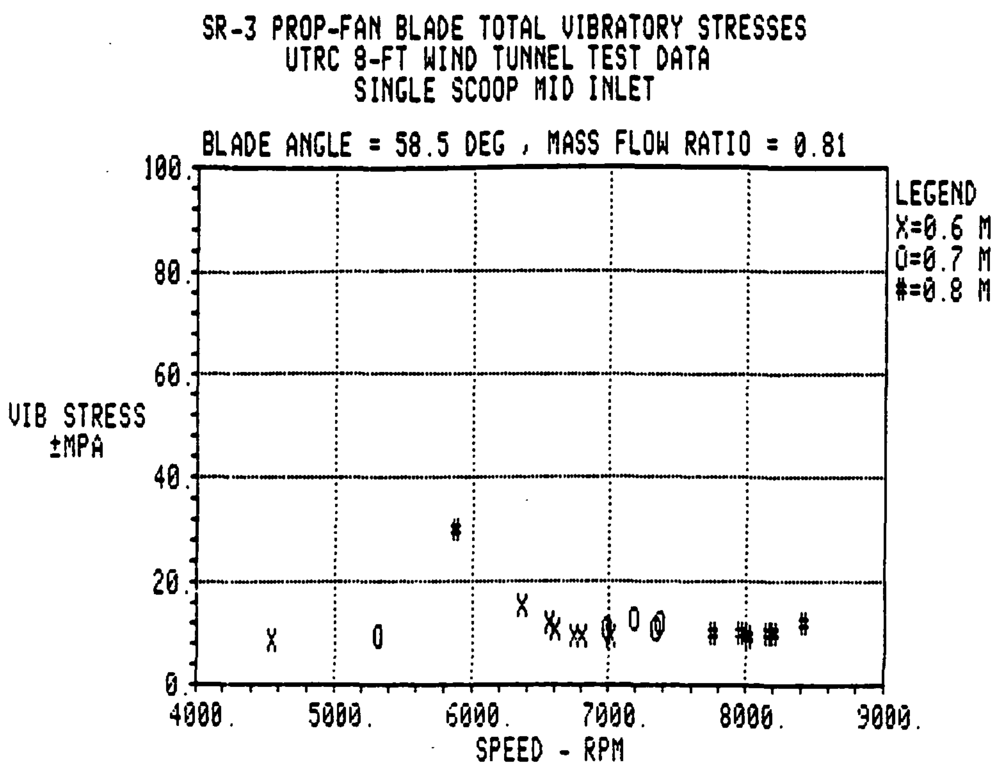

FIGURE 14. TIP BENDING (BG1-6) VS. PROP-FAN SPEED

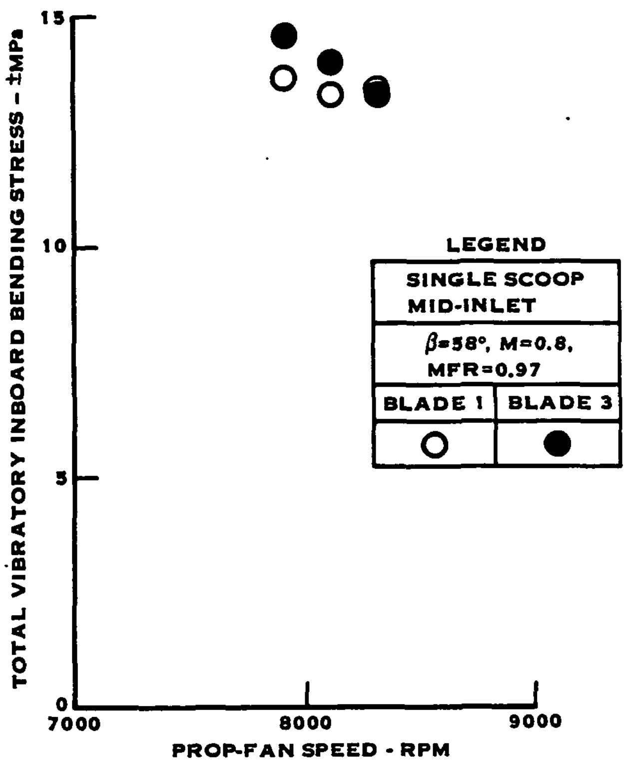

FIGURE 15. COMPARISON OF BLADE 1 AND BLADE 3 TOTAL VIBRATORY INBOARD BENDING STRESS

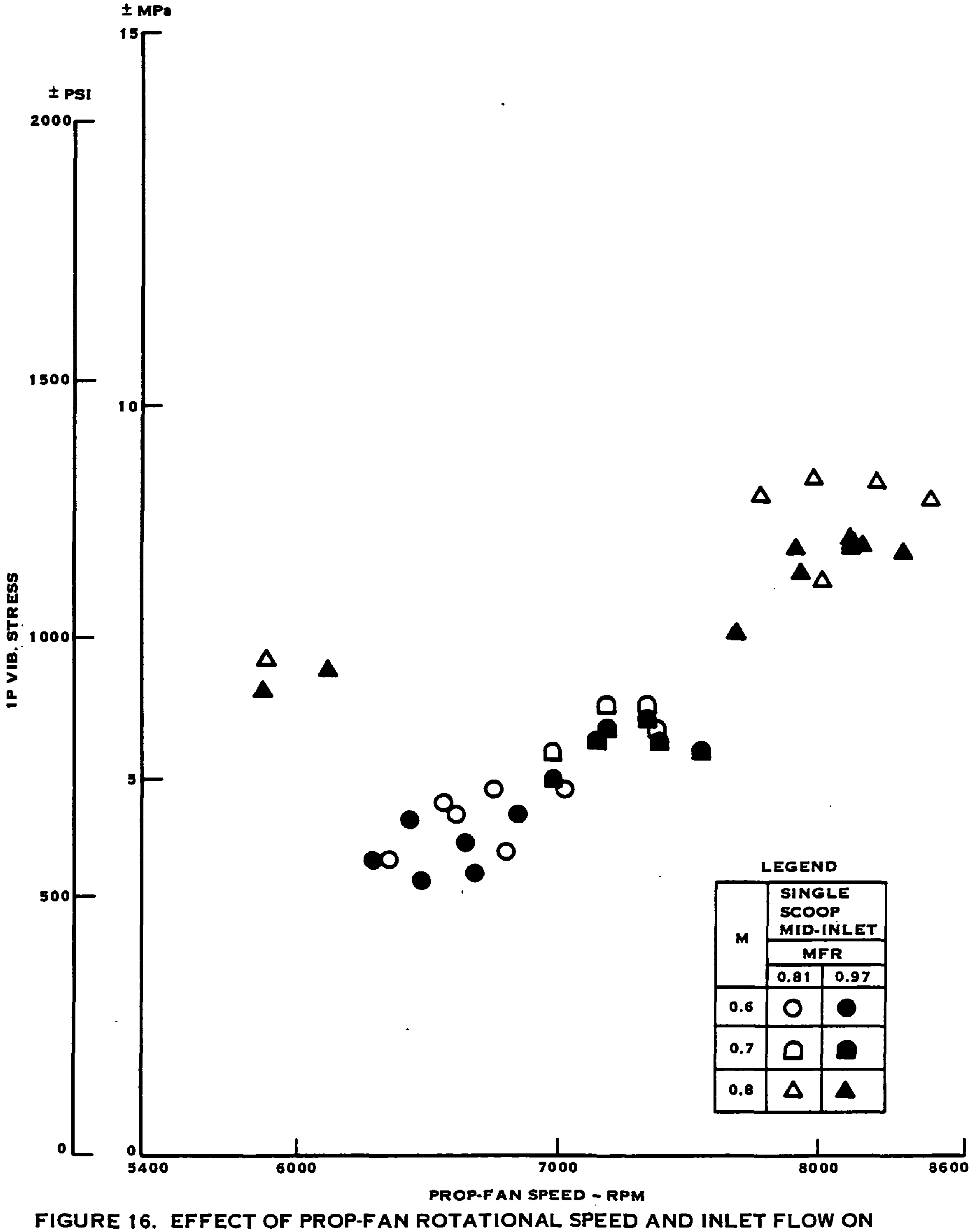

FIGURE 16. EFFECT OF PROP-FAN ROTATIONAL SPEED AND INLET FLOW ON INBOARD BENDING 1P STRESS OF BLADE #1 (SINGLE SCOOP MID-INLET, β=58.0° AND 59.2°)

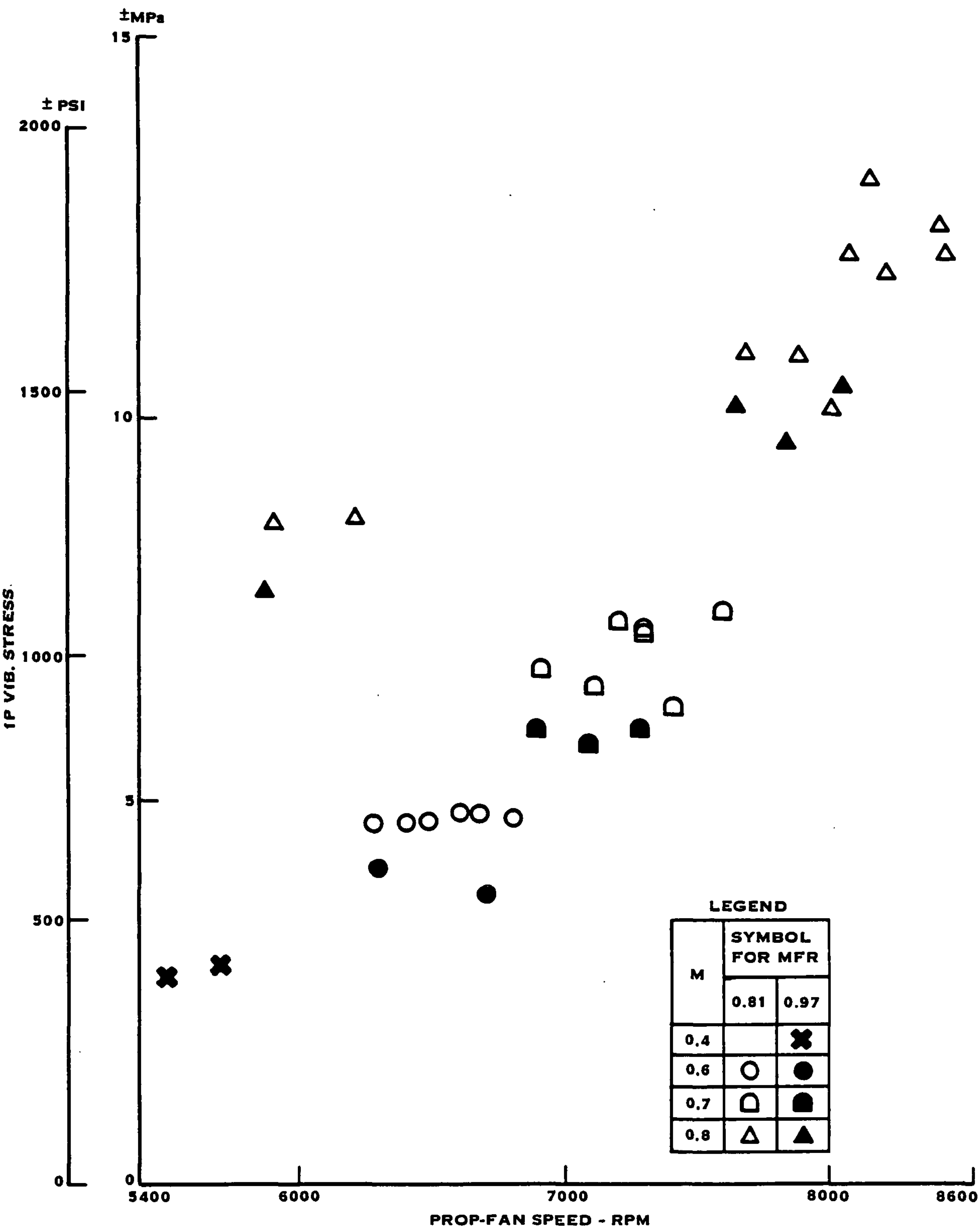

FIGURE 17. EFFECT OF PROP-FAN ROTATIONAL SPEED AND INLET FLOW ON INBOARD BENDING 1P STRESS OF BLADE #1 (SINGLE SCOOP FORWARD INLET, β=57.8° AND 59.0°)

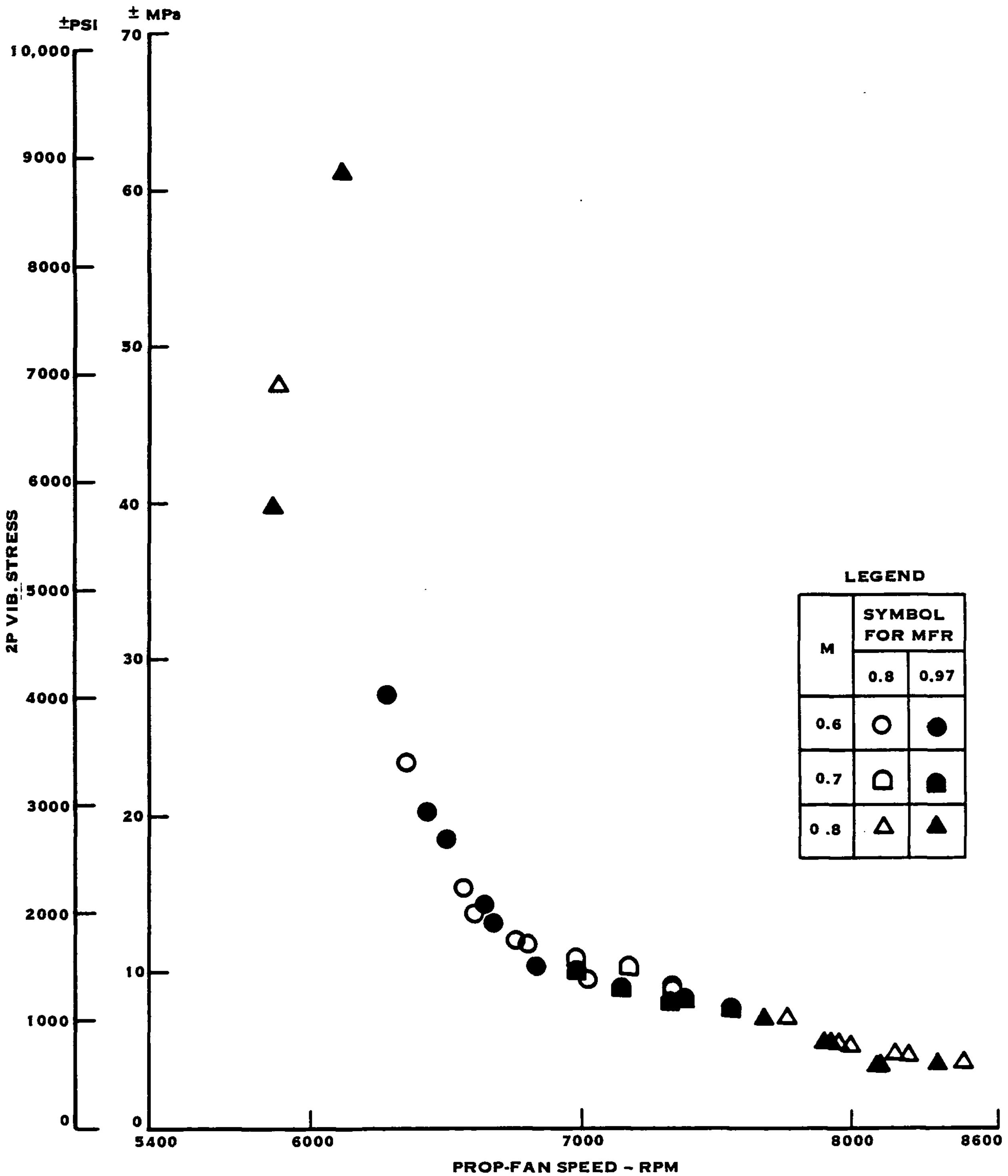

FIGURE 18. EFFECT OF PROP-FAN ROTATIONAL SPEED AND INLET FLOW ON INBOARD BENDING 2P STRESS OF BLADE #1 (SINGLE SCOOP MID-INLET, β=58.0° AND 59.2°)

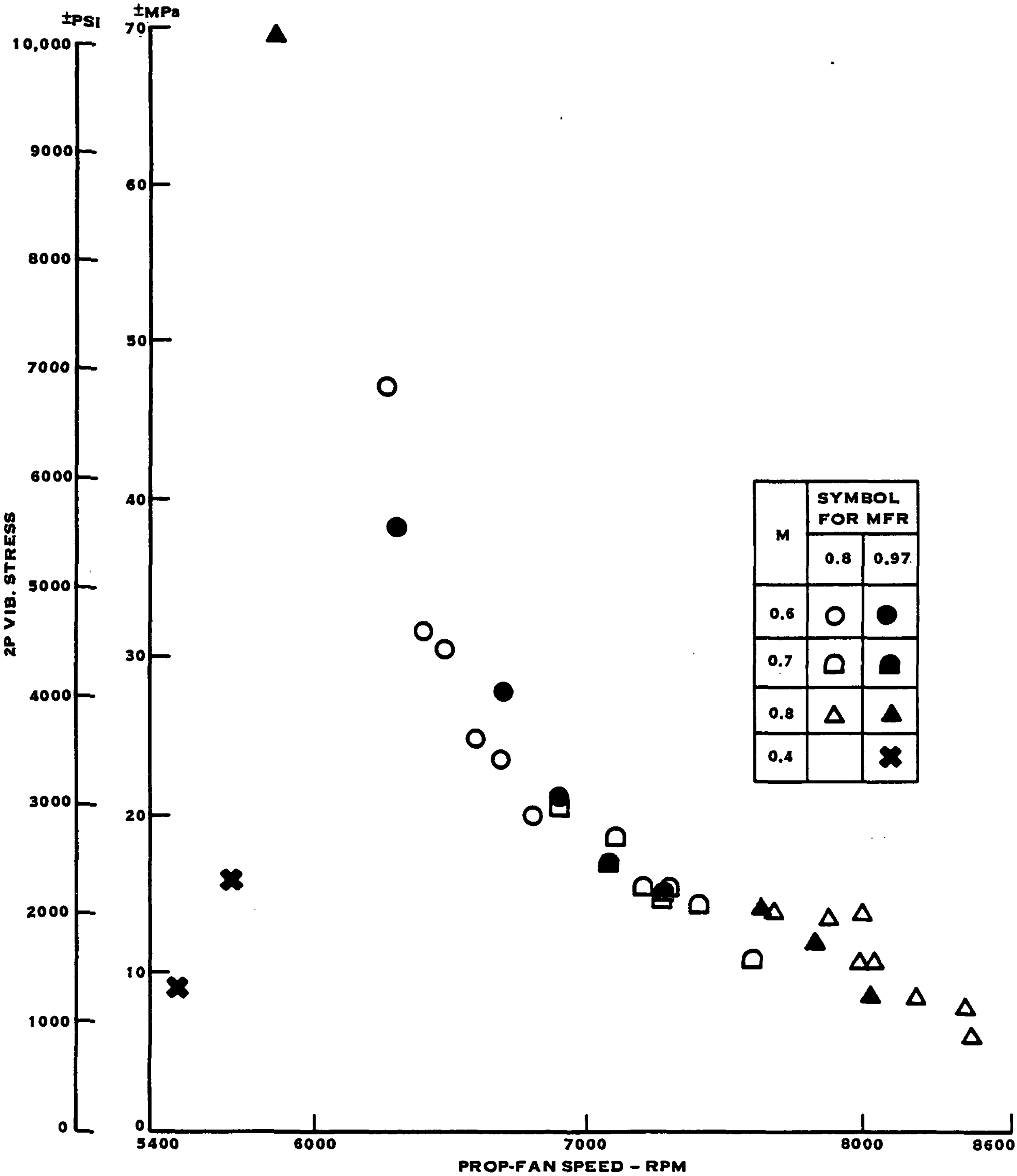

FIGURE 19. EFFECT OF PROP-FAN ROTATIONAL SPEED AND INLET FLOW ON INBOARD BENDING 2P STRESS OF BLADE #1 (SINGLE SCOOP FORWARD INLET, β=57.8° AND 59.0°)

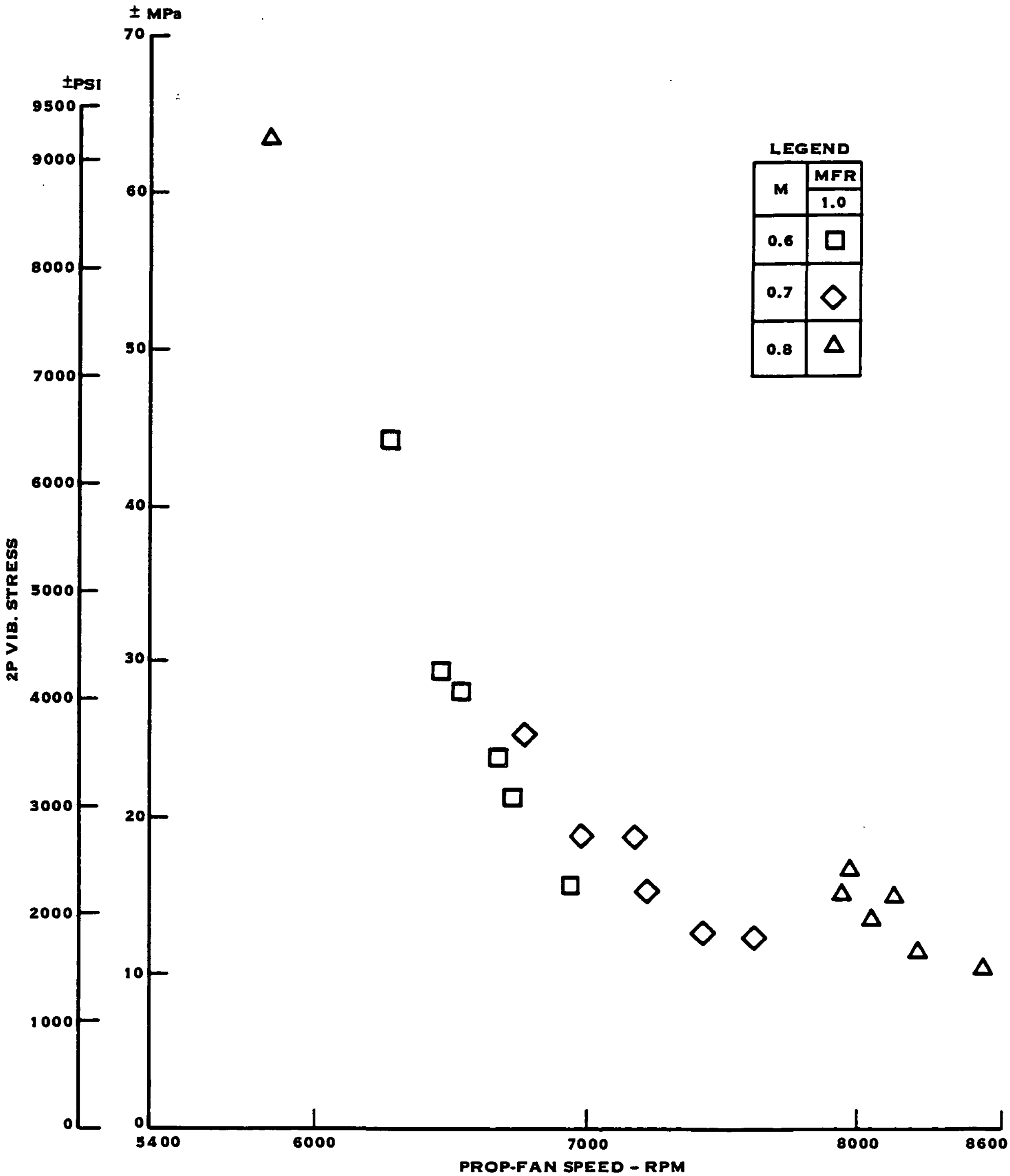

FIGURE 20. EFFECT OF PROP-FAN ROTATIONAL SPEED ON INBOARD BENDING 2P STRESS OF BLADE #3 (TWIN SCOOP FORWARD INLET, β=58.3° AND 59.1°)

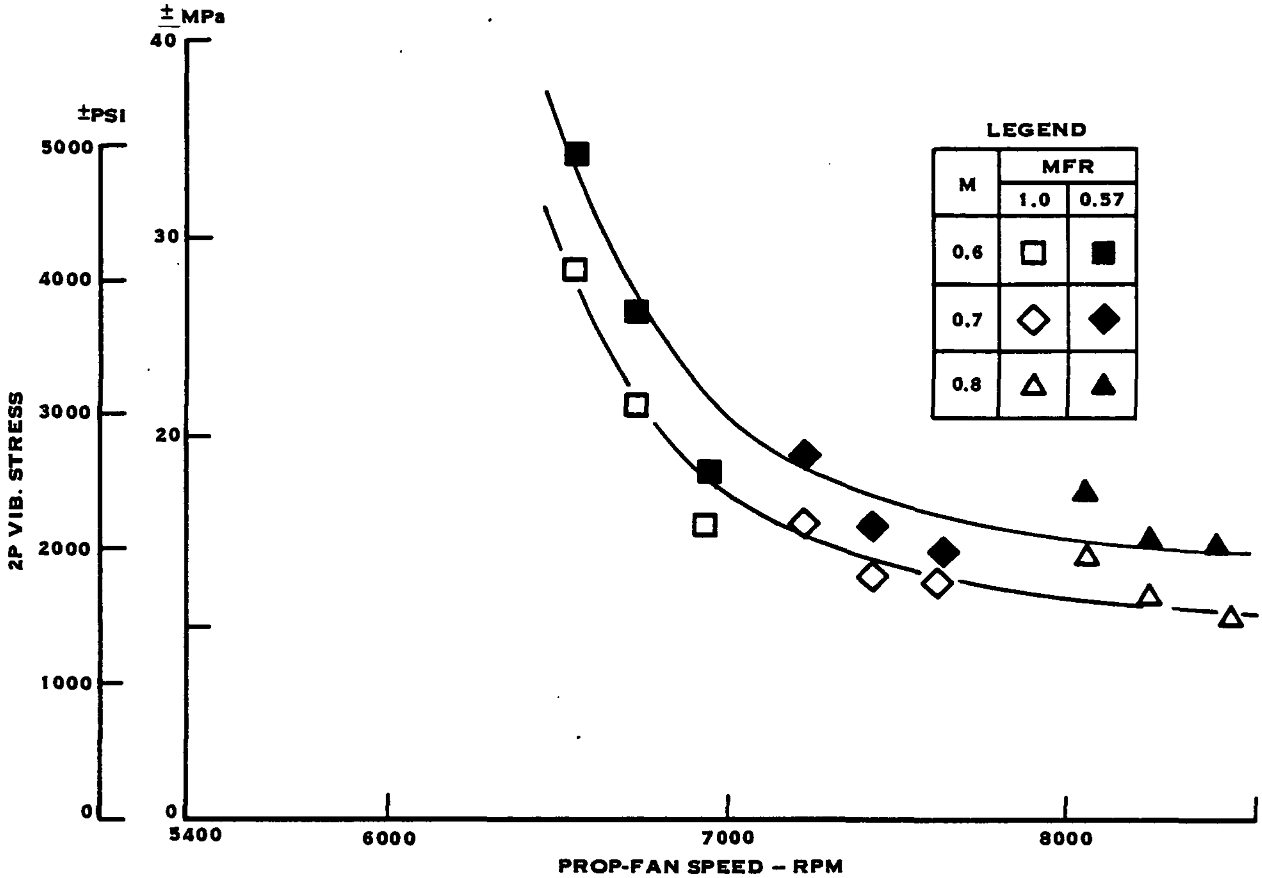

FIGURE 21. EFFECT OF PROP-FAN ROTATIONAL SPEED AND INLET FLOW ON INBOARD BENDING 2P STRESS OF BLADE #3 (TWIN SCOOP FORWARD INLET, β=58.3°)

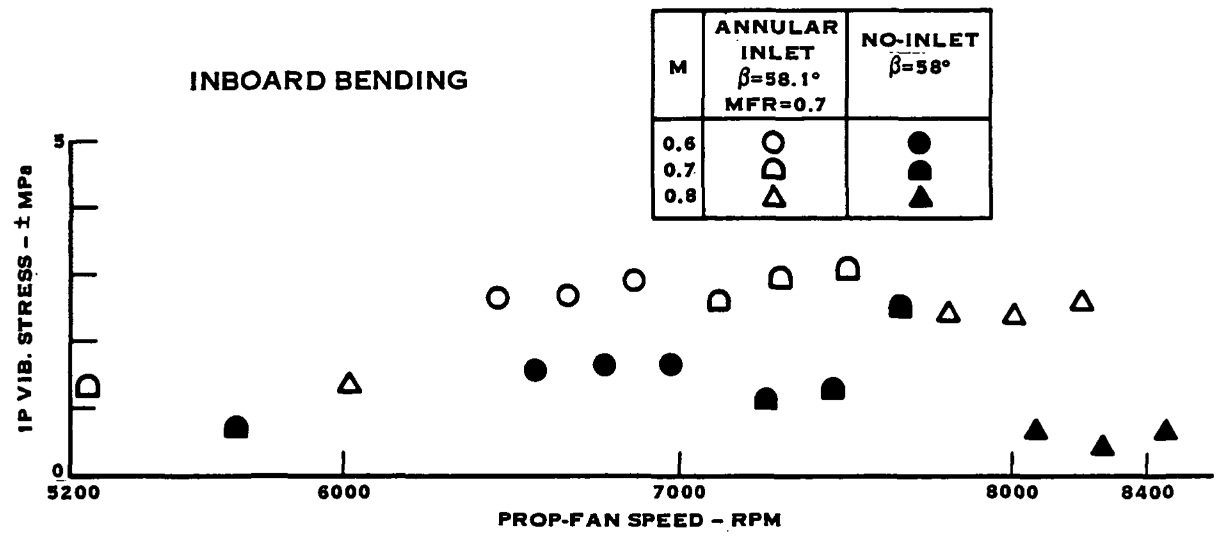

FIGURE 22. COMPARISON OF ANNULAR INLET AND NO-INLET 1P VIBRATORY STRESSES

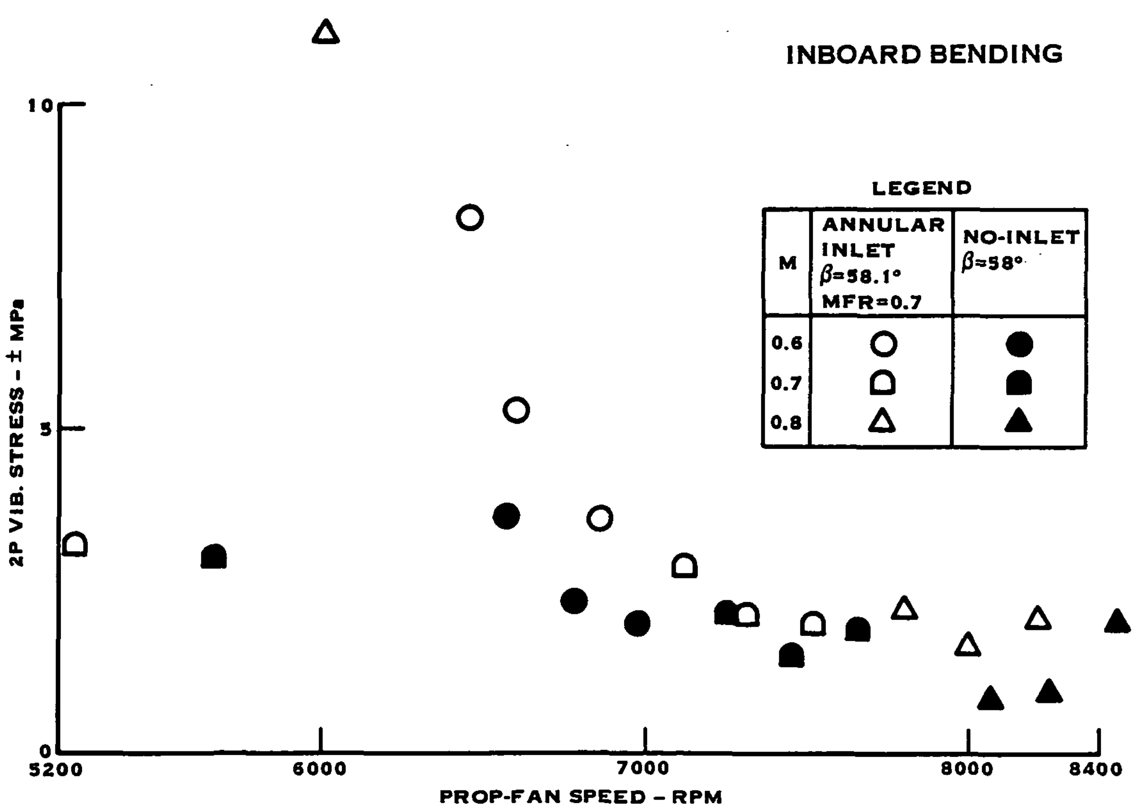

FIGURE 23. COMPARISON OF ANNULAR INLET AND NO-INLET 2P VIBRATORY STRESSES

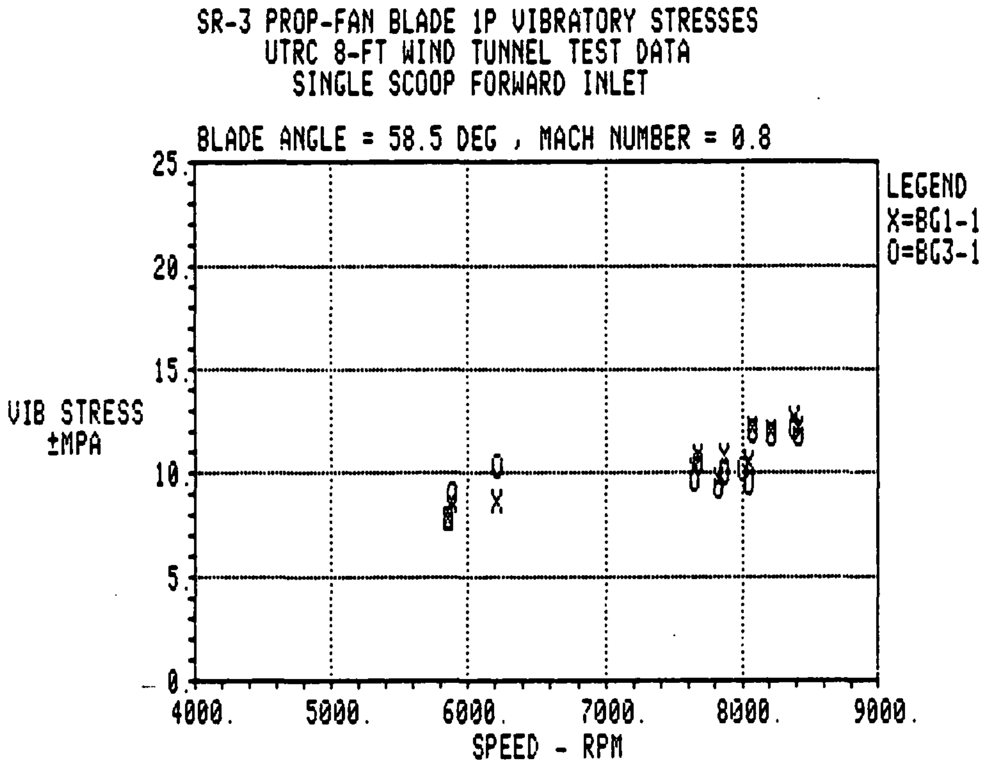

FIGURE 24. INBOARD BENDING VS. PROP-FAN SPEED

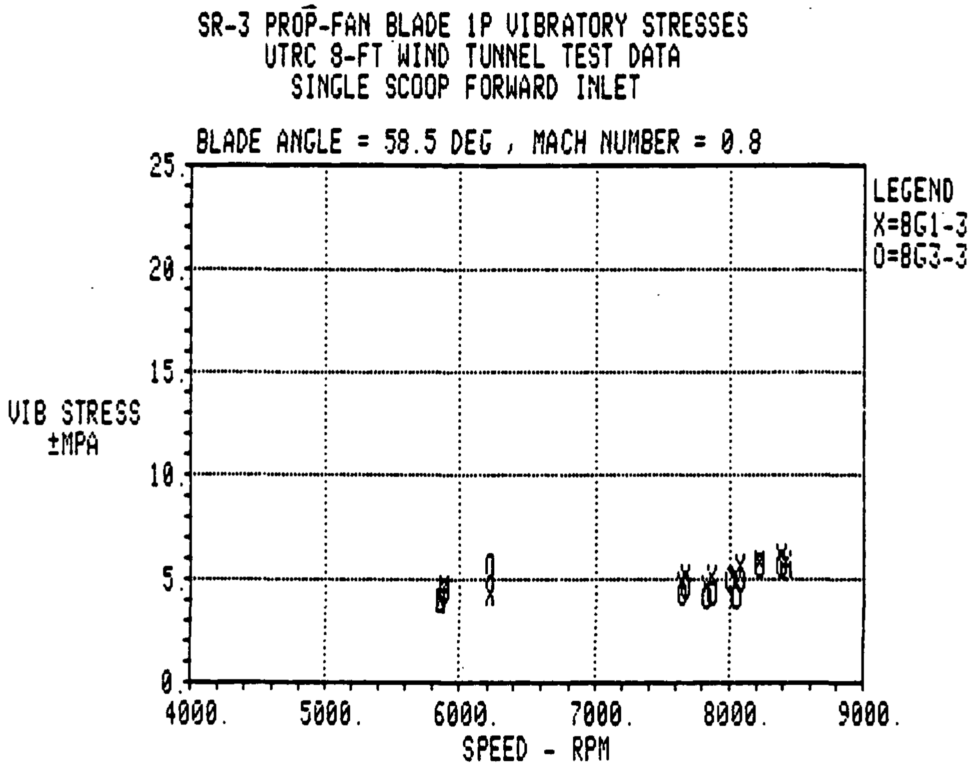

FIGURE 25. MID BLADE BENDING VS. PROP-FAN SPEED

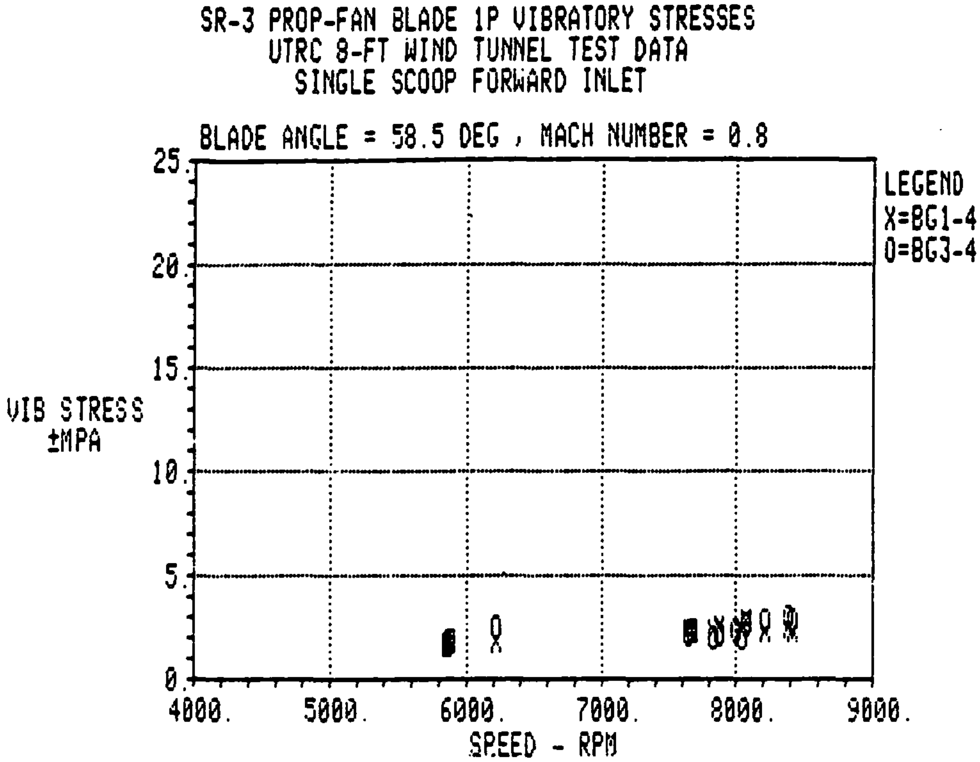

FIGURE 26. MID BLADE TORSION VS. PROP-FAN SPEED

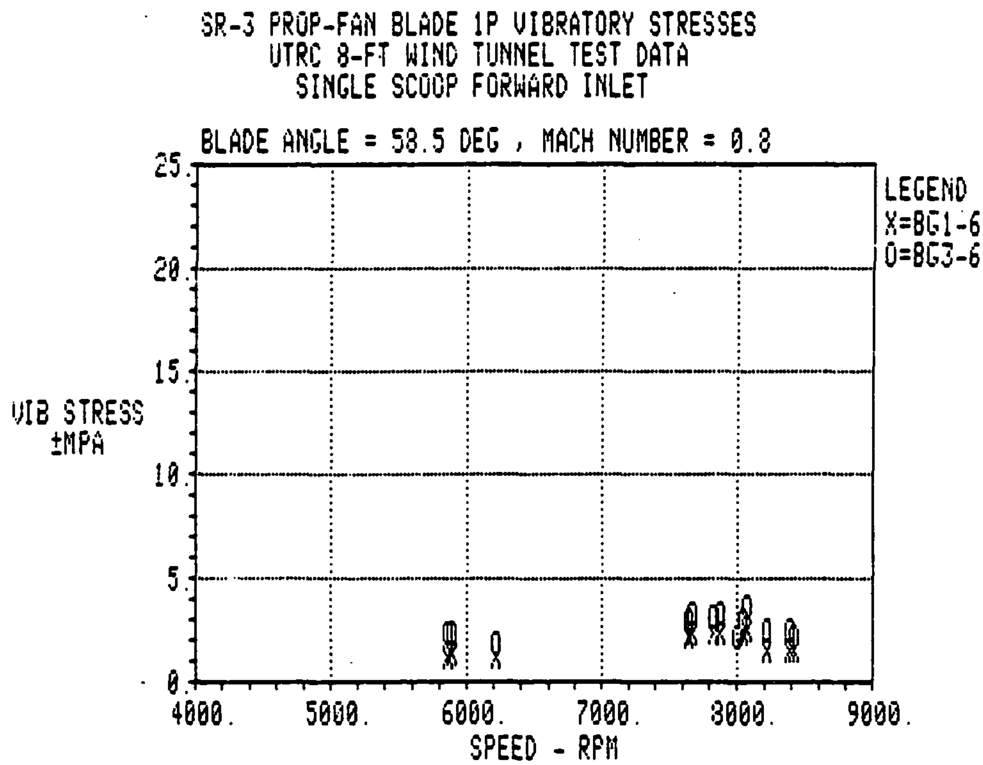

FIGURE 27. TIP BENDING VS. PROP-FAN SPEED

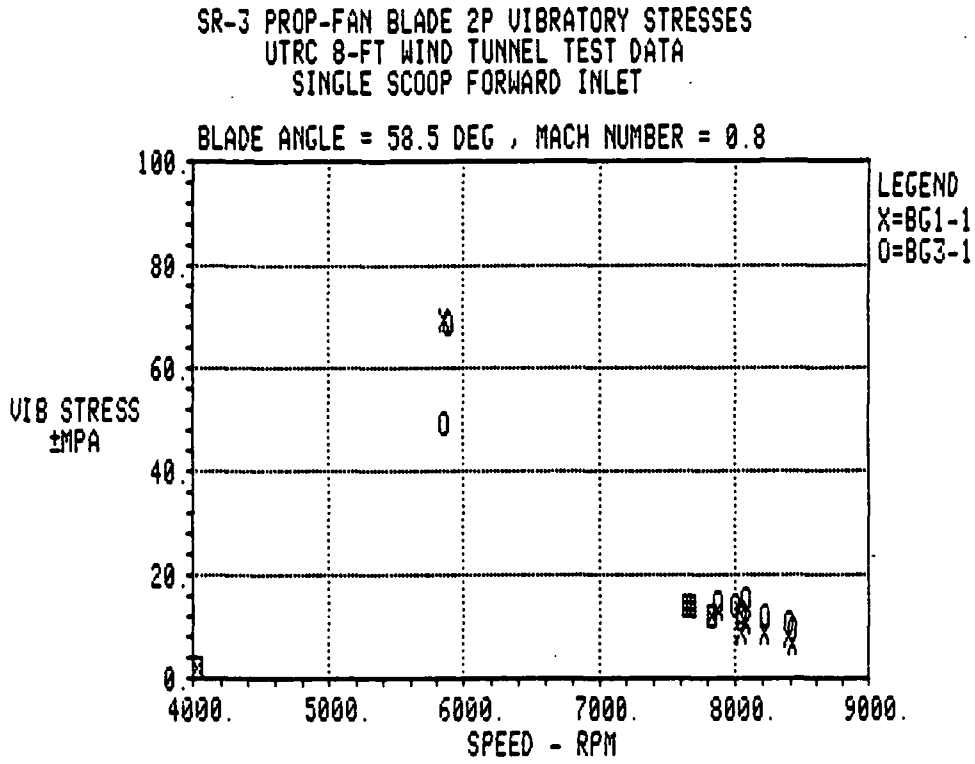

FIGURE 28. INBOARD BENDING VS. PROP-FAN SPEED

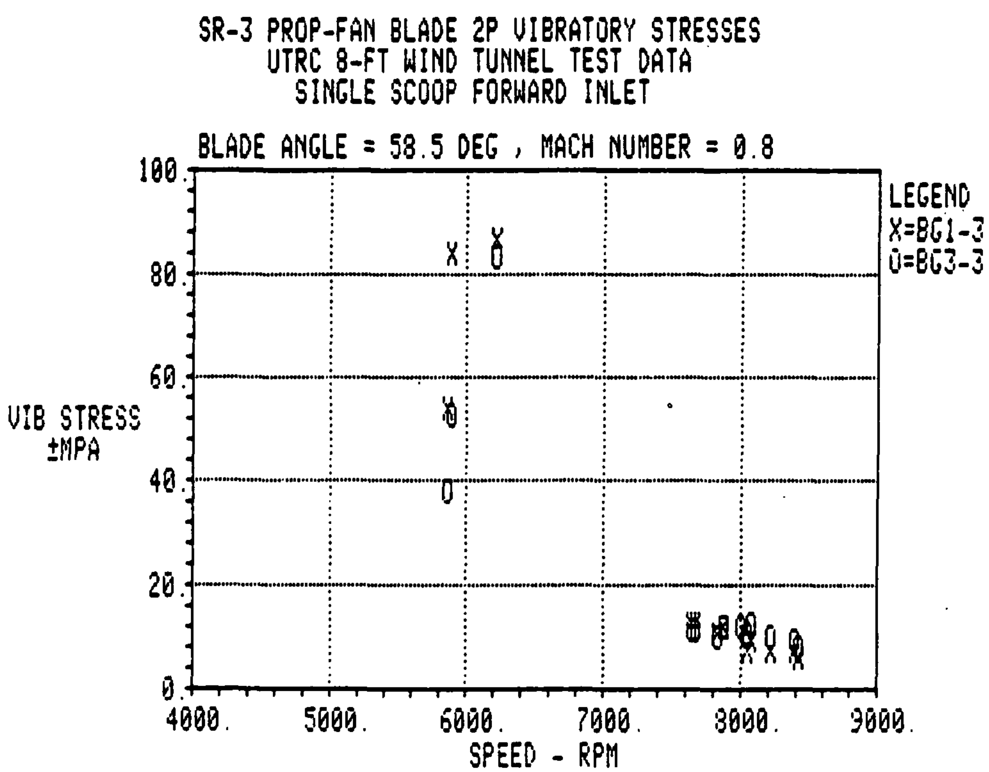

FIGURE 29. MID BLADE BENDING VS. PROP-FAN SPEED

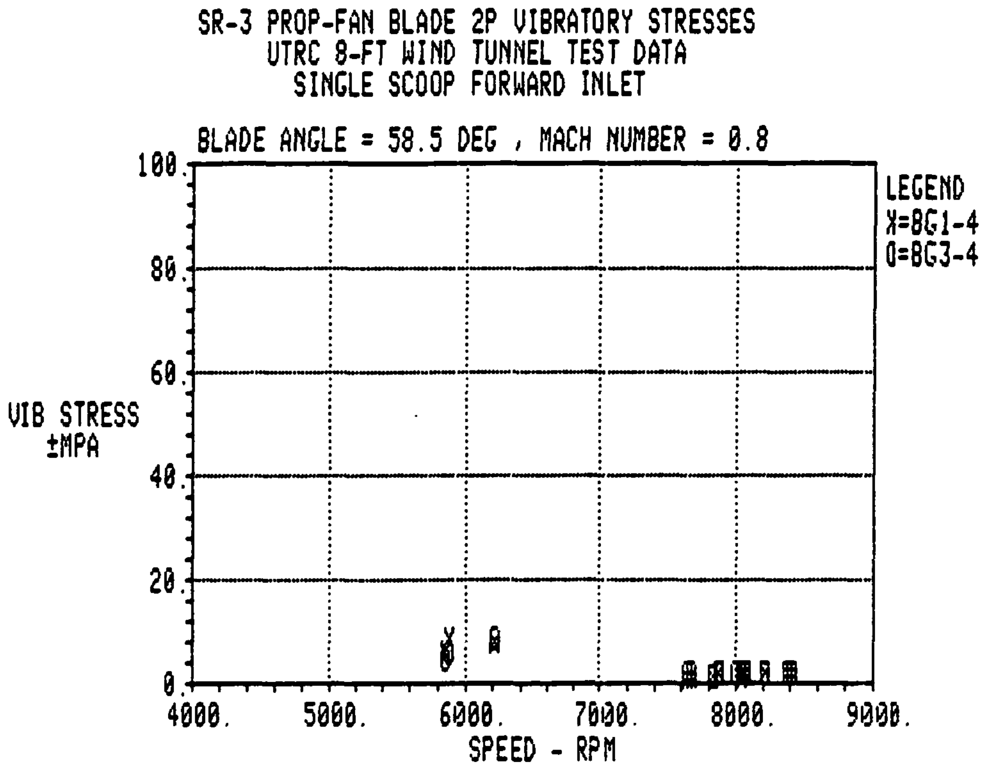

FIGURE 30. MID BLADE TORSION VS. PROP-FAN SPEED

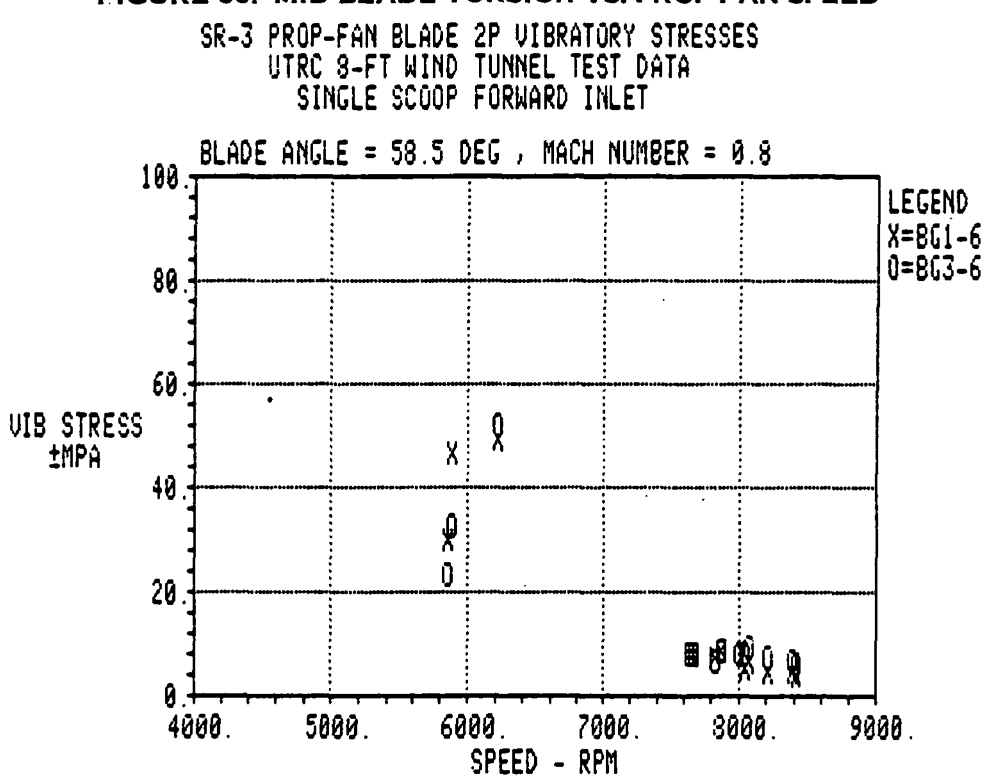

FIGURE 31. TIP BENDING VS. PROP-FAN SPEED

SR-3 SINGLE SCOOP MID-INLET RUN #37.2 (LGC CALCULATED DATA) M=0.8, MFR=0.81

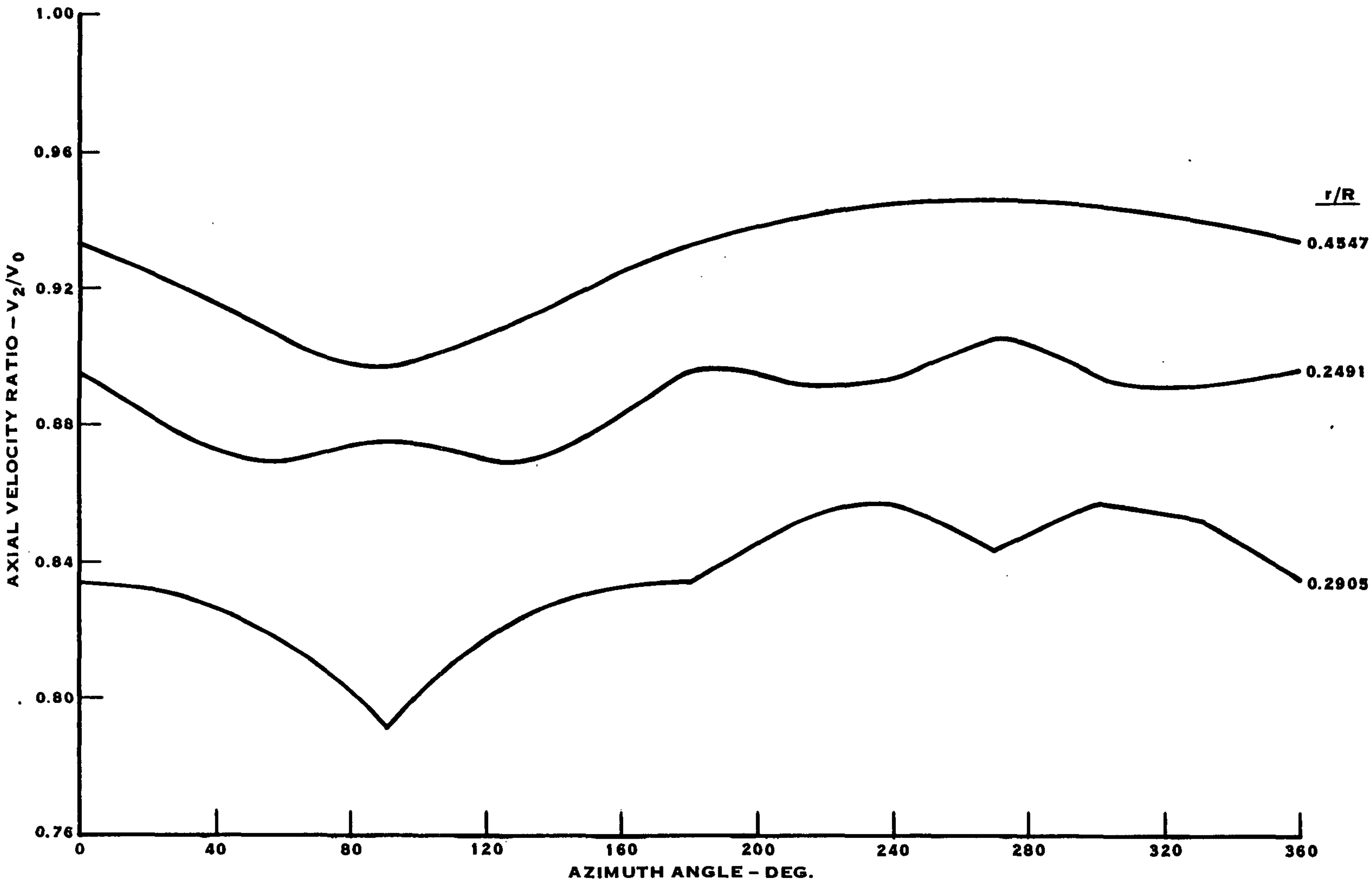

FIGURE 32. FLOW FIELD INPUT TO AERO LOAD CALCULATION

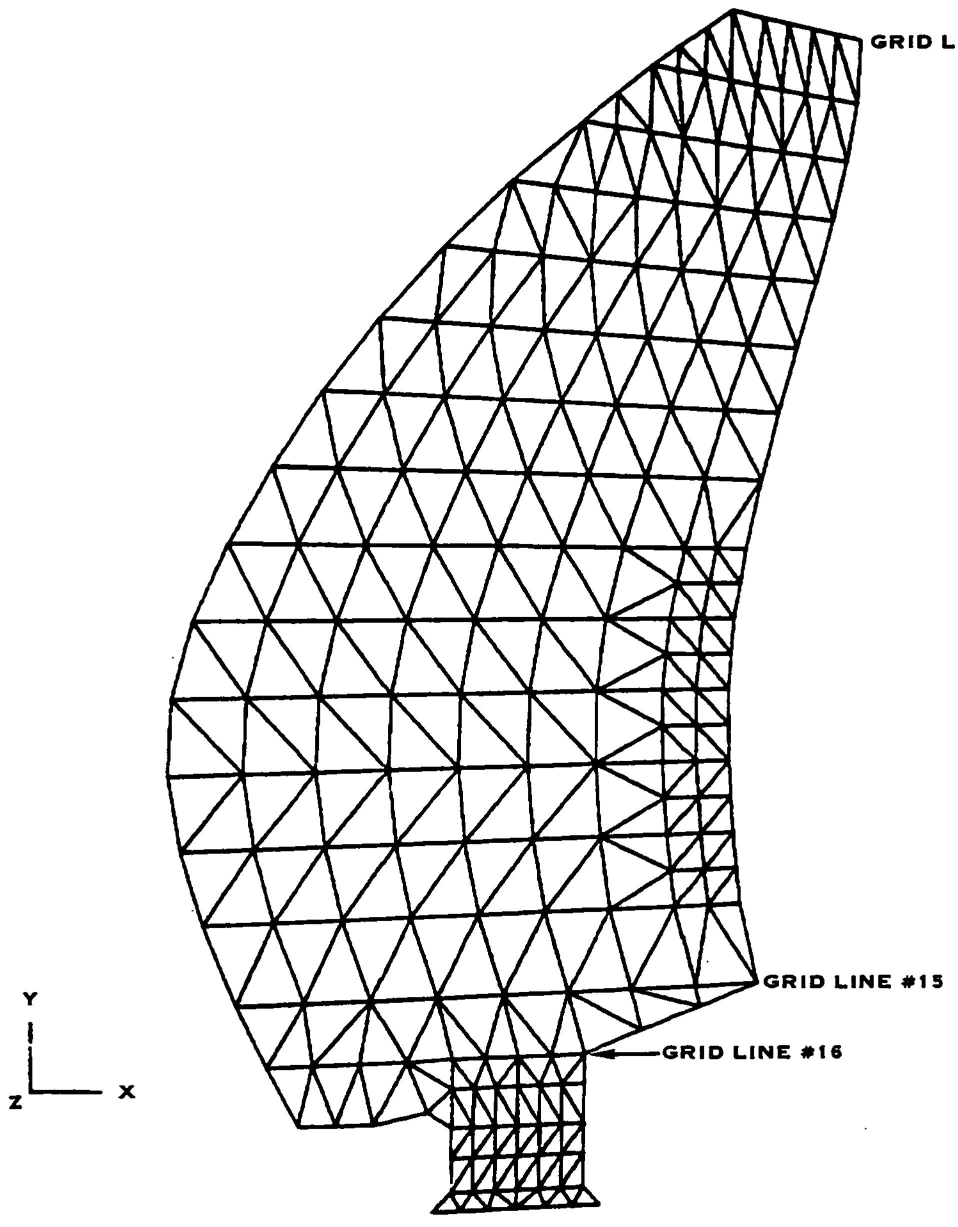

FIGURE 33. SR-3 FINITE ELEMENT MODEL

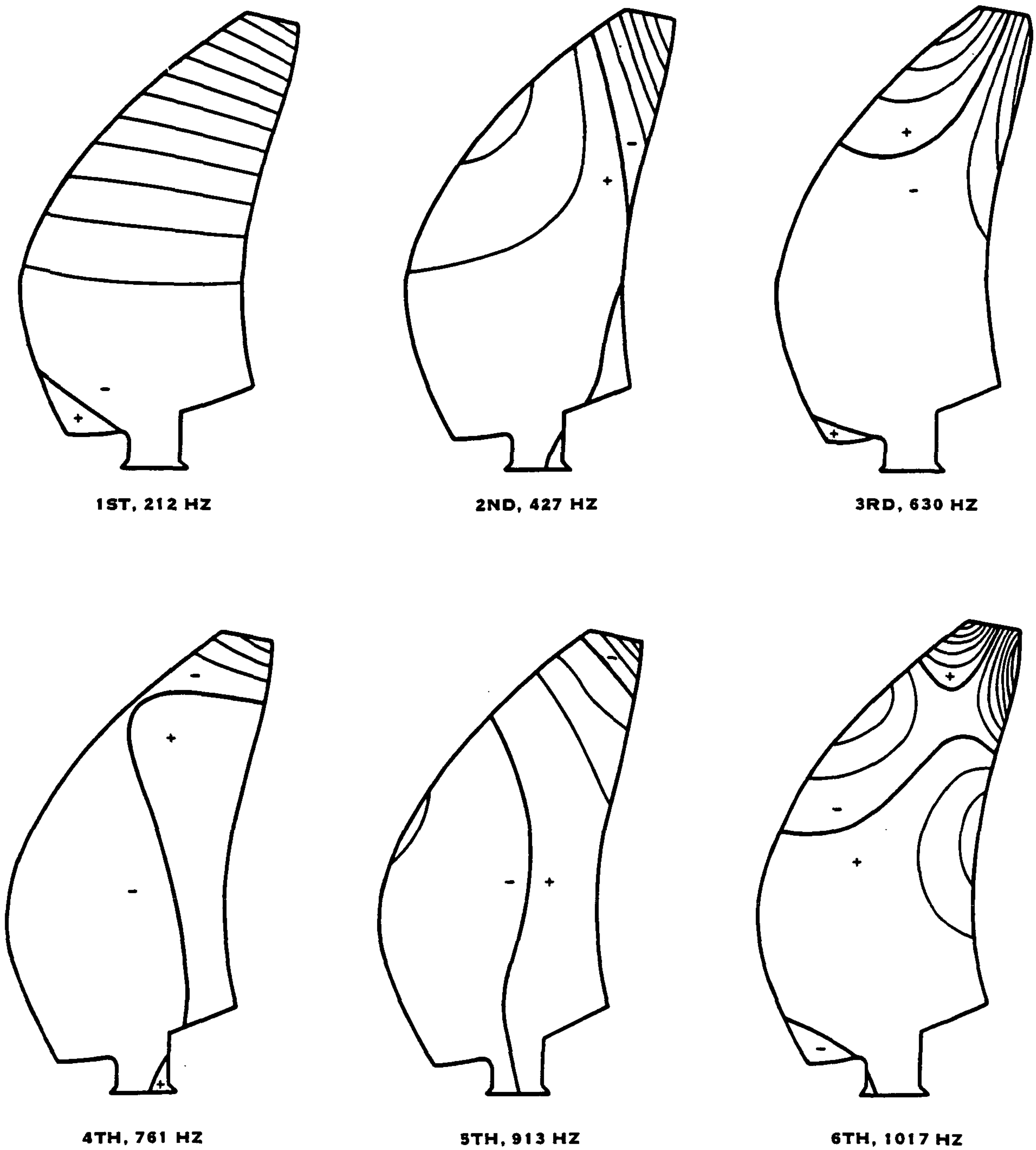

FIGURE 34. PREDICTED MODE SHAPES AT 7015 RPM, TEST RUN 35.2
(M=0.6, 7015 RPM, 0.81 MFR)

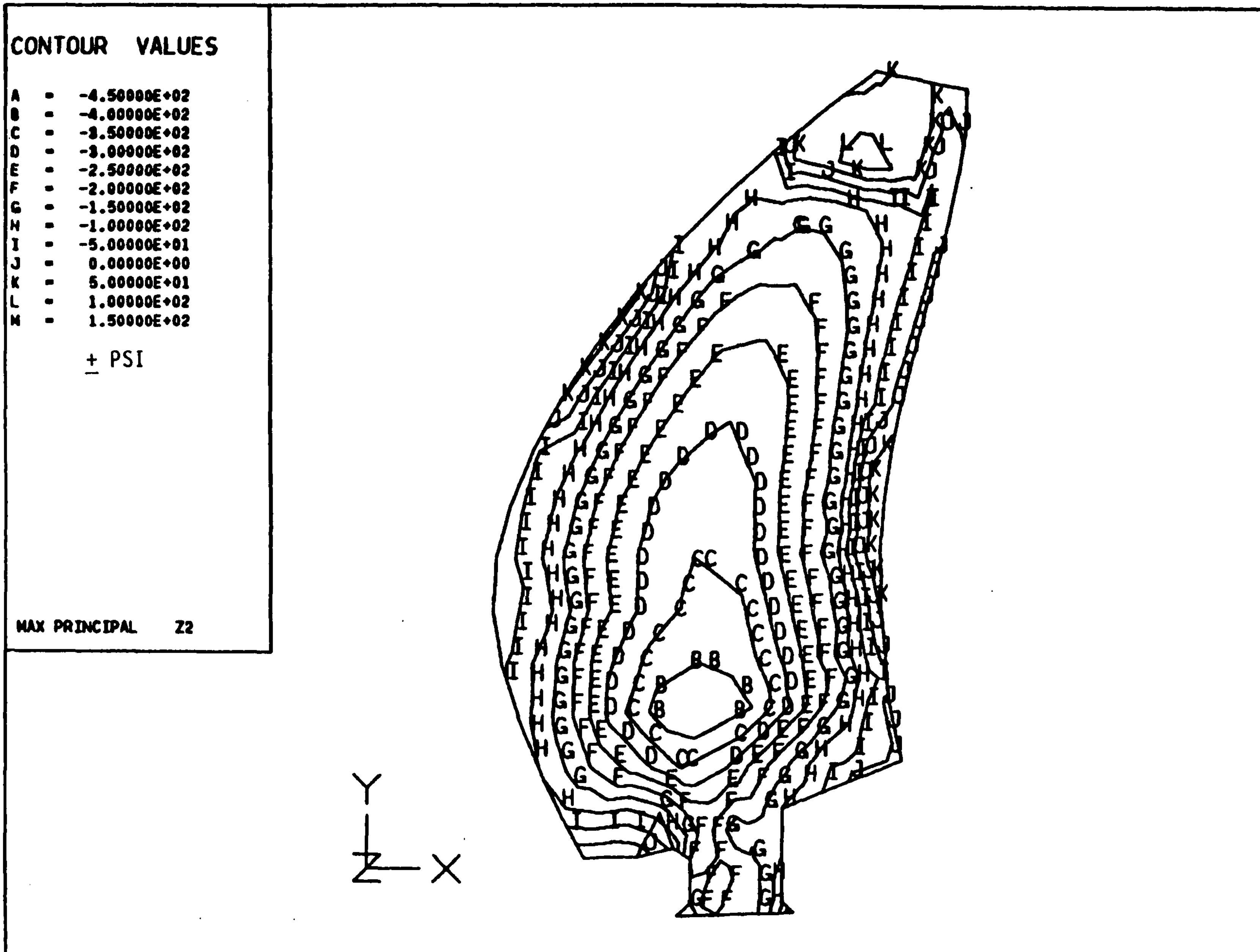

FIGURE 35. SR-3 MID INLET TEST 35.2: PREDICTED 1P STRESS CONTOURS

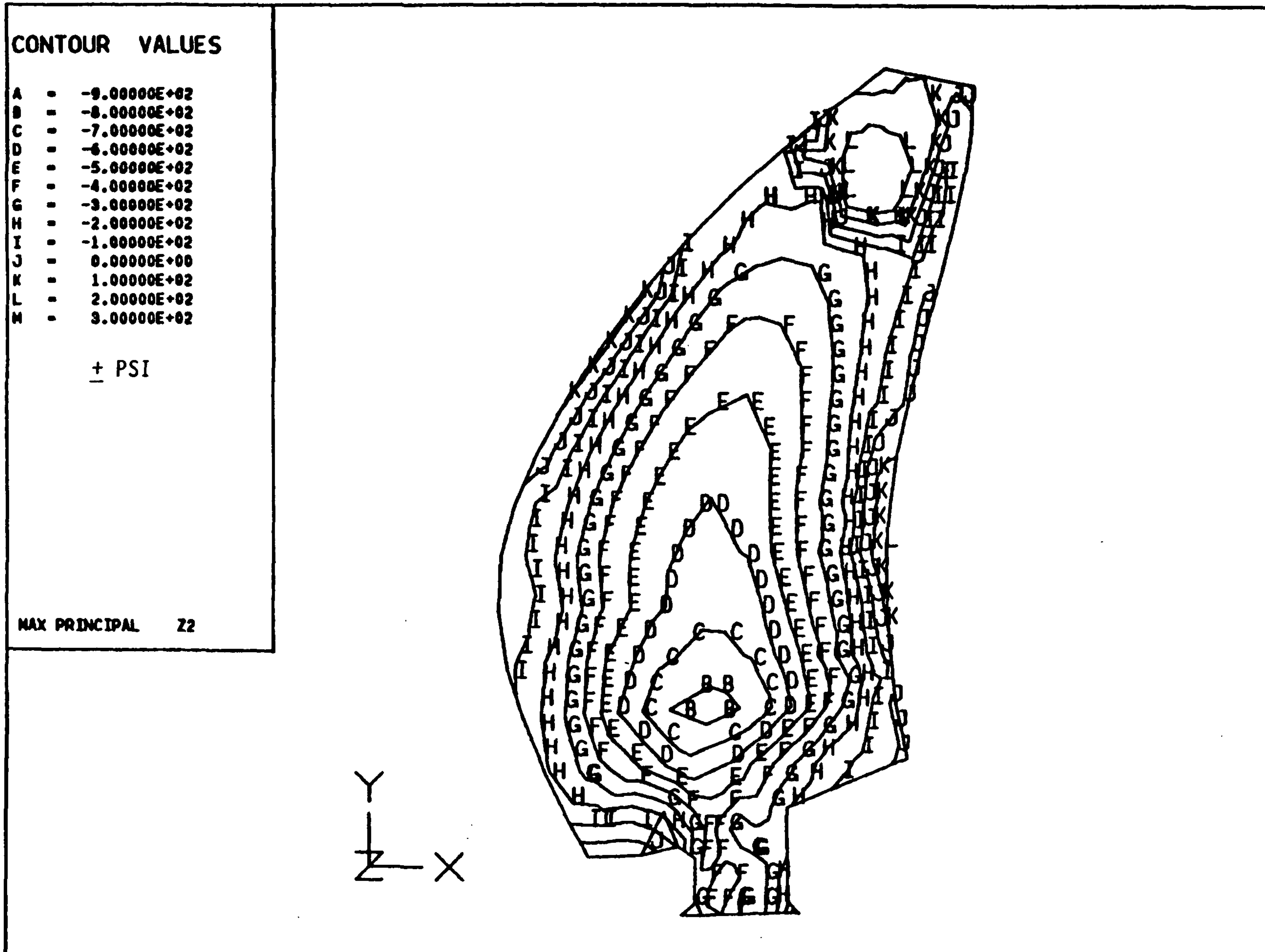

FIGURE 36. SR-3 MID INLET TEST 37.2: PREDICTED 1P STRESS CONTOURS

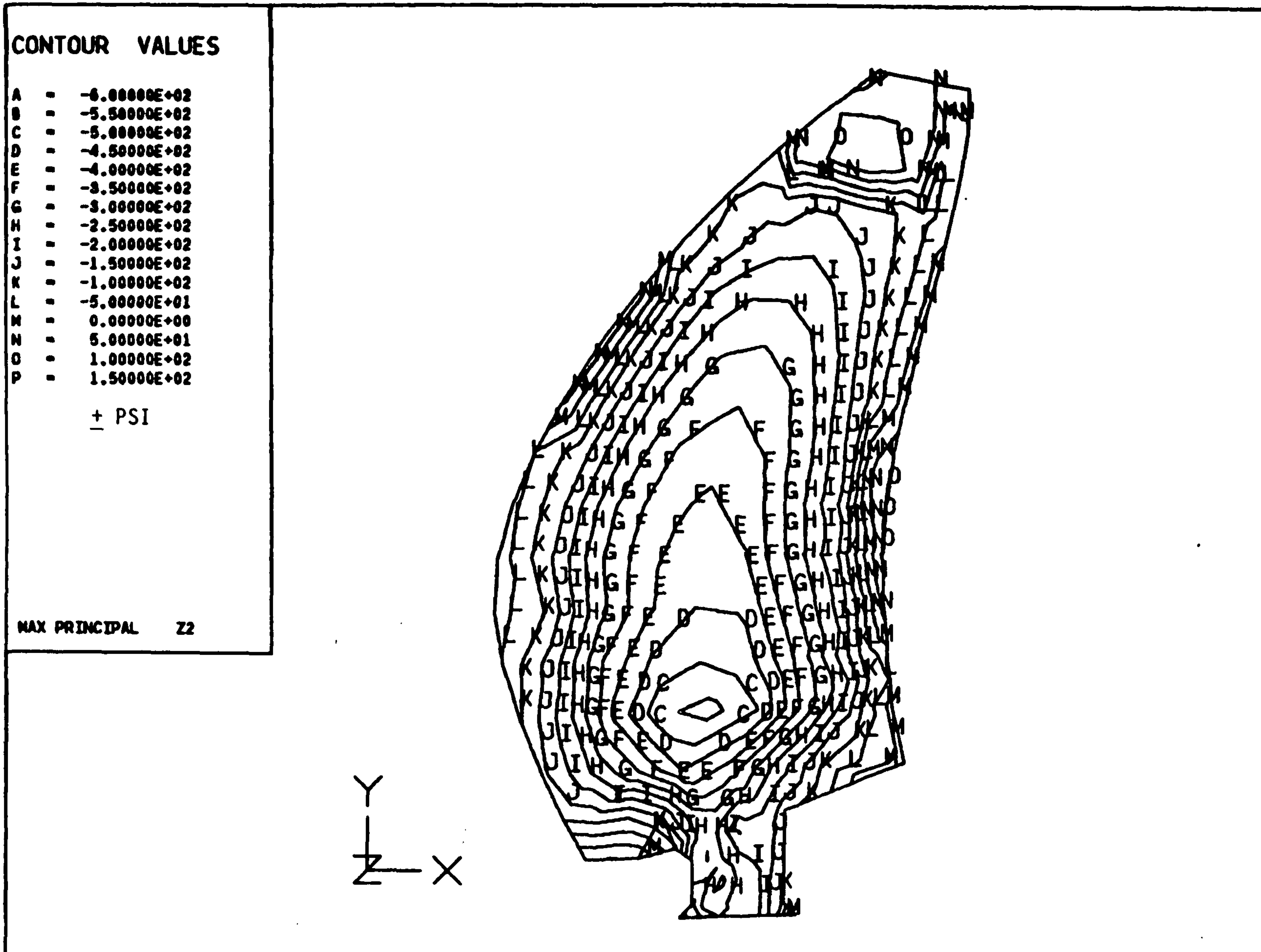

FIGURE 37. SR-3 FWD INLET TEST 10.2: PREDICTED 1P STRESS CONTOURS

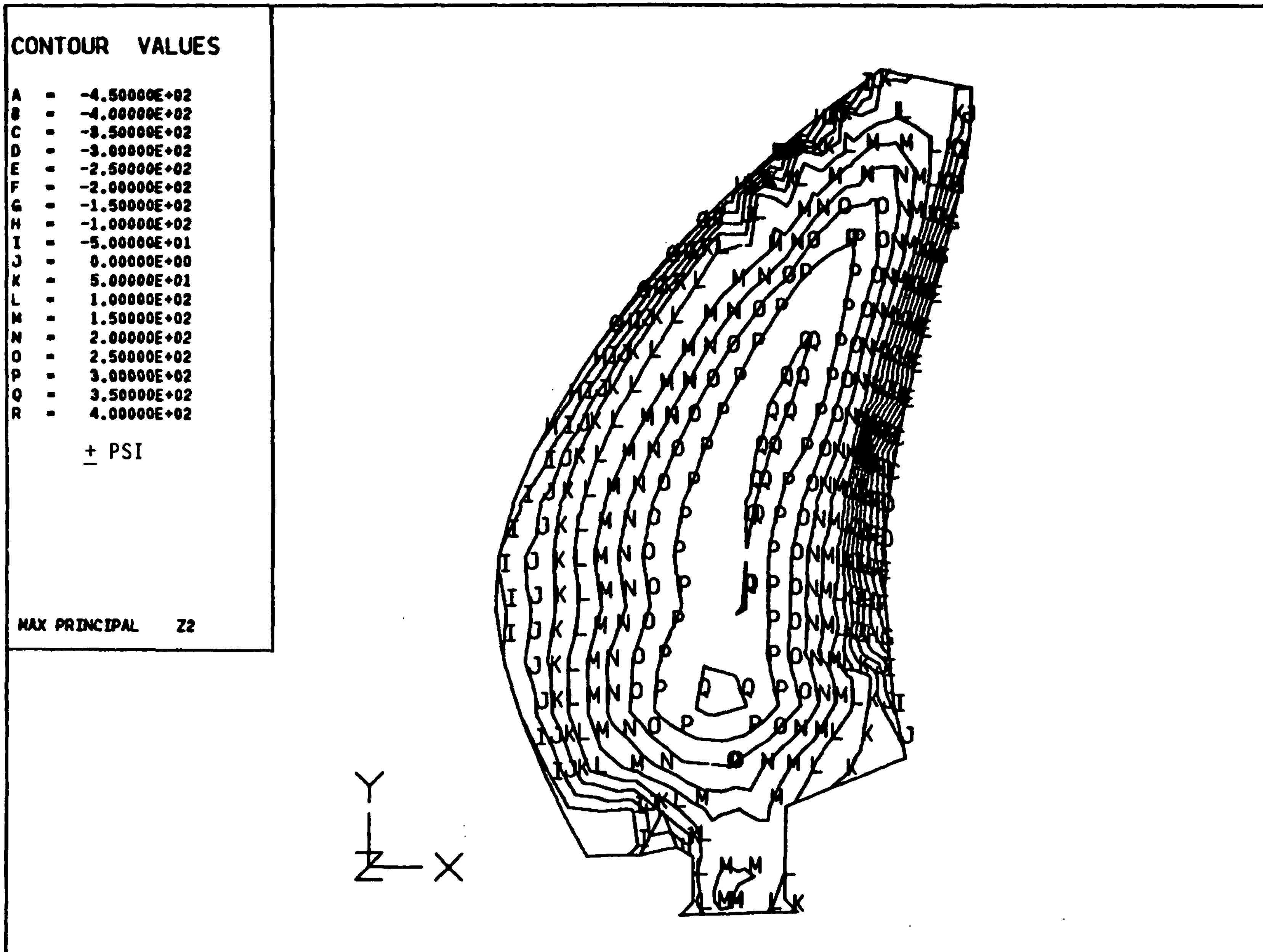

FIGURE 38. SR-3 MID INLET TEST 35.2: PREDICTED 2P STRESS CONTOURS

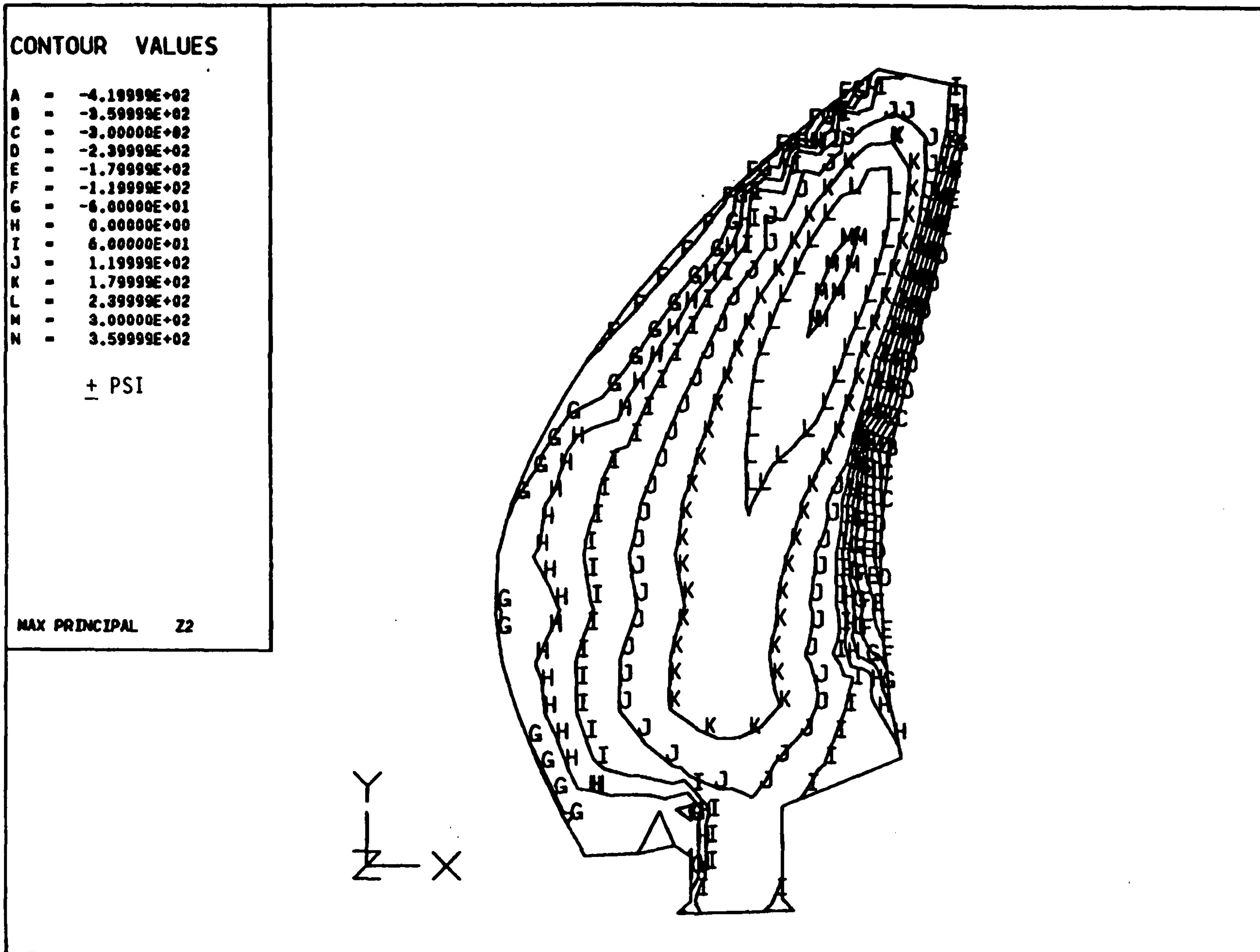

FIGURE 39. SR-3 MID INLET TEST 37.2: PREDICTED 2P STRESS CONTOURS

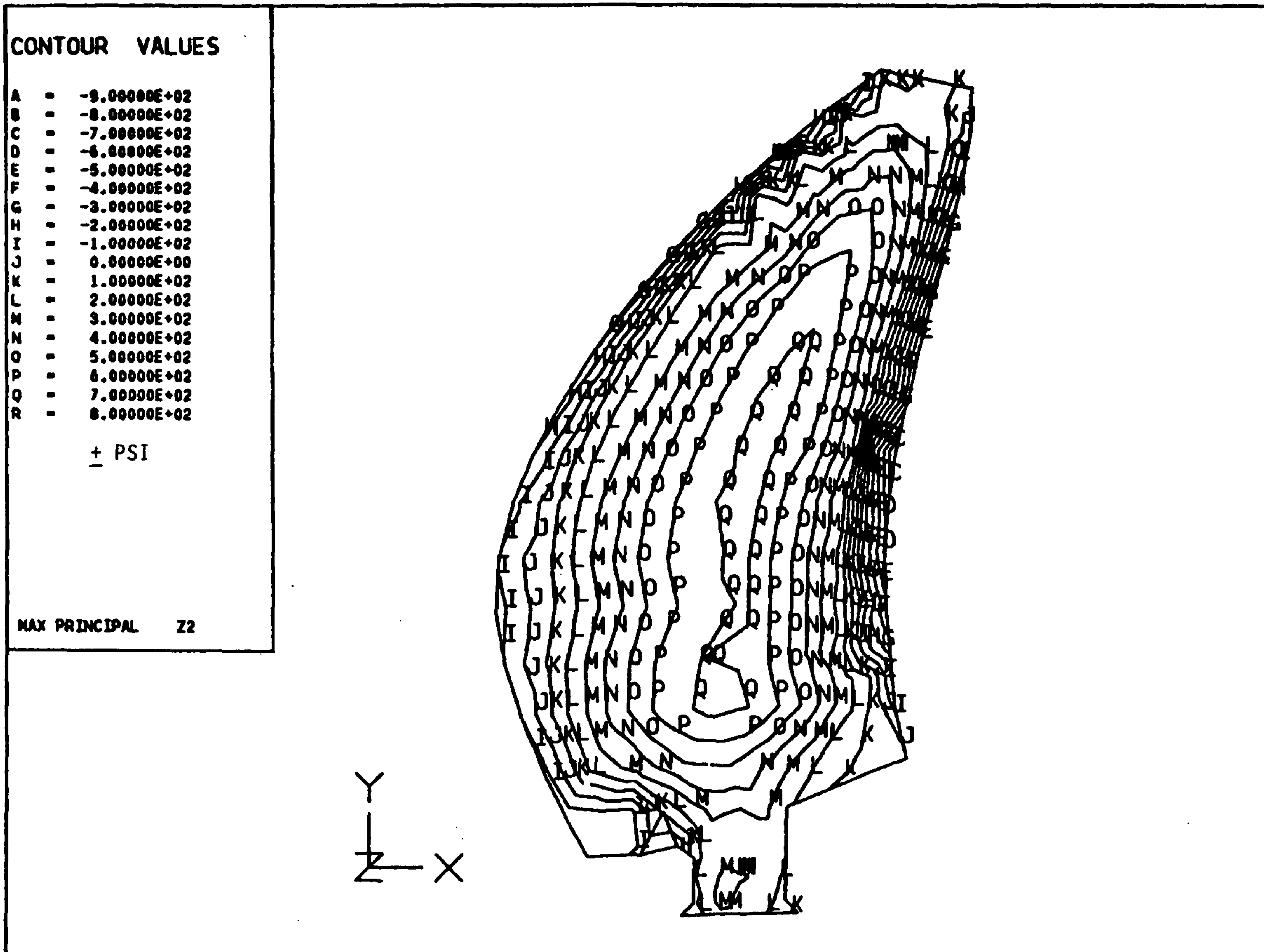

FIGURE 40. SR-3 FWD INLET TEST 10.2: PREDICTED 2P STRESS CONTOURS

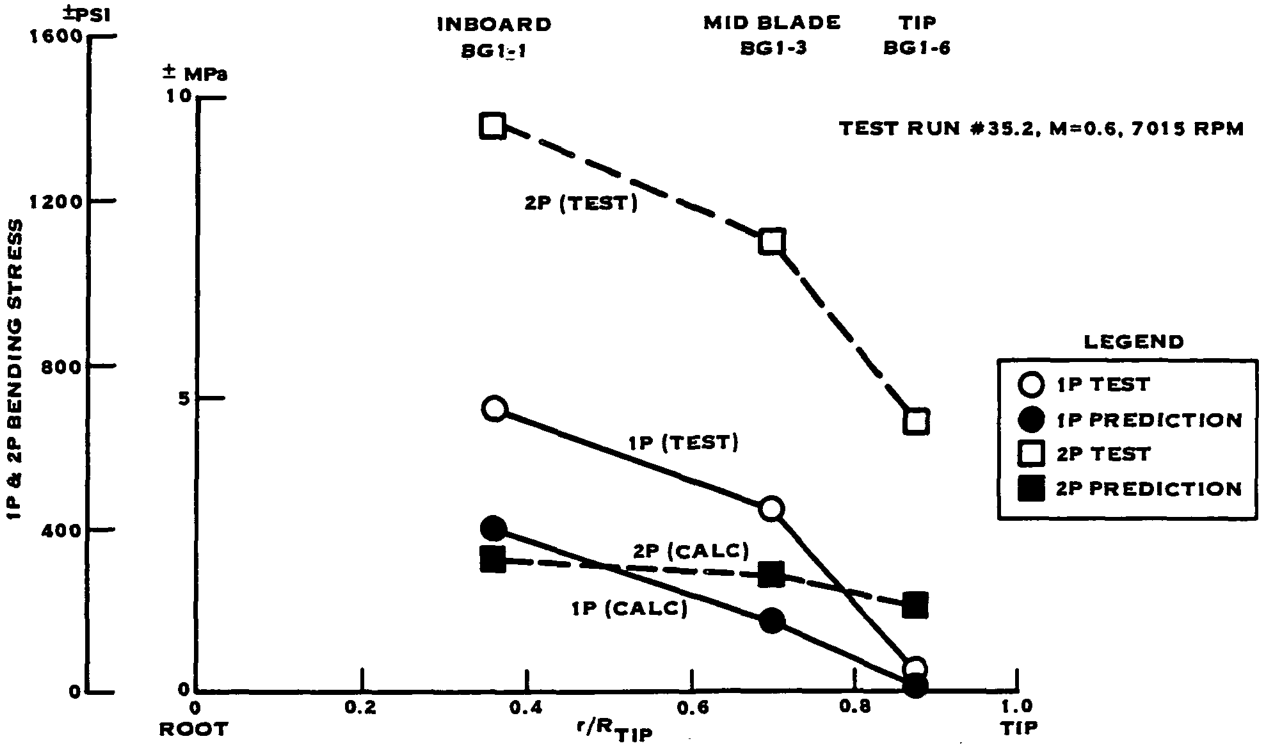

FIGURE 41. TEST VS. PREDICTED BENDING STRESSES FOR SINGLE SCOOP MID INLET

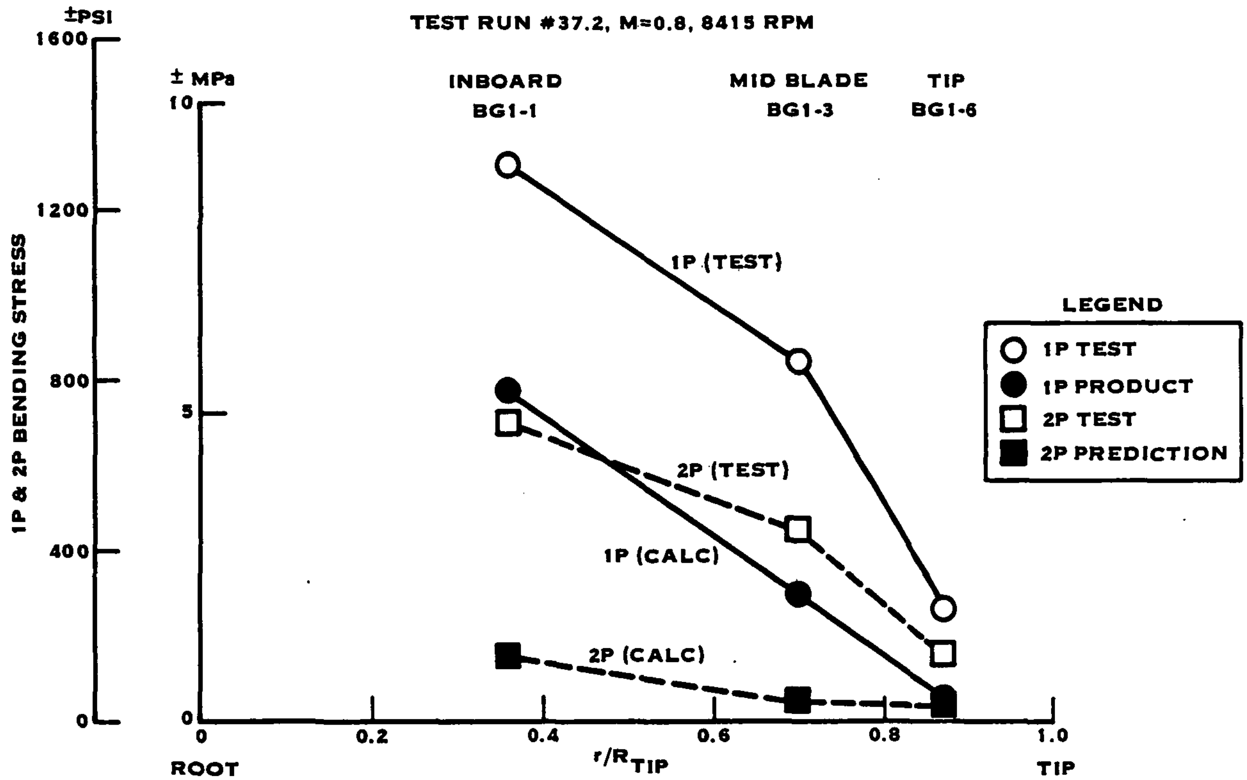

FIGURE 42. TESTED VS. PREDICTED BENDING STRESSES FOR SINGLE SCOOP MID INLET

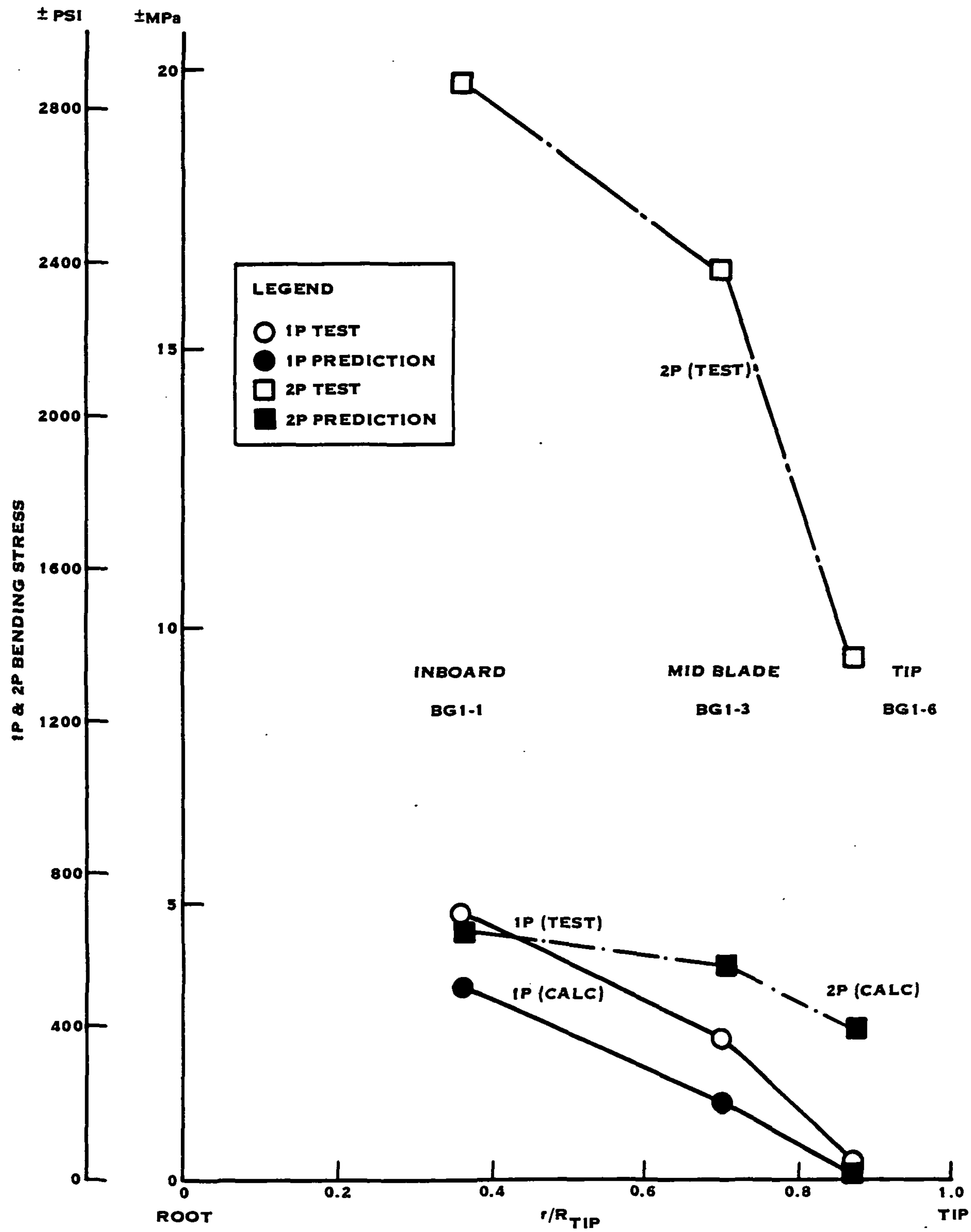

FIGURE 43. TESTED VS. PREDICTED BENDING STRESSES FOR SINGLE SCOOP FORWARD INLET.

APPENDIX

The appendix includes the operating conditions (table A-I), the total vibratory stresses (table A-II) and the P-order stresses (tables A-III to A-VII) for all the test points.

The data tables contain zero entries that indicate that no test data were available for those test points.

The tables are organized as follows:

Table No.	Title
A-I	Operating Conditions: SR-3 Inlet Tests
A-II	Total Vibratory Stresses ($\bar{X} + 2\sigma$): SR-3 Inlet Tests
A-III	P-Order Stresses: Single Scoop Forward Inlet
A-IV	P-Order Stresses: Single Scoop Mid-Inlet
A-V	P-Order Stresses: Twin Scoop Forward Inlet
A-VI	P-Order Stresses: Annular Forward Inlet
A-VII	P-Order Stresses: No-Inlet

TABLE A-I. OPERATING CONDITIONS FOR SR-3 INLET TESTS AT UTRC WIND TUNNEL

Run No.	MACH. No. (M)	BLADE ANGLE (deg)	PROP SPEED (rpm)	SHAFT HORSE power (shp)	POWER COEFF (cp)	FREE STREAM PARAMETERS V ft/sec	RHO $\frac{lbs\text{-}sec^2}{ft^4}$	P (psf)	t F^o
6.3	.41	57.8	5698	301.4	2.46693	447.3	.00217	1876.9	61.71
6.4	.41	57.8	5499	263.7	2.40261	446.7	.00217	1877.7	62.19
6.5	.40	57.8	5303	230.7	2.34153	441.6	.00217	1883.1	62.61
6.6	.40	57.8	5101	198.5	2.26451	441.2	.00217	1883.9	63.06
7.2	.61	57.8	6900	378.1	1.96206	664.3	.00193	1640.8	73.71
7.3	.60	57.8	6701	328.9	1.87251	663.1	.00192	1645.2	77.49
7.4	.61	57.8	6506	277.3	1.73873	668.9	.00190	1640.5	80.72
8.1	.71	57.8	5331	-5.542	-.06852	777.9	.00175	1506.5	91.83
8.2	.71	57.8	7645	403.1	1.70473	779.7	.00174	1509.6	97.58
8.3	.71	57.8	7449	350.8	1.60788	780.5	.00173	1509.9	99.04
8.4	.71	57.8	7252	300.4	1.49786	783.8	.00173	1506.7	100.27
9.1	.81	57.8	6205	-9.198	-.07931	886.3	.00159	1372.6	107.90
9.2	.81	57.8	8560	437.6	1.47270	896.3	.00155	1373.7	122.00
9.3	.81	57.8	8454	425.0	1.45478	889.3	.00159	1369.6	109.22
9.4	.81	57.8	8278	382.5	1.39293	888.5	.00159	1369.9	108.56
9.5	.81	57.8	8050	330.1	1.30413	886.9	.00159	1371.3	107.80
10.1	.61	57.8	4369	-5.232	-.10290	653.2	.00200	1661.7	59.96
10.2	.61	57.8	6802	363.8	1.92559	659.9	.00197	1659.6	67.66
10.3	.60	57.8	6609	302.0	1.78854	664.0	.00192	1666.8	83.08
10.4	.61	57.8	6403	249.1	1.63187	672.7	.00191	1656.4	83.84
11.1	.71	57.8	5304	-8.544	-.10596	777.1	.00177	1524.3	91.63
11.2	.71	57.8	7596	390.2	1.66663	783.5	.00175	1521.1	97.10
11.3	.71	57.8	7403	344.0	1.58980	781.1	.00175	1526.8	99.52
11.4	.71	57.8	7201	285.6	1.44137	784.2	.00174	1524.6	101.69
11.5	.81	57.8	6258	-14.56	-.12219	894.0	.00159	1381.7	111.71
11.6	.80	57.8	8413	424.3	1.46763	888.2	.00159	1395.3	116.43
12.1	.81	57.8	8397	446.3	1.52025	882.8	.00163	1386.7	101.85
12.2	.81	57.8	8204	396.6	1.45266	884.2	.00162	1386.8	103.48
12.3	.81	57.8	8009	338.5	1.33653	887.5	.00162	1382.3	103.83
13.1	.61	59.0	4264	-3.895	-.08440	665.4	.00195	1660.3	72.62
13.2	.60	59.0	6670	363.6	2.08244	664.8	.00193	1667.4	80.48
13.3	.61	59.0	6480	312.6	1.96706	669.1	.00192	1664.3	83.53

TABLE A-I.

RUN	M	β	rpm	SHP	Cp	V	ρ	P	t
13.4	.61	59.0	6273	263.3	1.83542	672.5	.00191	1661.6	85.67
14.1	.71	59.0	5041	-5.623	-.08103	776.9	.00178	1527.5	91.45
14.2	.71	59.0	7297	379.5	1.82250	779.3	.00176	1530.4	97.98
14.3	.71	59.0	7096	321.0	1.69154	784.9	.00174	1526.9	102.22
14.4	.71	59.0	6907	278.0	1.59366	784.3	.00174	1530.2	104.86
14.5	.71	59.0	7307	364.1	1.77262	787.4	.00173	1528.5	107.38
15.1	.81	59.0	5906	-9.573	-.09486	890.5	.00161	1386.2	108.74
15.2	.81	59.0	8073	411.4	1.60700	891.8	.00160	1389.0	113.43
15.3	.81	59.0	7870	363.1	1.52496	890.2	.00160	1388.7	111.19
15.4	.81	59.0	7670	316.4	1.43421	888.6	.00160	1391.2	111.40
16.1	.61	59.0	4311	-3.448	-.07355	669.8	.00192	1663.2	82.42
16.2	.61	59.0	6701	358.3	2.05386	673.5	.00190	1662.4	87.28
16.3	.61	59.0	6511	313.9	1.96511	671.5	.00190	1666.5	89.18
16.4	.61	59.0	6308	262.4	1.81428	677.2	.00189	1660.1	90.21
17.1	.71	59.0	5110	-4.167	-.05811	782.4	.00176	1523.5	94.63
17.2	.71	59.0	7280	379.7	1.83134	778.4	.00176	1531.4	96.92
17.3	.71	59.0	7087	330.8	1.73325	779.0	.00176	1531.8	98.14
17.4	.71	59.0	6885	280.1	1.60827	784.2	.00175	1525.6	99.31
18.1	.81	59.0	5864	-6.184	-.06212	885.0	.00162	1390.3	105.48
18.2	.81	59.0	8037	412.2	1.61572	888.4	.00161	1387.7	107.50
18.3	.81	59.0	7835	368.8	1.55942	886.1	.00161	1392.3	108.60
18.4	.81	59.0	7640	317.2	1.44831	885.9	.00161	1391.4	109.38
19.1	.61	59.0	4327	-2.891	-.06044	666.4	.00194	1669.0	79.31
19.2	.61	59.0	6688	367.3	2.09378	669.4	.00192	1667.5	82.59
19.3	.61	59.0	6486	315.9	1.98432	671.5	.00191	1667.0	85.11
19.4	.61	59.0	6280	267.4	1.85443	673.3	.00191	1665.4	86.14
20.1	.71	59.0	5149	-4.170	-.05671	780.4	.00177	1530.6	95.76
20.2	.71	59.0	7351	396.1	1.85974	782.0	.00176	1531.1	98.38
20.3	.71	59.0	7149	338.9	1.73755	784.5	.00175	1529.5	100.46
20.4	.71	59.0	6946	289.4	1.62368	785.4	.00174	1530.9	102.97
21.1	.80	59.0	5978	-5.983	-.05711	887.4	.00161	1396.6	111.59
21.2	.81	59.0	8176	428.5	1.61536	893.5	.00159	1393.5	116.72
21.3	.81	59.0	7962	367.4	1.50998	897.6	.00158	1391.0	119.73
21.4	.81	59.0	7770	321.2	1.42288	896.7	.00158	1394.2	121.71
22.1	.61	58.0	4597	-2.582	-.04593	675.3	.00190	1663.4	88.72
22.2	.61	58.0	6970	379.2	1.95377	676.1	.00188	1666.8	94.79
22.3	.60	58.0	6774	333.3	1.87518	674.7	.00188	1670.3	96.86
22.4	.61	58.0	6567	282.0	1.74808	678.0	.00187	1667.2	98.31
23.1	.71	58.0	5471	-2.889	-.03328	778.6	.00174	1524.3	102.73
23.2	.71	58.0	7653	410.5	1.72604	785.8	.00174	1528.8	103.44
23.3	.71	58.0	7456	355.9	1.62266	788.1	.00174	1526.3	104.33
23.4	.71	58.0	7256	310.2	1.53370	786.4	.00174	1529.0	104.69
24.1	.81	58.0	6325	-3.800	-.03058	891.1	.00161	1387.2	109.40
24.2	.81	58.0	8453	453.7	1.53358	885.6	.00161	1398.5	112.55
24.3	.81	58.0	8277	391.0	1.41470	891.2	.00160	1391.3	113.25
24.4	.81	58.0	8072	340.9	1.32699	892.0	.00160	1387.9	111.09
25.1	.61	58.0	4502	-3.859	-.07237	667.5	.00192	1644.9	77.43
25.2	.61	58.0	6837	357.7	1.91585	664.8	.00192	1649.2	78.49

TABLE A-I.

RUN	M	β	rpm	SHP	Cp	V	ρ	P	t
25.3	.61	58.0	6645	304.4	1.78577	671.1	.00191	1642.0	79.73
25.4	.61	58.0	6431	259.3	1.68142	670.9	.00190	1643.3	81.16
26.1	.71	58.0	5302	-5.215	-.06485	775.6	.00177	1509.6	87.21
26.2	.71	58.0	7538	391.4	1.70308	776.9	.00176	1511.2	90.81
26.3	.71	58.0	7334	338.3	1.60369	777.4	.00176	1512.3	92.74
27.1	.80	58.0	6117	-7.904	-.07050	881.8	.00161	1379.8	105.30
27.2	.81	58.0	8308	409.8	1.47306	887.2	.00159	1377.1	109.87
27.3	.81	58.0	8105	351.4	1.36850	892.2	.00158	1372.0	111.75
27.4	.81	58.0	7902	305.9	1.28875	893.0	.00158	1372.4	113.31
28.1	.61	59.2	4293	-3.574	-.07837	672.2	.00189	1641.5	83.62
28.2	.60	59.2	6669	356.3	2.08866	667.3	.00189	1649.9	86.81
28.3	.61	59.2	6484	307.0	1.97105	674.0	.00187	1642.7	88.75
28.4	.61	59.2	6280	256.0	1.81753	679.3	.00187	1636.6	89.75
29.1	.71	59.2	5085	-4.622	-.06618	780.6	.00174	1508.4	95.39
29.2	.71	59.2	7341	383.3	1.84070	782.5	.00173	1510.9	100.99
30.1	.71	59.2	5061	-5.154	-.07512	777.1	.00174	1490.6	90.54
30.2	.71	59.2	7383	389.8	1.85229	783.5	.00172	1487.4	96.48
30.3	.71	59.2	7181	340.0	1.75893	783.0	.00171	1489.6	98.18
30.4	.71	59.2	6983	293.0	1.65053	782.3	.00171	1491.8	99.52
31.1	.81	59.2	5877	-7.309	-.07516	887.6	.00157	1357.1	108.89
31.2	.81	59.2	8104	428.6	1.67264	885.2	.00158	1357.3	106.25
31.3	.80	59.2	7902	384.2	1.61304	882.1	.00158	1361.0	105.78
31.4	.81	59.2	7695	330.2	1.50252	883.6	.00158	1358.5	105.55
32.1	.61	59.2	4313	-3.719	-.08141	669.8	.00187	1624.1	84.21
32.2	.60	59.2	6748	360.0	2.07378	669.4	.00185	1629.0	89.69
32.3	.61	59.2	6556	307.0	1.94061	676.8	.00184	1620.7	91.16
32.4	.61	59.2	6354	264.7	1.84022	676.6	.00184	1621.5	91.91
33.1	.71	59.2	5086	-5.042	-.07322	779.2	.00172	1493.5	97.58
33.2	.71	59.2	7380	385.2	1.84418	781.7	.00171	1493.8	101.62
33.3	.71	59.2	7181	328.4	1.71818	787.9	.00169	1487.4	103.71
33.4	.71	59.2	6980	282.8	1.61263	787.9	.00169	1488.5	104.75
34.1	.81	59.2	5867	-7.387	-.07666	887.9	.00157	1359.2	111.85
34.2	.80	59.2	8153	430.2	1.67508	888.5	.00156	1363.9	117.12
34.3	.81	59.2	7960	365.1	1.54013	896.4	.00154	1355.0	119.04
34.4	.81	59.2	7763	325.3	1.48017	895.3	.00154	1358.0	120.48
35.1	.61	58.3	4542	-3.840	-.07350	678.6	.00183	1620.1	94.66
35.2	.61	58.3	7015	376.0	1.96345	677.1	.00182	1624.8	98.70
35.3	.61	58.3	6797	314.6	1.81500	684.2	.00181	1616.7	99.50
38.1	.53	58.2	4365	-2.946	-.05627	584.7	.00207	1764.3	66.61
38.2	.61	58.2	4420	-3.270	-.06427	666.4	.00193	1672.8	81.45
38.3	.60	58.2	6863	368.4	1.95291	668.6	.00191	1673.6	86.82
38.4	.61	58.2	6861	364.1	1.93933	671.1	.00191	1671.8	88.43
38.5	.60	58.2	6859	363.1	1.93789	670.6	.00191	1672.8	89.33
38.6	.60	58.2	6856	362.2	1.93706	670.9	.00190	1672.8	89.73

TABLE A-I.

RUN	M	β	rpm	SHP	Cp	V	ρ	P	t
40.1	.61	58.2	6924	400.3	2.03730	668.4	.00194	1662.5	76.31
40.2	.61	58.2	6922	392.0	2.01121	672.3	.00193	1660.1	79.64
40.3	.61	58.2	6921	392.1	2.01615	670.8	.00192	1663.5	81.37
40.4	.61	58.2	6917	388.5	2.00877	671.5	.00192	1664.5	83.60
40.5	.61	58.2	6720	377.6	1.90758	671.8	.00191	1665.4	84.99
40.6	.61	58.2	6716	335.0	1.90088	673.3	.00191	1664.5	86.30
40.7	.61	58.2	6716	333.8	1.89778	673.3	.00190	1665.4	87.54
40.8	.61	58.2	6528	291.8	1.80656	670.7	.00191	1669.4	88.40
40.9	.61	58.2	6525	291.9	1.81282	671.2	.00190	1669.5	89.46
40.10	.60	58.2	6526	291.8	1.81540	671.0	.00190	1670.8	90.72
41.1	.71	58.2	5258	-3.443	-.04388	779.6	.00177	1529.3	94.29
41.2	.71	58.2	7623	431.3	1.81055	782.4	.00176	1534.2	97.49
41.3	.71	58.2	7623	424.6	1.79156	781.5	.00176	1532.3	99.81
41.4	.71	58.2	7617	415.3	1.76714	784.9	.00174	1530.6	102.75
41.5	.71	58.2	7601	410.7	1.76217	784.4	.00174	1532.9	104.35
41.6	.71	58.2	7431	363.2	1.67055	785.1	.00174	1533.1	105.48
41.7	.71	58.2	7428	361.1	1.66867	787.8	.00173	1530.8	106.83
41.8	.71	58.2	7431	359.3	1.66190	788.6	.00173	1530.9	108.18
41.9	.71	58.2	7230	311.9	1.56658	786.8	.00173	1534.0	108.87
41.10	.70	58.2	7229	312.9	1.57220	785.5	.00173	1536.4	109.57
41.11	.71	58.2	7233	308.8	1.55584	789.7	.00172	1531.9	110.84
42.1	.81	58.2	6139	-3.870	-.03388	885.0	.00162	1396.1	107.56
42.2	.81	58.2	8505	478.6	1.59590	890.3	.00160	1396.1	115.04
42.3	.81	58.2	8460	472.7	1.59190	888.8	.00161	1393.1	110.54
42.4	.81	58.2	8444	471.9	1.59761	888.8	.00161	1392.7	110.23
42.5	.81	58.2	8250	412.6	1.49914	889.5	.00161	1392.0	110.47
42.6	.81	58.2	8252	412.2	1.49764	890.7	.00161	1390.3	110.41
42.7	.81	58.2	8252	411.6	1.49562	890.9	.00161	1389.6	110.17
42.8	.81	58.2	8058	364.8	1.42193	889.3	.00161	1392.2	110.30
42.9	.81	58.2	8058	367.4	1.42972	887.4	.00161	1394.6	110.04
42.10	.81	58.2	8059	367.8	1.42973	886.6	.00161	1396.1	110.18
43.1	.81	59.1	5842	-3.628	-.03699	889.3	.00161	1391.9	108.64
43.2	.81	59.1	8141	458.5	1.74911	892.2	.00159	1397.4	117.30
43.3	.80	59.1	8134	451.5	1.73753	893.6	.00158	1400.5	121.94
43.4	.80	59.1	8159	443.7	1.71288	895.9	.00158	1400.0	124.56
43.5	.81	59.1	7939	395.8	1.63451	896.2	.00159	1391.7	117.79
43.6	.81	59.1	7938	396.9	1.63037	895.9	.00160	1387.4	113.41
43.7	.81	59.1	7925	400.7	1.64793	892.6	.00160	1391.0	112.29
43.8	.81	59.1	7747	359.7	1.57920	890.1	.00161	1393.6	111.44
43.9	.81	59.1	7747	364.2	1.59369	887.6	.00161	1396.3	110.43
43.10	.81	59.1	7743	363.0	1.58895	888.0	.00161	1394.2	109.12

TABLE A-I.

RUN	M	θ	rpm	SHP	Cp	V	ρ	P	t
44.1	.71	59.1	4887	-3.440	-.05161	759.6	.00187	1530.5	64.32
44.2	.70	59.1	7177	409.7	1.95028	756.4	.00186	1540.0	69.24
44.3	.71	59.1	7181	401.8	1.92647	763.6	.00185	1532.6	72.10
44.4	.71	59.1	7184	398.1	1.91495	764.2	.00184	1534.8	75.02
44.5	.71	59.1	7183	395.5	1.90879	764.3	.00183	1537.0	77.26
44.6	.71	59.1	6985	340.5	1.79325	766.0	.00183	1536.0	78.71
44.7	.71	59.1	6986	337.2	1.78365	768.9	.00182	1534.2	81.02
44.8	.71	59.1	6988	334.9	1.77567	770.6	.00181	1533.1	82.23
44.9	.70	59.1	6773	287.0	1.67408	767.8	.00181	1540.2	85.72
44.10	.71	59.1	6775	277.4	1.62930	775.3	.00180	1531.0	86.88
45.1	.61	59.1	4236	-3.384	-.07149	670.0	.00192	1671.2	85.46
45.2	.60	59.1	6669	361.8	2.08494	667.3	.00192	1675.1	85.74
45.3	.61	59.1	6663	358.4	2.07453	670.6	.00192	1671.1	86.00
45.4	.61	59.1	6660	355.9	2.06292	670.9	.00192	1670.6	85.89
45.5	.61	59.1	6461	305.6	1.94462	673.7	.00191	1667.3	86.34
45.6	.61	59.1	6459	307.0	1.95449	672.5	.00191	1668.8	86.27
45.7	.61	59.1	6459	307.0	1.95325	672.0	.00191	1669.6	86.25
45.8	.61	59.1	6281	270.2	1.86896	670.1	.00191	1672.6	86.77
45.9	.61	59.1	6281	269.8	1.86783	670.4	.00191	1672.3	87.21
45.10	.61	59.1	6281	268.3	1.86022	671.9	.00191	1671.0	87.71
215.1	.61	59.0	4212	-2.878	-.06380	655.7	.00198	1641.1	58.81
215.2	.61	59.0	6632	370.5	2.12340	656.1	.00196	1645.1	64.62
215.3	.60	59.0	6432	320.4	2.02071	656.1	.00196	1647.0	66.98
215.4	.61	59.0	6234	270.8	1.88680	660.8	.00194	1642.6	69.09
216.1	.71	59.0	5007	-3.290	-.04778	765.8	.00180	1511.0	78.33
216.2	.71	59.0	7258	403.4	1.87063	776.7	.00178	1500.3	82.72
216.3	.71	59.0	7145	355.6	1.80082	772.1	.00178	1508.9	85.01
216.4	.71	59.0	6954	305.5	1.68387	772.9	.00177	1510.0	87.17
217.1	.81	59.0	5794	-4.690	-.04864	876.2	.00163	1375.8	97.08
217.2	.80	59.0	7964	431.3	1.70736	871.9	.00164	1376.8	92.52
217.3	.81	59.0	7758	371.9	1.59803	876.3	.00164	1370.6	92.66
217.4	.80	59.0	7565	327.8	1.51597	872.6	.00164	1376.7	93.19
218.1	.61	59.0	4311	-2.699	-.05721	664.7	.00193	1640.9	72.16
218.2	.61	59.0	6671	361.7	2.07330	663.9	.00193	1643.0	73.41
218.3	.61	59.0	6473	314.9	1.97751	663.3	.00193	1644.6	74.36
218.4	.61	59.0	6269	270.0	1.86760	662.9	.00193	1645.4	74.90
219.1	.71	59.0	5056	-2.991	-.04244	770.0	.00179	1507.9	80.69
219.2	.71	59.0	7277	388.1	1.85094	769.2	.00179	1511.5	82.96
219.3	.71	59.0	7082	340.8	1.76500	769.3	.00178	1511.9	83.51
219.4	.71	59.0	6878	289.5	1.64015	770.8	.00178	1510.7	84.41
220.1	.81	59.0	5777	-4.124	-.04258	870.8	.00165	1375.5	89.62
220.2	.80	59.0	7041	420.6	1.67061	871.4	.00164	1376.4	91.16
220.3	.80	59.0	7736	370.4	1.59697	870.1	.00164	1379.6	92.32
220.4	.80	59.0	7540	318.2	1.48619	872.8	.00164	1376.7	93.12
221.1	.61	58.1	4470	-2.425	-.04588	663.9	.00194	1639.8	69.12
221.2	.61	58.1	6856	376.1	1.97744	662.3	.00194	1643.9	71.50
221.3	.61	58.1	6660	325.8	1.87065	662.2	.00193	1644.6	72.26
221.4	.61	58.1	6455	279.3	1.76413	664.5	.00193	1641.8	72.54

TABLE A-I.

RUN	M	θ	rpm	SHP	Cp	V	ρ	P	t
222.1	.71	58.1	5253	-2.691	-.03394	769.7	.00180	1507.1	78.84
222.2	.71	58.1	7518	407.9	1.76131	770.2	.00179	1508.9	81.36
222.3	.71	58.1	7315	354.6	1.66454	770.1	.00179	1510.4	82.68
222.4	.71	58.1	7119	308.2	1.57067	769.8	.00178	1511.1	83.05
223.1	.81	58.1	6014	-3.779	-.03451	870.9	.00165	1374.0	88.14
223.2	.80	58.1	8210	441.9	1.58874	869.8	.00165	1378.0	90.19
223.3	.81	58.1	8001	380.5	1.48221	872.1	.00164	1375.7	91.09
223.4	.81	58.1	7801	333.8	1.40476	872.3	.00164	1376.3	91.83

ORIGINAL PAGE IS
OF POOR QUALITY

TABLE A-II. TOTAL VIBRATORY STRESSES ($\overline{X}+2\sigma$,±kPa): SR-3 INLET TESTS

RUN#	1-1	1-3	1-4	1-6	3-1	3-3	3-4	3-6
6.3	20404.	16180.	3645.	11846.	17505.	13914.	3193.	12109.
6.4	14458.	11382.	2758.	8776.	13578.	10717.	2703.	9694.
6.5	12086.	9326.	2299.	7347.	10932.	8498.	2256.	7872.
6.6	0.	0.	0.	0.	8798.	6711.	1849.	6593.
10.1	12431.	10552.	3081.	8492.	8806.	9404.	3648.	8449.
10.2	26156.	20480.	3106.	14761.	28426.	21808.	3490.	16929.
10.3	31729.	24668.	3483.	17303.	34439.	26801.	3740.	19527.
10.4	40413.	32163.	4005.	22976.	44936.	35576.	4376.	25086.
11.1	27118.	19821.	4686.	13756.	25615.	18690.	4575.	14518.
11.2	21473.	15515.	4675.	14597.	22132.	15475.	5775.	13559.
11.3	22407.	16267.	4713.	15534.	23581.	15994.	5100.	14739.
11.4	25612.	17919.	6203.	15880.	25061.	17745.	5584.	15390.
11.5	126506.	103374.	12750.	68103.	129348.	103323.	15741.	79369.
11.6	21922.	16869.	7536.	19229.	24007.	17134.	6745.	17539.
11.7	22891.	18378.	7426.	19029.	23987.	16990.	6171.	16030.
11.8	21469.	15653.	6344.	14783.	25344.	17654.	6271.	15705.
11.9	21915.	15967.	5999.	14341.	26193.	18685.	6376.	15103.
13.1	14289.	11604.	3327.	9180.	8638.	9307.	3168.	9119.
13.2	29888.	23965.	3275.	17324.	32245.	25011.	3510.	18553.
13.3	38646.	31245.	3776.	21273.	42420.	33722.	3882.	24949.
13.4	53194.	43152.	4540.	27455.	57622.	46762.	5300.	33370.
14.1	23482.	17003.	4058.	13266.	21628.	15234.	3924.	12758.
14.2	25678.	17567.	4732.	16638.	25565.	17553.	4733.	16766.
14.3	28396.	20116.	6034.	17463.	27317.	19319.	4861.	16791.
14.4	30022.	22760.	6577.	17425.	30160.	22309.	5836.	19504.
14.5	24739.	17735.	4804.	18105.	24616.	17137.	4650.	15776.
15.1	128416.	100754.	12952.	59346.	90270.	69213.	11337.	47320.
15.2	23975.	17038.	6223.	15966.	26474.	18755.	6354.	17807.
15.3	26814.	19975.	6144.	17517.	25583.	17692.	5811.	15863.
15.4	27930.	20606.	5544.	17402.	26012.	17840.	5617.	15508.
16.1	12401.	10327.	3755.	8795.	9462.	9232.	3462.	10134.
16.2	26604.	21102.	2974.	14857.	28686.	21414.	3162.	16960.
16.2.1	33283.	26679.	3193.	17857.	28686.	21414.	3162.	16960.
16.3	47435.	37666.	3978.	23516.	50949.	40580.	4478.	29049.
17.1	21906.	15892.	3875.	12053.	20347.	14931.	3797.	12601.
17.2	23394.	16593.	4394.	16103.	23704.	16286.	4295.	15490.
17.3	26301.	18643.	5572.	16938.	25437.	18259.	4556.	16078.
17.4	29017.	21257.	5662.	16683.	29108.	20967.	5120.	18293.
18.1	91778.	71646.	9971.	43602.	66638.	51694.	9402.	35745.
18.2	22051.	15334.	5475.	13871.	23432.	16797.	5270.	15944.
18.3	23973.	18359.	5444.	15216.	22251.	15809.	5118.	14378.
18.4	25007.	18275.	5104.	15629.	23189.	15937.	4926.	14535.
19.1	6595.	6189.	2073.	6123.	6158.	5473.	2339.	5838.
19.2	6994.	5835.	2396.	6361.	7168.	6369.	2227.	6810.
19.3	7088.	6587.	2087.	6813.	7584.	6885.	1851.	5759.
19.4	9036.	7839.	1887.	7586.	10171.	9047.	2161.	8715.
20.1	6414.	5690.	2182.	6326.	5844.	5427.	2232.	6212.
20.2	5818.	5905.	3228.	8395.	5858.	6017.	3586.	7006.
20.3	6788.	6380.	5504.	8876.	5795.	5691.	4187.	6970.
20.4	6736.	5912.	5051.	7564.	5849.	6118.	3868.	7128.

NOTE: ZERO-VALUE ENTRIES INDICATE ABSENCE OF DATA

ORIGINAL PAGE IS
OF POOR QUALITY

TABLE A-II. TOTAL VIBRATORY STRESSES ($\overline{X}+2\sigma$,±kPa): SR-3 INLET TESTS

RUN#	1-1	1-3	1-4	1-6	3-1	3-3	3-4	3-6
21-1	15475.	13769.	3545.	13360.	9735.	9208.	3803.	10300.
21-2	6237.	7052.	3078.	9954.	6083.	7129.	3234.	9239.
21-3	5658.	7285.	3081.	10141.	6121.	7169.	3256.	9285.
21-4	6007.	6832.	3754.	9109.	5805.	6716.	3013.	7756.
22-1	5064.	5765.	2690.	7671.	5515.	5886.	2504.	6241.
22-2	5963.	5347.	3186.	6889.	7068.	7120.	3229.	6452.
22-3	6408.	5759.	2484.	6206.	7294.	7049.	2679.	7282.
22-4	7230.	6292.	2076.	5988.	7560.	7279.	2385.	6943.
23-1	6194.	6026.	2169.	6340.	5843.	5840.	2457.	6476.
23-2	0.	0.	0.	0.	6554.	7907.	3498.	8668.
23-4	6133.	6848.	5167.	8344.	7095.	7492.	3948.	7050.
24-2	7280.	11403.	4550.	15597.	6679.	9213.	3157.	11893.
24-3	5678.	7418.	3539.	11296.	5958.	7500.	2944.	10159.
24-4	4754.	5792.	3005.	8860.	5605.	7602.	3206.	10336.
25-1	0.	0.	0.	0.	7074.	7067.	3294.	7305.
25-2	16713.	12735.	2963.	9890.	18237.	14174.	2949.	11156.
25-3	19488.	15138.	3186.	10846.	21456.	16511.	2920.	12814.
25-4	24857.	19756.	3155.	14602.	27222.	21170.	3093.	14858.
26-1	14820.	11749.	3198.	8782.	12835.	10871.	3337.	9078.
26-2	13614.	10268.	4239.	9365.	14571.	10418.	4464.	10713.
26-3	14665.	10723.	4672.	11456.	14902.	10846.	4517.	10301.
26-4	15822.	12580.	6254.	11876.	16091.	11135.	4661.	10481.
27-1	76511.	58795.	8794.	41909.	49322.	40658.	7257.	29388.
27-2	13400.	11175.	4202.	10071.	13295.	10631.	4007.	10383.
27-3	13259.	10330.	4138.	9563.	14006.	11737.	4182.	11516.
27-4	13696.	10662.	3879.	9368.	14598.	11540.	3872.	10601.
28-1	9584.	7687.	2570.	7485.	17297.	14365.	3176.	9381.
28-2	18968.	14470.	2573.	10504.	21093.	16367.	3226.	12380.
28-3	23594.	18151.	2851.	12966.	26411.	20768.	3556.	14931.
28-4	32218.	25139.	3215.	16990.	36998.	29260.	4462.	20370.
29-1	14613.	11862.	3059.	9109.	13839.	11569.	3598.	9667.
30-1	14729.	12371.	3504.	9036.	0.	0.	0.	0.
30-2	14633.	11461.	4717.	9619.	0.	0.	0.	0.
30-3	15917.	13159.	5679.	11617.	0.	0.	0.	0.
30-4	16191.	13977.	4956.	10459.	0.	0.	0.	0.
31-1	56107.	45455.	6850.	27176.	0.	0.	0.	0.
31-2	12857.	10327.	4343.	9062.	0.	0.	0.	0.
31-3	13582.	11838.	4163.	9850.	0.	0.	0.	0.
31-4	14738.	12741.	4024.	8883.	0.	0.	0.	0.
32-2	17135.	13929.	2860.	9558.	0.	0.	0.	0.
32-3	21270.	17432.	2897.	11727.	0.	0.	0.	0.
32-4	28672.	23319.	3073.	15310.	0.	0.	0.	0.
33-2	15629.	12252.	4584.	11703.	0.	0.	0.	0.
33-3	17099.	14164.	5961.	12553.	0.	0.	0.	0.
33-4	17413.	15243.	5564.	10875.	0.	0.	0.	0.
34-1	62829.	50723.	7424.	29725.	0.	0.	0.	0.
34-2	14086.	10970.	4419.	9964.	0.	0.	0.	0.
34-3	14797.	11756.	4742.	9686.	0.	0.	0.	0.
34-4	15866.	13113.	4452.	9721.	0.	0.	0.	0.
35-1	9993.	9037.	3904.	8549.	0.	0.	0.	0.

NOTE: ZERO-VALUE ENTRIES INDICATE ABSENCE OF DATA

TABLE A-II: TOTAL VIBRATORY STRESSES ($\overline{X}+2\sigma$,±kPa): SR-3 INLET TESTS

RUN#	1-1	1-3	1-4	1-6	3-1	3-3	3-4	3-6
35.2	14593.	11258.	3691.	9651.	0.	0.	0.	0.
35.3	16442.	13173.	3237.	9583.	0.	0.	0.	0.
36.1	19270.	15477.	2864.	10638.	0.	0.	0.	0.
36.2	17412.	14346.	3415.	9531.	0.	0.	0.	0.
36.5	15116.	11343.	4709.	10917.	0.	0.	0.	0.
37.2	14376.	13336.	4694.	11847.	0.	0.	0.	0.
37.3	14186.	11489.	4368.	10203.	0.	0.	0.	0.
37.4	14186.	11593.	4556.	9330.	0.	0.	0.	0.
38.1	14553.	11618.	4204.	8759.	14407.	12527.	4828.	9762.
40.1	0.	0.	0.	0.	32064.	27807.	4292.	20742.
40.2	0.	0.	0.	0.	21757.	19328.	3571.	14260.
40.3	0.	0.	0.	0.	23121.	20178.	3633.	14604.
40.4	0.	0.	0.	0.	24709.	21491.	3560.	16046.
40.5	0.	0.	0.	0.	30618.	25828.	3546.	19350.
40.6	0.	0.	0.	0.	28215.	23837.	3341.	18078.
40.7	0.	0.	0.	0.	25408.	21794.	3149.	16672.
40.8	0.	0.	0.	0.	33192.	27668.	3304.	19624.
40.9	0.	0.	0.	0.	36162.	30126.	3557.	21736.
40.10	0.	0.	0.	0.	39083.	32646.	3910.	23726.
41.1	0.	0.	0.	0.	31649.	24257.	5708.	18250.
41.2	0.	0.	0.	0.	24379.	22513.	5364.	17216.
41.3	0.	0.	0.	0.	17138.	15357.	4721.	12591.
41.4	0.	0.	0.	0.	18351.	16589.	4923.	13525.
41.5	0.	0.	0.	0.	19999.	17863.	5159.	15060.
41.6	0.	0.	0.	0.	20849.	19094.	4778.	14529.
41.7	0.	0.	0.	0.	19036.	17567.	4683.	13550.
41.8	0.	0.	0.	0.	17674.	16181.	4615.	12507.
41.9	0.	0.	0.	0.	19549.	17793.	4550.	12967.
41.10	0.	0.	0.	0.	21248.	19116.	4588.	14409.
41.11	0.	0.	0.	0.	22987.	20528.	4701.	15258.
42.1	0.	0.	0.	0.	187258.	161219.	19524.	100238.
42.2	0.	0.	0.	0.	15698.	14867.	4287.	14300.
42.3	0.	0.	0.	0.	17377.	15905.	4296.	14529.
42.4	0.	0.	0.	0.	19095.	17618.	4587.	15458.
42.5	0.	0.	0.	0.	20823.	18442.	4627.	16491.
42.6	0.	0.	0.	0.	19094.	17116.	4290.	15518.
42.7	0.	0.	0.	0.	17687.	15723.	4077.	14660.
42.8	0.	0.	0.	0.	18120.	16050.	4189.	14384.
42.9	0.	0.	0.	0.	20078.	17826.	4532.	15446.
42.10	0.	0.	0.	0.	21806.	19639.	4880.	16570.
43.1	0.	0.	0.	0.	70514.	55166.	7851.	37076.
43.2	0.	0.	0.	0.	18536.	16588.	3966.	15459.
43.3	0.	0.	0.	0.	20486.	18282.	4202.	16798.
43.4	0.	0.	0.	0.	22077.	19466.	4354.	17770.
43.5	0.	0.	0.	0.	23231.	20701.	4477.	17169.
43.6	0.	0.	0.	0.	21727.	19512.	4049.	16318.
43.7	0.	0.	0.	0.	19882.	17875.	3694.	15124.
43.8	0.	0.	0.	0.	19293.	17286.	4072.	14905.
43.9	0.	0.	0.	0.	21045.	18862.	4369.	16052.
43.10	0.	0.	0.	0.	23047.	20751.	4639.	17604.

NOTE: ZERO-VALUE ENTRIES INDICATE ABSENCE OF DATA

TABLE A-II. TOTAL VIBRATORY STRESSES ($\bar{X}+2\sigma$,±kPa): SR-3 INLET TESTS

RUN#	1-1	1-3	1-4	1-6	3-1	3-3	3-4	3-6
44.1	0.	0.	0.	0.	25261.	20131.	4952.	17150.
44.2	0.	0.	0.	0.	33711.	28810.	5229.	20977.
44.3	0.	0.	0.	0.	22505.	19537.	4744.	13819.
44.4	0.	0.	0.	0.	24065.	21018.	4983.	14627.
44.5	0.	0.	0.	0.	26194.	22398.	4941.	15519.
44.6	0.	0.	0.	0.	30560.	26677.	4468.	19525.
44.7	0.	0.	0.	0.	28342.	24876.	4546.	18161.
44.8	0.	0.	0.	0.	25633.	22622.	4621.	16221.
44.9	0.	0.	0.	0.	31901.	26338.	3970.	20366.
44.10	0.	0.	0.	0.	34033.	28294.	4244.	21062.
44.11	0.	0.	0.	0.	37899.	31291.	4412.	23881.
45.1	0.	0.	0.	0.	11500.	9068.	3889.	7609.
45.2	0.	0.	0.	0.	32375.	27099.	3424.	20808.
45.3	0.	0.	0.	0.	30022.	25256.	3409.	19276.
46.4	0.	0.	0.	0.	27640.	23174.	3314.	17823.
46.5	0.	0.	0.	0.	37467.	30731.	3125.	22242.
46.6	0.	0.	0.	0.	41355.	33878.	3431.	24519.
46.7	0.	0.	0.	0.	44814.	36785.	3757.	26768.
46.8	0.	0.	0.	0.	59109.	49112.	4920.	34619.
46.9	0.	0.	0.	0.	54769.	45413.	4640.	31721.
46.10	0.	0.	0.	0.	48619.	40230.	4225.	27975.
215.1	5287.	5573.	1850.	5983.	4444.	4833.	2104.	5821.
215.2	10163.	8680.	2047.	7431.	9432.	8184.	2434.	7088.
215.3	13534.	11622.	2194.	8753.	11735.	10522.	2482.	9481.
215.4	17207.	14482.	2864.	13811.	15245.	12873.	3137.	11887.
216.1	6056.	6272.	2193.	6627.	6440.	6240.	2413.	6468.
216.2	6757.	6785.	4100.	7167.	6943.	7254.	4006.	8529.
216.3	6966.	6542.	5825.	6958.	7840.	8005.	3854.	9143.
216.4	6835.	7426.	4166.	10525.	7805.	7226.	3834.	8005.
217.1	11276.	9948.	3124.	9723.	14149.	11646.	3316.	9915.
217.2	6291.	6394.	2544.	10395.	5923.	6626.	3441.	10446.
217.3	6093.	6742.	2699.	7874.	6343.	6033.	2758.	7495.
217.4	6036.	5893.	2804.	6626.	0.	0.	0.	0.
218.1	4898.	5644.	2455.	8088.	6254.	6247.	2627.	5881.
218.2	9644.	8148.	2383.	10007.	8950.	7405.	2448.	6426.
218.3	12661.	10757.	2001.	8511.	10853.	9384.	2599.	8012.
218.4	16431.	14281.	2836.	19503.	13714.	11701.	2868.	10260.
219.1	6841.	6409.	2308.	4991.	6936.	6240.	2379.	6530.
219.2	7194.	6671.	4590.	6325.	8426.	8246.	3510.	8598.
219.3	7241.	6972.	5863.	9960.	8564.	8205.	3737.	9067.
219.4	8035.	7330.	3501.	10903.	8695.	7585.	3682.	7653.
220.1	11510.	10162.	3002.	9465.	15162.	12252.	3110.	10611.
220.2	6858.	6688.	2647.	9087.	6785.	6288.	3365.	8336.
220.3	6469.	6652.	2702.	4988.	6888.	6619.	2965.	7343.
220.4	6622.	6189.	2949.	7514.	7247.	7074.	3310.	7109.
221.1	5414.	6215.	4040.	6939.	6716.	6861.	3192.	7054.
221.2	8663.	7468.	2493.	8832.	7709.	6481.	2289.	6716.
221.3	9629.	8249.	2306.	6460.	8143.	7102.	1944.	6888.
221.4	12661.	10965.	2003.	6545.	9515.	8653.	2103.	8895.
222.1	6397.	6298.	2083.	4308.	6516.	5875.	2227.	6212.

NOTE: ZERO-VALUE ENTRIES INDICATE ABSENCE OF DATA

TABLE A-II. TOTAL VIBRATORY STRESSES ($\overline{X}+2\sigma$, ±kPa): SR-3 INLET TESTS

RUN#	1-1	1-3	1-4	1-6	3-1	3-3	3-4	3-6
2222	7246.	7456.	3068.	4070.	6178.	6557.	3089.	8550.
2223	7006.	6780.	4002.	5534.	6399.	7274.	2992.	8377.
2224	7407.	7124.	5748.	8031.	7557.	8233.	2965.	8922.
2231	16278.	13738.	3153.	10832.	24208.	20009.	3799.	15093.
2232	7190.	7147.	2445.	8969.	5288.	5895.	2503.	7716.
2233	6915.	6598.	2624.	8362.	5288.	5868.	2434.	7702.
2234	6915.	6955.	2928.	8023.	5647.	6495.	2544.	7667.

NOTE: ZERO-VALUE ENTRIES INDICATE ABSENCE OF DATA

TABLE A-III: P-ORDER STRESSES (±kPa), SINGLE SCOOP FORWARD INLET

RUN NO.	INLET TYPE	INLET POS.	MASS FLOW RATIO	BLADE ANGLE DEG	POWER COEFF	PROP SPEED RPM	MACH NO.	BLADE GAGE	P ORDER COMPONENTS 1	2	3	4	5	6
63	SINGLE	FWD	0.97	57.80	2.467	5696.	0.403	BG1-1	2845.	15882.	537.	432.	229.	183.
								BG1-3	1643.	12154.	974.	873.	219.	210.
								BG1-4	595.	998.	0.	0.	0.	0.
								BG1-6	596.	6569.	924.	1031.	0.	182.
								BG3-1	2228.	13752.	256.	504.	268.	180.
								BG3-3	899.	10389.	929.	721.	216.	206.
								BG3-4	253.	922.	0.	0.	0.	0.
								BG3-6	1016.	6428.	830.	918.	180.	182.
64	SINGLE	FWD	0.97	57.80	2.403	5499.	0.403	BG1-1	2673.	9198.	561.	455.	248.	0.
								BG1-3	1550.	6920.	1006.	470.	271.	0.
								BG1-4	537.	624.	0.	0.	0.	0.
								BG1-6	561.	3681.	968.	585.	236.	0.
								BG3-1	2130.	8822.	321.	411.	265.	0.
								BG3-3	916.	6575.	883.	673.	263.	0.
								BG3-4	268.	632.	0.	0.	0.	0.
								BG3-6	979.	3982.	732.	833.	262.	0.
65	SINGLE	FWD	0.97	57.80	2.342	5302.	0.403	BG1-1	2322.	8281.	613.	445.	263.	0.
								BG1-3	1380.	6183.	1039.	365.	281.	0.
								BG1-4	456.	580.	0.	0.	0.	0.
								BG1-6	364.	3219.	938.	422.	261.	0.
								BG3-1	1979.	7709.	322.	332.	259.	0.
								BG3-3	950.	5748.	803.	648.	254.	0.
								BG3-4	276.	575.	0.	0.	0.	0.
								BG3-6	805.	3424.	625.	777.	260.	0.
66	SINGLE	FWD	0.97	57.80	2.265	5101.	0.403	BG3-1	2203.	5943.	432.	242.	190.	0.
								BG3-3	1180.	4338.	853.	505.	267.	0.
								BG3-4	367.	446.	0.	0.	0.	0.
								BG3-6	715.	2503.	598.	574.	355.	0.
101	SINGLE	FWD	0.81	57.80	-0.103	4365.	0.600	BG1-1	4096.	8683.	2591.	0.	0.	322.
								BG1-3	2249.	6956.	3092.	797.	283.	449.
								BG1-4	834.	996.	276.	0.	0.	186.
								BG1-6	1186.	3636.	2006.	765.	351.	618.
								BG3-1	4362.	2981.	3721.	184.	0.	546.
								BG3-3	2728.	2296.	4392.	645.	409.	654.
								BG3-4	1134.	585.	395.	0.	0.	0.
								BO3-6	911.	1277.	3385.	641.	466.	1106.
102	SINGLE	FWD	0.81	57.80	1.926	6801.	0.600	BG1-1	4778.	20065.	0.	945.	0.	420.
								BG1-3	2419.	16762.	1779.	802.	0.	324.
								BG1-4	803.	1026.	395.	381.	0.	701.
								BG1-6	344.	9710.	1686.	1485.	0.	922.
								BG3-1	5019.	22311.	242.	829.	225.	400.
								BG3-3	2616.	17712.	1430.	1566.	0.	290.
								BG3-4	1081.	1289.	412.	256.	0.	596.
								BG3-6	879.	11472.	1609.	2601.	0.	815.
103	SINGLE	FWD	0.81	57.80	1.789	6604.	0.600	BG1-1	4901.	24880.	298.	813.	0.	360.
								BG1-3	2435.	20551.	1581.	655.	0.	206.
								BG1-4	886.	1304.	429.	427.	0.	534.
								BG1-6	0.	11908.	1432.	1241.	194.	759.
								BG3-1	5512.	27412.	328.	573.	217.	339.
								BG3-3	2901.	21769.	1546.	1363.	0.	189.
								BG3-4	1277.	1544.	415.	313.	0.	509.
								BG3-6	900.	14048.	1739.	2189.	0.	1264.

NOTE: ZERO-VALUE ENTRIES INDICATE ABSENCE OF DATA

ORIGINAL PAGE IS
OF POOR QUALITY

TABLE A-III: P-ORDER STRESSES (±kPa), SINGLE SCOOP FORWARD INLET

RUN NO.	INLET TYPE	INLET POS.	MASS FLOW RATIO	BLADE ANGLE DEG	POWER COEFF	PROP SPEED RPM	MACH NO.	BLADE GAGE	P ORDER COMPONENTS 1	2	3	4	5	6
110	SINGLE	FWD	0.81	57.80	1.632	6412.	0.600	BG1-1	4752.	31958.	374.	1099.	0.	237.
								BG1-3	2437.	26255.	1598.	956.	0.	256.
								BG1-4	996.	1803.	396.	430.	0.	321.
								BG1-6	0.	15224.	1421.	1567.	229.	981.
								BG3-1	5243.	37358.	353.	1150.	176.	0.
								BG3-3	2753.	29649.	1503.	1943.	0.	210.
								BG3-4	1294.	2217.	393.	563.	0.	298.
								BG3-6	810.	19214.	1618.	3191.	251.	1192.
111	SINGLE	FWD	0.81	57.80	-0.106	5293.	0.700	BG1-1	5151.	20727.	1366.	409.	189.	320.
								BG1-3	2749.	15732.	2257.	1409.	196.	223.
								BG1-4	1012.	2288.	229.	258.	0.	246.
								BG1-6	1068.	8646.	1745.	1646.	392.	329.
								BG3-1	0.	19082.	1137.	570.	0.	280.
								BG3-3	0.	14282.	2026.	1373.	178.	197.
								BG3-4	0.	2282.	0.	195.	0.	285.
								BG3-6	0.	8784.	1785.	1714.	340.	351.
112	SINGLE	FWD	0.81	57.80	1.667	7592.	0.700	BG1-1	7508.	10932.	625.	699.	0.	626.
								BG1-3	3846.	9331.	3226.	0.	0.	342.
								BG1-4	1523.	1342.	854.	0.	446.	524.
								BG1-6	822.	5399.	3395.	291.	1540.	1286.
								BG3-1	7709.	11386.	492.	428.	0.	701.
								BG3-3	3916.	8955.	2045.	388.	234.	354.
								BG3-4	1935.	1466.	883.	503.	833.	539.
								BG3-6	1951.	5484.	2618.	455.	1862.	1278.
113	SINGLE	FWD	0.81	57.80	1.590	7405.	0.700	BG1-1	6262.	14269.	405.	912.	0.	696.
								BG1-3	3140.	12212.	2663.	316.	191.	394.
								BG1-4	1272.	1560.	631.	209.	654.	773.
								BG1-6	629.	7294.	2707.	851.	1702.	1435.
								BG3-1	6695.	14367.	419.	332.	0.	851.
								BG3-3	3395.	11405.	1848.	725.	0.	503.
								BG3-4	1696.	1623.	649.	430.	406.	951.
								BG3-6	1638.	7263.	2314.	787.	532.	1314.
114	SINGLE	FWD	0.81	57.80	1.441	7200.	0.700	BG1-1	7387.	15492.	464.	652.	0.	1356.
								BG1-3	3564.	13205.	2618.	402.	186.	1216.
								BG1-4	1455.	1466.	609.	0.	517.	2424.
								BG1-6	730.	7954.	2592.	497.	1018.	2492.
								BG3-1	7404.	16047.	376.	579.	281.	800.
								BG3-3	3795.	12769.	1743.	955.	186.	685.
								BG3-4	1860.	1547.	673.	274.	417.	1409.
								BG3-6	1675.	8258.	2058.	1323.	565.	1514.
115	SINGLE	FWD	0.81	57.80	-0.122	6221.	0.800	BG1-1	8715.	108740.	609.	3862.	468.	1034.
								BG1-3	4384.	86592.	2170.	7552.	471.	399.
								BG1-4	1894.	8037.	588.	1449.	0.	671.
								BG1-6	1231.	49054.	2101.	10611.	676.	4916.
								BG3-1	10352.	106827.	718.	8741.	445.	294.
								BG3-3	5696.	83208.	2247.	11862.	724.	611.
								BG3-4	2545.	8750.	309.	2884.	340.	1337.
								BG3-6	1799.	52134.	2566.	19340.	651.	6081.

NOTE: ZERO-VALUE ENTRIES INDICATE ABSENCE OF DATA

TABLE A-III: P-ORDER STRESSES (±kPa), SINGLE SCOOP FORWARD INLET

RUN NO.	INLET TYPE	INLET POS.	MASS FLOW RATIO	BLADE ANGLE DEG	POWER COEFF	PROP SPEED RPM	MACH NO.	BLADE GAGE	P ORDER COMPONENTS 1	2	3	4	5	6
116	SINGLE	FWD	0.81	57.80	1.468	8417.	0.800	BG1-1	12202.	6700.	3307.	665.	0.	624.
								BG1-3	5768.	5968.	6514.	402.	553.	411.
								BG1-4	2344.	1834.	2221.	416.	846.	0.
								BG1-6	1434.	3812.	8938.	494.	1049.	2372.
								BG3-1	11848.	9523.	2029.	366.	293.	636.
								BG3-3	5516.	8279.	3965.	832.	202.	545.
								BG3-4	2794.	1971.	1492.	623.	532.	173.
								BG3-6	2158.	5773.	5777.	864.	704.	3890.
117	SINGLE	FWD	0.81	57.80	0.000	8392.	0.800	BG1-1	12608.	7820.	3546.	583.	0.	560.
								BG1-3	6121.	7068.	6970.	352.	462.	398.
								BG1-4	2462.	2064.	2157.	371.	676.	230.
								BG1-6	1561.	4676.	9035.	260.	725.	2823.
								BG3-1	12119.	10703.	1341.	457.	0.	561.
								BG3-3	5683.	9344.	2688.	552.	295.	493.
								BG3-4	2958.	2182.	1172.	339.	336.	0.
								BG3-6	2513.	6624.	3818.	972.	412.	4082.
118	SINGLE	FWD	0.81	57.80	0.000	8208.	0.800	BG1-1	11945.	8465.	1759.	662.	0.	585.
								BG1-3	5781.	7445.	3820.	370.	378.	300.
								BG1-4	2312.	1923.	1350.	370.	636.	216.
								BG1-6	1465.	4779.	4729.	447.	776.	2317.
								BG3-1	11894.	11785.	1459.	371.	0.	614.
								BG3-3	5594.	10164.	2552.	659.	180.	362.
								BG3-4	2808.	2046.	1144.	596.	372.	0.
								BG3-6	2461.	7011.	3786.	908.	579.	3166.
119	SINGLE	FWD	0.81	57.80	0.000	8007.	0.800	BG3-1	10152.	13880.	1049.	419.	0.	546.
								BG3-3	4933.	12042.	1980.	673.	0.	323.
								BG3-4	2389.	2173.	990.	612.	223.	263.
								BG3-6	2184.	8227.	2887.	967.	316.	2404.
131	SINGLE	FWD	0.81	59.00	-0.084	4295.	0.600	BG1-1	0.	8371.	2939.	0.	267.	372.
								BG1-3	0.	6723.	3436.	747.	435.	420.
								BG1-4	0.	948.	253.	0.	0.	0.
								BG1-6	0.	3558.	2285.	658.	594.	661.
								BG3-1	0.	2006.	4016.	310.	201.	709.
								BG3-3	0.	1600.	4754.	670.	384.	721.
								BG3-4	0.	478.	478.	0.	0.	0.
								BG3-6	0.	885.	3442.	718.	499.	1280.
132	SINGLE	FWD	0.81	59.00	2.082	6676.	0.600	BG1-1	4837.	23578.	783.	717.	260.	226.
								BG1-3	2453.	19582.	2464.	493.	0.	375.
								BG1-4	905.	1006.	267.	345.	0.	517.
								BG1-6	495.	11559.	2512.	805.	0.	621.
								BG3-1	4674.	26495.	524.	349.	188.	221.
								BG3-3	1897.	21089.	2117.	970.	0.	389.
								BG3-4	769.	1270.	498.	259.	0.	534.
								BG3-6	1612.	13852.	2422.	1511.	211.	702.
133	SINGLE	FWD	0.81	59.00	1.967	6480.	0.600	BG1-1	4758.	30610.	953.	1522.	284.	248.
								BG1-3	2390.	25179.	2403.	1426.	0.	305.
								BG1-4	1041.	1484.	267.	590.	0.	354.
								BG1-6	598.	14773.	2394.	2350.	0.	501.
								BG3-1	4751.	34573.	559.	1049.	262.	198.
								BG3-3	1914.	27407.	2016.	2412.	0.	286.
								BG3-4	865.	1798.	457.	514.	0.	327.
								BG3-6	1585.	17825.	2255.	3799.	208.	769.

NOTE: ZERO-VALUE ENTRIES INDICATE ABSENCE OF DATA

TABLE A-III: P-ORDER STRESSES (±kPa), SINGLE SCOOP FORWARD INLET

RUN NO.	INLET TYPE	INLET POS.	MASS FLOW RATIO	BLADE ANGLE DEG	POWER COEFF	PROP SPEED RPM	MACH NO.	BLADE GAGE	P ORDER COMPONENTS 1	2	3	4	5	6
134	SINGLE	FWD	0.81	59.00	1.835	6273.	0.600	BG1-1	4715.	47304.	931.	1915.	247.	216.
								BG1-3	2323.	38563.	2142.	2489.	0.	324.
								BG1-4	1166.	2583.	307.	746.	0.	0.
								BG1-6	628.	22338.	2090.	3736.	221.	1591.
								BG3-1	4610.	52035.	401.	2102.	0.	320.
								BG3-3	1795.	41193.	1691.	4285.	0.	215.
								BG3-4	911.	3046.	399.	976.	0.	493.
								BG3-6	1556.	26585.	1876.	6643.	232.	2072.
141	SINGLE	FWD	0.81	59.00	-0.081	5063.	0.700	BG1-1	5531.	15211.	2011.	0.	400.	0.
								BG1-3	3062.	11397.	3089.	1277.	357.	287.
								BG1-4	1255.	1697.	272.	0.	0.	284.
								BG1-6	613.	6038.	2500.	1416.	531.	247.
								BG3-1	5394.	13328.	1604.	308.	580.	0.
								BG3-3	2759.	9929.	2693.	1048.	646.	269.
								BG3-4	1157.	1610.	191.	219.	0.	275.
								BG3-6	1562.	5886.	2347.	1270.	1015.	325.
142	SINGLE	FWD	0.81	59.00	1.823	7293.	0.700	BG1-1	7315.	14952.	180.	748.	503.	710.
								BG1-3	3549.	12634.	2967.	238.	386.	621.
								BG1-4	1704.	1222.	680.	221.	343.	1103.
								BG1-6	1523.	7852.	3299.	638.	1243.	1407.
								BG3-1	7303.	15491.	487.	288.	484.	564.
								BG3-3	3103.	12187.	2164.	754.	311.	424.
								BG3-4	1537.	1297.	738.	376.	370.	862.
								BG3-6	2459.	8069.	2762.	1265.	665.	1276.
143	SINGLE	FWD	0.81	59.00	1.692	7098.	0.700	BG1-1	6489.	18866.	327.	824.	528.	1092.
								BG1-3	3124.	15994.	2497.	388.	291.	922.
								BG1-4	1556.	1292.	604.	0.	236.	1942.
								BG1-6	1423.	9953.	2633.	757.	818.	1972.
								BG3-1	6278.	19725.	286.	617.	330.	685.
								BG3-3	2615.	15672.	2096.	1105.	425.	404.
								BG3-4	1343.	1411.	634.	233.	399.	1011.
								BG3-6	2052.	10490.	2488.	1841.	346.	1271.
144	SINGLE	FWD	0.81	59.00	1.594	6900.	0.700	BG1-1	6752.	20819.	472.	956.	535.	1084.
								BG1-3	3195.	17397.	2291.	269.	363.	1142.
								BG1-4	1663.	1296.	557.	230.	0.	2285.
								BG1-6	1389.	10719.	2513.	592.	425.	1655.
								BG3-1	6592.	21343.	399.	419.	413.	802.
								BG3-3	2586.	16920.	2025.	937.	403.	774.
								BG3-4	1406.	1394.	626.	313.	249.	1627.
								BG3-6	1963.	11353.	2516.	1725.	431.	1706.
145	SINGLE	FWD	0.81	59.00	1.773	7302.	0.700	BG1-1	7200.	15532.	0.	764.	605.	676.
								BG1-3	3461.	13134.	2521.	194.	375.	837.
								BG1-4	1729.	1280.	679.	182.	428.	1377.
								BG1-6	1523.	8316.	2738.	558.	1477.	1508.
								BG3-1	7310.	15778.	215.	259.	529.	653.
								BG3-3	3007.	12458.	2094.	725.	373.	530.
								BG3-4	1496.	1315.	654.	326.	497.	999.
								BG3-6	2474.	8360.	2612.	1317.	744.	1278.

NOTE: ZERO-VALUE ENTRIES INDICATE ABSENCE OF DATA

TABLE A-III: P-ORDER STRESSES (±kPa), SINGLE SCOOP FORWARD INLET

RUN NO.	INLET TYPE	INLET POS.	MASS FLOW RATIO	BLADE ANGLE DEG	POWER COEFF	PROP SPEED RPM	MACH NO.	BLADE GAGE	P ORDER COMPONENTS 1	2	3	4	5	6
151	SINGLE	FWD	0.81	59.00	-0.095	5889.	0.800	BG1-1	8637.	106994.	1358.	2627.	461.	440.
								BG1-3	4693.	83674.	2596.	4691.	262.	225.
								BG1-4	1839.	8933.	173.	662.	0.	715.
								BG1-6	1394.	46538.	2251.	6603.	382.	1620.
								BG3-1	8972.	68425.	1312.	2673.	0.	376.
								BG3-3	4458.	52800.	2713.	3457.	501.	0.
								BG3-4	1900.	6290.	301.	524.	241.	503.
								BG3-6	2393.	32780.	2919.	4916.	605.	626.
152	SINGLE	FWD	0.81	59.00	1.607	8066.	0.800	BG1-1	12213.	10773.	1551.	344.	345.	320.
								BG1-3	5749.	9304.	4082.	365.	503.	404.
								BG1-4	2773.	1824.	1573.	561.	666.	223.
								BG1-6	2561.	6595.	5384.	410.	1048.	1693.
								BG3-1	11944.	15260.	786.	0.	520.	421.
								BG3-3	5069.	12811.	2844.	0.	0.	402.
								BG3-4	2639.	2100.	1137.	523.	337.	262.
								BG3-6	3658.	9134.	3811.	702.	754.	2162.
153	SINGLE	FWD	0.81	59.00	1.525	7876.	0.800	BG1-1	10849.	13439.	1253.	408.	441.	381.
								BG1-3	5111.	12136.	3932.	419.	408.	386.
								BG1-4	2429.	1771.	1333.	451.	457.	355.
								BG1-6	2415.	8355.	4866.	187.	536.	1459.
								BG3-1	10055.	14806.	600.	207.	548.	470.
								BG3-3	4395.	12088.	2387.	193.	0.	365.
								BG3-4	2249.	2078.	1130.	491.	304.	386.
								BG3-6	3386.	8577.	3213.	747.	553.	1737.
154	SINGLE	FWD	0.81	59.00	1.434	7674.	0.800	BG1-1	10911.	14005.	777.	546.	351.	395.
								BG1-3	5118.	12441.	3297.	592.	280.	438.
								BG1-4	2395.	1539.	1121.	370.	297.	459.
								BG1-6	2367.	8236.	3962.	383.	391.	1180.
								BG3-1	10433.	13679.	580.	335.	346.	462.
								BG3-3	4663.	11102.	2378.	0.	183.	302.
								BG3-4	2285.	1740.	1047.	572.	0.	336.
								BG3-6	3413.	7845.	3151.	397.	1017.	1116.
161	SINGLE	FWD	0.97	59.00	-0.074	4310.	0.600	BG1-1	0.	8760.	2304.	0.	315.	221.
								BG1-3	0.	6751.	2749.	384.	188.	270.
								BG1-4	0.	1051.	298.	0.	0.	0.
								BG1-6	0.	3457.	1777.	499.	319.	325.
								BG3-1	0.	5198.	3208.	301.	0.	511.
								BG3-3	0.	4244.	3944.	904.	338.	590.
								BG3-4	0.	748.	283.	0.	0.	211.
								BG3-6	0.	2385.	2963.	743.	381.	1052.
162	SINGLE	FWD	0.97	59.00	2.054	6703.	0.600	BG1-1	3788.	28039.	651.	793.	327.	234.
								BG1-3	1672.	23038.	1730.	1093.	286.	242.
								BG1-4	815.	1268.	205.	263.	0.	302.
								BG1-6	750.	13510.	1463.	1645.	266.	505.
								BG3-1	3902.	31628.	577.	1075.	298.	248.
								BG3-3	1469.	25054.	1753.	1360.	286.	233.
								BG3-4	610.	1613.	349.	462.	0.	302.
								BG3-6	1405.	16258.	2056.	2296.	336.	554.

NOTE: ZERO-VALUE ENTRIES INDICATE ABSENCE OF DATA

TABLE A-III: P-ORDER STRESSES (±kPa), SINGLE SCOOP FORWARD INLET

RUN NO.	INLET TYPE	INLET POS.	MASS FLOW RATIO	BLADE ANGLE DEG	POWER COEFF	PROP SPEED RPM	MACH NO.	BLADE GAGE	P ORDER COMPONENTS 1	2	3	4	5	6
163	SINGLE	FWD	0.97	59.00	1.965	6308.	0.600	BG1-1	4126.	38336.	602.	1232.	342.	176.
								BG1-3	1698.	31246.	1632.	1487.	235.	229.
								BG1-4	991.	2016.	236.	448.	0.	0.
								BG1-6	914.	18065.	1338.	2320.	242.	1136.
								BG3-1	4226.	42688.	415.	1451.	254.	0.
								BG3-3	1659.	33811.	1385.	2687.	265.	0.
								BG3-4	717.	2442.	325.	696.	0.	333.
								BG3-6	1610.	21705.	1639.	4291.	373.	1544.
171	SINGLE	FWD	0.97	59.00	-0.058	5105.	0.700	BG1-1	4893.	15108.	1494.	209.	438.	223.
								BG1-3	2551.	11446.	2180.	843.	0.	367.
								BG1-4	1141.	1723.	186.	0.	0.	268.
								BG1-6	467.	6073.	1609.	996.	223.	338.
								BG3-1	5080.	13842.	1407.	0.	301.	194.
								BG3-3	2567.	10397.	2071.	1088.	484.	374.
								BG3-4	1011.	1695.	0.	0.	0.	292.
								BG3-6	1816.	6186.	1959.	1316.	810.	486.
172	SINGLE	FWD	0.97	59.00	1.831	7280.	0.700	BG1-1	5981.	14751.	430.	357.	292.	769.
								BG1-3	2685.	12495.	2381.	303.	244.	687.
								BG1-4	1407.	1147.	586.	0.	0.	1341.
								BG1-6	1557.	7698.	2346.	668.	297.	1683.
								BG3-1	6218.	15213.	427.	549.	283.	626.
								BG3-3	2781.	12076.	2116.	354.	303.	640.
								BG3-4	1189.	1229.	672.	263.	279.	1143.
								BG3-6	2323.	7989.	2783.	701.	332.	1352.
173	SINGLE	FWD	0.97	59.00	1.733	7087.	0.700	BG1-1	5736.	16926.	439.	296.	358.	948.
								BG1-3	2517.	14454.	2143.	493.	275.	1007.
								BG1-4	1354.	1119.	430.	0.	293.	2040.
								BG1-6	1566.	8943.	1917.	793.	289.	1777.
								BG3-1	5790.	17394.	499.	849.	287.	501.
								BG3-3	2706.	13946.	1950.	744.	389.	565.
								BG3-4	1153.	1204.	588.	0.	334.	1078.
								BG3-6	2150.	9277.	2348.	1239.	0.	1052.
174	SINGLE	FWD	0.97	59.00	1.608	6885.	0.700	BG1-1	5960.	21393.	573.	293.	271.	764.
								BG1-3	2445.	18059.	2366.	487.	255.	1106.
								BG1-4	1382.	1285.	401.	0.	0.	2154.
								BG1-6	1579.	11071.	2206.	804.	0.	1283.
								BG3-1	6045.	22247.	482.	884.	339.	523.
								BG3-3	2715.	17786.	2063.	702.	265.	803.
								BG3-4	1200.	1445.	607.	361.	0.	1542.
								BG3-6	2107.	11789.	2594.	1282.	179.	1298.
181	SINGLE	FWD	0.97	59.00	-0.062	5864.	0.800	BG1-1	7764.	69617.	1169.	1894.	447.	183.
								BG1-3	3983.	54272.	2232.	3612.	195.	247.
								BG1-4	1685.	5963.	0.	323.	0.	601.
								BG1-6	1170.	30030.	1767.	5064.	349.	[illegible]
								BG3-1	7785.	49006.	1275.	1873.	0.	0.
								BG3-3	4006.	37721.	2224.	3476.	462.	265.
								BG3-4	1610.	4645.	255.	497.	224.	565.
								BG3-6	2409.	23276.	2438.	4944.	583.	333.

NOTE: ZERO-VALUE ENTRIES INDICATE ABSENCE OF DATA

TABLE A-III: P-ORDER STRESSES (±kPa), SINGLE SCOOP FORWARD INLET

RUN NO.	INLET TYPE	INLET POS.	MASS FLOW RATIO	BLADE ANGLE DEG	POWER COEFF	PROP SPEED RPM	MACH NO.	BLADE GAGE	P ORDER COMPONENTS 1	2	3	4	5	6
182	SINGLE	FWD	0.97	59.00	1.616	8037.	0.800	BG1-1	10478.	8661.	1124.	0.	279.	414.
								BG1-3	4846.	7603.	2643.	311.	369.	378.
								BG1-4	2399.	1417.	1164.	449.	467.	309.
								BG1-6	2253.	5474.	3479.	525.	554.	1592.
								BG3-1	9514.	12796.	355.	361.	413.	470.
								BG3-3	4177.	10809.	1519.	0.	0.	445.
								BG3-4	2057.	1765.	850.	346.	218.	336.
								BG3-6	3072.	7847.	2146.	406.	371.	2266.
183	SINGLE	FWD	0.97	59.00	1.559	7833.	0.800	BG1-1	9709.	12120.	710.	189.	214.	319.
								BG1-3	4734.	10841.	2906.	455.	418.	351.
								BG1-4	2273.	1512.	993.	319.	381.	358.
								BG1-6	2328.	7466.	3449.	321.	295.	1245.
								BG3-1	9379.	12169.	641.	325.	367.	409.
								BG3-3	4208.	9800.	1785.	0.	0.	336.
								BG3-4	2065.	1646.	932.	432.	244.	402.
								BG3-6	3111.	6987.	2517.	257.	304.	1678.
184	SINGLE	FWD	0.97	59.00	1.448	7640.	0.800	BG1-1	10162.	14289.	689.	253.	231.	414.
								BG1-3	4772.	12443.	2661.	607.	290.	505.
								BG1-4	2307.	1480.	921.	234.	210.	630.
								BG1-6	2194.	8194.	3195.	541.	267.	1063.
								BG3-1	9725.	14092.	597.	345.	275.	381.
								BG3-3	4328.	11293.	1683.	333.	254.	358.
								BG3-4	2134.	1674.	830.	444.	414.	410.
								BG3-6	3070.	7975.	2297.	240.	1948.	1309.

*** END DATA ***

NOTE: ZERO-VALUE ENTRIES INDICATE ABSENCE OF DATA

TABLE A-IV: P-ORDER STRESSES (±kPa), SINGLE SCOOP MID INLET

RUN NO.	INLET TYPE	INLET POS.	MASS FLOW RATIO	BLADE ANGLE DEG	POWER COEFF	PROP SPEED RPM	MACH NO.	BLADE GAGE	P ORDER COMPONENTS 1	2	3	4	5	6
251	SINGLE	MID	0.97	58.00	-0.072	4496.	0.600	BG1-1	3655.	5375.	878.	0.	371.	222.
								BG1-3	2681.	4146.	807.	230.	447.	486.
								BG1-4	980.	596.	0.	0.	0.	0.
								BG1-6	947.	2308.	556.	240.	607.	578.
								BG3-1	3223.	3455.	698.	0.	382.	253.
								BG3-3	2260.	2815.	685.	176.	489.	498.
								BG3-4	893.	440.	0.	0.	0.	0.
								BG3-6	854.	1762.	500.	0.	764.	773.
252	SINGLE	MID	0.97	58.00	1.916	6834.	0.600	BG1-1	4552.	10508.	391.	443.	0.	321.
								BG1-3	2945.	8377.	400.	610.	0.	373.
								BG1-4	1142.	502.	0.	0.	0.	587.
								BG1-6	452.	4928.	580.	946.	0.	610.
								BG3-1	4035.	11529.	349.	423.	0.	334.
								BG3-3	2466.	8821.	375.	478.	0.	381.
								BG3-4	1094.	605.	0.	0.	0.	602.
								BG3-6	852.	5743.	303.	885.	0.	697.
253	SINGLE	MID	0.97	58.00	1.786	6644.	0.600	BG1-1	4160.	14599.	309.	0.	0.	253.
								BG1-3	2689.	11641.	289.	311.	0.	241.
								BG1-4	1133.	766.	0.	0.	0.	402.
								BG1-6	395.	6843.	393.	474.	0.	471.
								BG3-1	3729.	16003.	342.	0.	0.	261.
								BG3-3	2299.	12355.	523.	0.	0.	226.
								BG3-4	1067.	867.	0.	0.	0.	375.
								BG3-6	842.	8042.	478.	271.	0.	692.
254	SINGLE	MID	0.97	58.00	1.681	6433.	0.600	BG1-1	4479.	20273.	185.	278.	0.	192.
								BG1-3	2870.	16208.	285.	621.	0.	188.
								BG1-4	1248.	1114.	179.	0.	0.	237.
								BG1-6	427.	9477.	408.	896.	0.	701.
								BG3-1	4080.	22097.	414.	336.	0.	175.
								BG3-3	2499.	17245.	576.	703.	0.	191.
								BG3-4	1196.	1260.	0.	0.	0.	254.
								BG3-6	969.	11225.	533.	1108.	0.	779.
261	SINGLE	MID	0.97	58.00	-0.065	5303.	0.700	BG1-1	4355.	9877.	683.	306.	0.	241.
								BG1-3	3040.	7733.	608.	0.	0.	0.
								BG1-4	1102.	948.	0.	0.	0.	262.
								BG1-6	817.	4286.	451.	0.	192.	0.
								BG3-1	4102.	8019.	589.	0.	0.	226.
								BG3-3	2826.	6305.	550.	181.	268.	0.
								BG3-4	1069.	859.	0.	0.	0.	270.
								BG3-6	1084.	3933.	359.	241.	504.	0.
262	SINGLE	MID	0.97	58.00	1.703	7540.	0.700	BG1-1	5383.	7496.	184.	0.	0.	351.
								BG1-3	3302.	5647.	293.	192.	0.	477.
								BG1-4	1467.	787.	0.	0.	427.	543.
								BG1-6	800.	3300.	542.	366.	1418.	892.
								BG3-1	4977.	7750.	526.	0.	183.	350.
								BG3-3	2777.	5405.	302.	294.	211.	549.
								BG3-4	1503.	818.	0.	0.	692.	682.
								BG3-6	1229.	3236.	557.	619.	1716.	888.

NOTE: ZERO-VALUE ENTRIES INDICATE ABSENCE OF DATA

TABLE A-IV: P-ORDER STRESSES (±kPa), SINGLE SCOOP MID INLET

RUN NO.	INLET TYPE	INLET POS.	MASS FLOW RATIO	BLADE ANGLE DEG	POWER COEFF	PROP SPEED RPM	MACH NO.	BLADE GAGE	P ORDER COMPONENTS 1	2	3	4	5	6
263	SINGLE	MID	0.97	58.00	1.604	7334.	0.700	BG1-1	5834.	8508.	372.	0.	0.	623.
								BG1-3	3607.	6595.	548.	314.	0.	846.
								BG1-4	1569.	710.	189.	0.	243.	1342.
								BG1-6	888.	3938.	826.	331.	695.	1481.
								BG3-1	5474.	8484.	294.	182.	0.	536.
								BG3-3	3097.	6054.	498.	366.	0.	718.
								BG3-4	1635.	777.	0.	0.	0.	1092.
								BG3-6	1382.	3770.	736.	429.	294.	991.
264	SINGLE	MID	0.97	58.00	0.000	7145.	0.700	BG1-1	5507.	8664.	397.	179.	0.	1379.
								BG1-3	3381.	6750.	485.	300.	0.	1736.
								BG1-4	1522.	709.	0.	0.	0.	3130.
								BG1-6	760.	4075.	765.	467.	391.	2651.
								BG3-1	5045.	8866.	398.	414.	0.	665.
								BG3-3	2849.	6504.	290.	685.	0.	861.
								BG3-4	1485.	738.	0.	179.	190.	1529.
								BG3-6	1253.	4135.	542.	1070.	316.	1329.
271	SINGLE	MID	0.97	58.00	-0.071	6110.	0.800	BG1-1	6512.	61227.	533.	1819.	190.	0.
								BG1-3	4629.	47850.	0.	2540.	0.	526.
								BG1-4	1583.	4754.	204.	332.	0.	1472.
								BG1-6	1159.	26926.	0.	3685.	228.	5079.
								BG3-1	6127.	38322.	721.	1695.	0.	285.
								BG3-3	4104.	29817.	499.	3154.	0.	228.
								BG3-4	1605.	3331.	0.	367.	0.	1134.
								BG3-6	1410.	18559.	451.	4788.	225.	3136.
272	SINGLE	MID	0.97	58.00	1.473	8311.	0.800	BG1-1	8083.	4248.	1045.	0.	0.	332.
								BG1-3	4990.	2839.	2168.	192.	192.	472.
								BG1-4	1619.	603.	526.	0.	281.	248.
								BG1-6	1289.	1799.	2878.	348.	443.	1525.
								BG3-1	7159.	5534.	856.	0.	0.	339.
								BG3-3	4041.	3979.	1023.	0.	0.	482.
								BG3-4	1665.	661.	364.	0.	0.	197.
								BG3-6	1835.	2737.	1728.	183.	231.	1871.
273	SINGLE	MID	0.97	58.00	1.369	8102.	0.800	BG1-1	8225.	4168.	715.	0.	0.	311.
								BG1-3	5051.	2773.	1506.	0.	0.	465.
								BG1-4	1628.	593.	332.	0.	0.	385.
								BG1-6	1213.	1770.	1890.	190.	269.	1528.
								BG3-1	7237.	6086.	957.	0.	0.	294.
								BG3-3	4126.	4589.	1369.	224.	0.	405.
								BG3-4	1698.	654.	469.	0.	0.	285.
								BG3-6	1932.	3246.	2235.	347.	274.	1625.
274	SINGLE	MID	0.97	58.00	1.289	7902.	0.800	BG1-1	8129.	5450.	523.	0.	0.	263.
								BG1-3	5099.	3901.	975.	0.	0.	437.
								BG1-4	1557.	679.	234.	0.	0.	478.
								BG1-6	1215.	2578.	1184.	237.	248.	1707.
								BG3-1	7226.	7308.	889.	0.	0.	321.
								BG3-3	4193.	5574.	953.	0.	0.	413.
								BG3-4	1682.	791.	333.	0.	0.	415.
								BG3-6	2069.	3961.	1620.	180.	335.	1390.

NOTE: ZERO-VALUE ENTRIES INDICATE ABSENCE OF DATA

TABLE A-IV: P-ORDER STRESSES (±kPa), SINGLE SCOOP MID INLET

RUN NO.	INLET TYPE	INLET POS.	MASS FLOW RATIO	BLADE ANGLE DEG	POWER COEFF	PROP SPEED RPM	MACH NO.	BLADE GAGE	P ORDER COMPONENTS 1	2	3	4	5	6
281	SINGLE	MID	0.97	59.20	-0.078	4292.	0.600	BG1-1	0.	5516.	818.	309.	0.	197.
								BG1-3	0.	4753.	648.	247.	370.	559.
								BG1-4	0.	561.	0.	0.	0.	185.
								BG1-6	0.	2401.	398.	285.	431.	552.
								BG3-1	0.	1433.	1784.	0.	0.	472.
								BG3-3	0.	1821.	1840.	0.	317.	659.
								BG3-4	0.	0.	212.	0.	0.	0.
								BG3-6	0.	1055.	1422.	0.	448.	1003.
282	SINGLE	MID	0.97	59.20	2.089	6678.	0.600	BG1-1	3774.	13133.	281.	215.	0.	462.
								BG1-3	2443.	10528.	694.	434.	225.	241.
								BG1-4	765.	624.	0.	0.	0.	387.
								BG1-6	1176.	5992.	627.	654.	197.	668.
								BG3-1	4776.	14003.	259.	399.	0.	461.
								BG3-3	3338.	10806.	477.	264.	214.	239.
								BG3-4	1285.	792.	0.	0.	0.	453.
								BG3-6	1032.	6953.	644.	479.	232.	836.
283	SINGLE	MID	0.97	59.20	1.971	6486.	0.600	BG1-1	3642.	18477.	308.	294.	0.	358.
								BG1-3	2423.	14824.	692.	411.	0.	193.
								BG1-4	832.	939.	0.	0.	0.	196.
								BG1-6	1164.	8514.	532.	651.	190.	596.
								BG3-1	4404.	20678.	334.	0.	0.	280.
								BG3-3	3137.	16093.	611.	439.	183.	199.
								BG3-4	1266.	1165.	0.	0.	0.	223.
								BG3-6	1013.	10417.	708.	688.	261.	730.
284	SINGLE	MID	0.97	59.20	1.818	6280.	0.600	BG1-1	3936.	27896.	374.	479.	0.	420.
								BG1-3	2680.	22457.	647.	308.	0.	237.
								BG1-4	989.	1582.	0.	0.	0.	207.
								BG1-6	1208.	12956.	422.	460.	0.	1540.
								BG3-1	4783.	31211.	414.	525.	0.	214.
								BG3-3	3431.	24584.	633.	1280.	227.	213.
								BG3-4	1479.	1969.	0.	319.	0.	460.
								BG3-6	1196.	15961.	690.	1959.	277.	2146.
291	SINGLE	MID	0.97	59.20	-0.066	5091.	0.700	BG1-1	4214.	9320.	700.	239.	453.	0.
								BG1-3	2664.	7433.	631.	275.	278.	223.
								BG1-4	857.	1159.	0.	0.	0.	280.
								BG1-6	1229.	4212.	435.	378.	399.	174.
								BG3-1	5414.	7942.	717.	382.	390.	0.
								BG3-3	4064.	6407.	615.	0.	454.	0.
								BG3-4	1549.	1105.	0.	0.	0.	265.
								BG3-6	1694.	4080.	614.	0.	784.	176.
301	SINGLE	MID	0.97	59.20	-0.075	5078.	0.700	BG1-1	4767.	9140.	976.	0.	183.	0.
								BG1-3	3330.	7359.	829.	0.	317.	325.
								BG1-4	1212.	1005.	0.	0.	0.	236.
								BG1-6	1296.	3990.	558.	0.	430.	209.
302	SINGLE	MID	0.97	59.20	1.852	7379.	0.700	BG1-1	5542.	8198.	378.	0.	0.	455.
								BG1-3	3623.	6361.	414.	215.	0.	692.
								BG1-4	1546.	786.	250.	0.	409.	1086.
								BG1-6	683.	3728.	798.	318.	885.	1313.

NOTE: ZERO-VALUE ENTRIES INDICATE ABSENCE OF DATA

TABLE A-IV: P-ORDER STRESSES (±kPa), SINGLE SCOOP MID INLET

RUN NO.	INLET TYPE	INLET POS.	MASS FLOW RATIO	BLADE ANGLE DEG	POWER COEFF	PROP SPEED RPM	MACH NO.	BLADE GAGE	P ORDER COMPONENTS 1	2	3	4	5	6
303	SINGLE	MID	0.97	59.20	1.759	7181.	0.700	BG1-1	5718.	9786.	277.	203.	0.	1176.
								BG1-3	3751.	7708.	488.	259.	0.	1442.
								BG1-4	1613.	812.	272.	0.	204.	2554.
								BG1-6	744.	4637.	837.	343.	293.	2424.
304	SINGLE	MID	0.97	59.20	1.651	6983.	0.700	BG1-1	5046.	10179.	375.	0.	0.	884.
								BG1-3	3255.	8108.	415.	229.	0.	1061.
								BG1-4	1455.	671.	177.	0.	0.	1990.
								BG1-6	510.	4933.	677.	364.	0.	1635.
311	SINGLE	MID	0.97	59.20	-0.075	5862.	0.800	BG1-1	6166.	40060.	425.	527.	0.	221.
								BG1-3	4401.	31685.	394.	950.	0.	0.
								BG1-4	1658.	3248.	0.	0.	0.	488.
								BG1-6	1009.	17761.	307.	1217.	293.	602.
312	SINGLE	MID	0.97	59.20	1.673	8102.	0.800	BG1-1	8178.	4309.	784.	0.	0.	289.
								BG1-3	5293.	2836.	1661.	0.	192.	437.
								BG1-4	1941.	685.	299.	0.	293.	422.
								BG1-6	1425.	1924.	2118.	0.	273.	1130.
313	SINGLE	MID	0.97	59.20	1.613	7917.	0.800	BG1-1	7749.	5372.	462.	0.	0.	282.
								BG1-3	5098.	4069.	1103.	0.	231.	402.
								BG1-4	1841.	702.	222.	0.	198.	460.
								BG1-6	1418.	2698.	1433.	259.	210.	1269.
314	SINGLE	MID	0.97	59.20	1.503	7679.	0.800	BG1-1	7029.	7161.	365.	0.	0.	305.
								BG1-3	4510.	5544.	871.	185.	0.	453.
								BG1-4	1679.	732.	0.	0.	218.	513.
								BG1-6	1075.	3425.	1104.	296.	369.	1239.
322	SINGLE	MID	0.81	59.20	2.074	6749.	0.600	BG1-1	4897.	12199.	313.	195.	0.	270.
								BG1-3	3122.	9761.	566.	290.	0.	283.
								BG1-4	1179.	490.	0.	0.	0.	519.
								BG1-6	589.	5722.	639.	519.	0.	548.
323	SINGLE	MID	0.81	59.20	1.941	6558.	0.600	BG1-1	4742.	15368.	271.	340.	0.	266.
								BG1-3	3041.	12410.	412.	360.	0.	256.
								BG1-4	1277.	666.	0.	0.	0.	418.
								BG1-6	555.	7245.	436.	609.	0.	378.
324	SINGLE	MID	0.81	59.20	1.840	6355.	0.600	BG1-1	3957.	23580.	269.	562.	0.	0.
								BG1-3	2541.	19062.	339.	1001.	0.	0.
								BG1-4	1122.	1131.	0.	0.	0.	250.
								BG1-6	466.	11034.	303.	1389.	0.	963.
332	SINGLE	MID	0.81	59.20	1.844	7377.	0.700	BG1-1	5699.	8912.	244.	0.	0.	630.
								BG1-3	3616.	6999.	735.	202.	0.	805.
								BG1-4	1582.	695.	194.	0.	256.	1283.
								BG1-6	953.	4135.	832.	317.	787.	1744.
333	SINGLE	MID	0.81	59.20	1.718	7181.	0.700	BG1-1	6006.	10572.	415.	244.	0.	1154.
								BG1-3	3806.	8375.	716.	261.	0.	1426.
								BG1-4	1706.	794.	0.	0.	0.	2554.
								BG1-6	1054.	5117.	745.	351.	340.	2353.
334	SINGLE	MID	0.81	59.20	1.613	6979.	0.700	BG1-1	5402.	10830.	453.	0.	0.	1054.
								BG1-3	3387.	8647.	470.	207.	0.	1293.
								BG1-4	1570.	659.	0.	0.	0.	2421.
								BG1-6	840.	5231.	428.	396.	0.	1865.

NOTE: ZERO-VALUE ENTRIES INDICATE ABSENCE OF DATA

C-2

TABLE A-IV: P-ORDER STRESSES (±kPa), SINGLE SCOOP MID INLET

RUN NO.	INLET TYPE	INLET POS.	MASS FLOW RATIO	BLADE ANGLE DEG	POWER COEFF	PROP SPEED RPM	MACH NO.	BLADE GAGE	P ORDER COMPONENTS 1	2	3	4	5	6
341	SINGLE	MID	0.81	59.20	-0.077	5877.	0.800	BG1-1	6670.	47835.	510.	592.	0.	278.
								BG1-3	4627.	37789.	279.	1072.	0.	0.
								BG1-4	1742.	3889.	0.	0.	0.	587.
								BG1-6	1211.	21134.	321.	1394.	273.	737.
342	SINGLE	MID	0.81	59.20	1.675	8153.	0.800	BG1-1	8165.	4839.	878.	0.	0.	353.
								BG1-3	5089.	3431.	1631.	0.	0.	399.
								BG1-4	1932.	738.	290.	0.	248.	255.
								BG1-6	1577.	2422.	2072.	0.	270.	1752.
343	SINGLE	MID	0.81	59.20	1.540	7959.	0.800	BG1-1	9078.	4849.	490.	0.	0.	388.
								BG1-3	5675.	3595.	1054.	177.	0.	398.
								BG1-4	2114.	671.	0.	0.	286.	546.
								BG1-6	1782.	2417.	1261.	311.	747.	1019.
344	SINGLE	MID	0.81	59.20	1.480	7764.	0.800	BG1-1	8836.	7296.	587.	0.	0.	364.
								BG1-3	5447.	5731.	1058.	261.	0.	459.
								BG1-4	2119.	738.	0.	0.	0.	565.
								BG1-6	1500.	3638.	1254.	554.	338.	1200.
351	SINGLE	MID	0.81	58.00	-0.074	4544.	0.600	BG1-1	3893.	5182.	1569.	0.	649.	207.
								BG1-3	2795.	4132.	1663.	0.	841.	527.
								BG1-4	988.	620.	198.	0.	0.	257.
								BG1-6	1293.	2272.	1086.	0.	1254.	691.
352	SINGLE	MID	0.81	58.00	1.963	7017.	0.600	BG1-1	4877.	9568.	678.	180.	0.	621.
								BG1-3	2950.	7606.	681.	277.	0.	897.
								BG1-4	1073.	476.	0.	0.	0.	1543.
								BG1-6	385.	4598.	804.	401.	0.	1229.
353	SINGLE	MID	0.81	58.00	1.815	6795.	0.600	BG1-1	4054.	11958.	561.	0.	0.	445.
								BG1-3	2493.	9565.	422.	0.	0.	421.
								BG1-4	1004.	609.	0.	0.	0.	825.
								BG1-6	232.	5721.	419.	0.	0.	588.
361	SINGLE	MID	0.81	58.00	0.000	6600.	0.600	BG1-1	4561.	13697.	433.	343.	0.	329.
								BG1-3	2860.	11054.	312.	272.	0.	204.
								BG1-4	1180.	655.	0.	0.	0.	476.
								BG1-6	232.	6509.	283.	418.	189.	422.
362	SINGLE	MID	0.81	58.00	0.000	5321.	0.700	BG1-1	0.	11601.	758.	257.	0.	217.
								BG1-3	0.	9159.	701.	319.	0.	0.
								BG1-4	0.	1084.	0.	0.	0.	320.
								BG1-6	0.	4917.	584.	377.	187.	0.
365	SINGLE	MID	0.81	58.00	0.000	7337.	0.700	BG1-1	6008.	8840.	371.	0.	0.	663.
								BG1-3	3695.	6919.	498.	346.	0.	946.
								BG1-4	1594.	870.	0.	0.	296.	1568.
								BG1-6	415.	4327.	706.	426.	864.	1563.
372	SINGLE	MID	0.81	58.00	0.000	8410.	0.800	BG1-1	8751.	4367.	2046.	0.	174.	176.
								BG1-3	5404.	3172.	4006.	0.	0.	530.
								BG1-4	1753.	793.	933.	0.	297.	260.
								BG1-6	1119.	2026.	5571.	0.	498.	1902.
373	SINGLE	MID	0.81	58.00	0.000	8204.	0.800	BG1-1	9000.	4971.	1118.	0.	0.	195.
								BG1-3	5590.	3574.	2142.	0.	0.	489.
								BG1-4	1819.	781.	488.	0.	0.	378.
								BG1-6	1134.	2334.	3029.	0.	278.	1737.

NOTE: ZERO-VALUE ENTRIES INDICATE ABSENCE OF DATA

TABLE A-IV: P-ORDER STRESSES (±kPa), SINGLE SCOOP MID INLET

RUN NO.	INLET TYPE	INLET POS.	MASS FLOW RATIO	BLADE ANGLE DEG	POWER COEFF	PROP SPEED RPM	MACH NO.	BLADE GAGE	P ORDER COMPONENTS 1	2	3	4	5	6
374	SINGLE	MID	0.81	58.00	0.000	8009.	0.800	BG1-1	7713.	5477.	777.	0.	0.	309.
								BG1-3	4807.	3927.	1328.	0.	184.	586.
								BG1-4	1538.	788.	317.	0.	0.	743.
								BG1-6	924.	2572.	1865.	0.	423.	989.

*** END DATA ***

NOTE: ZERO-VALUE ENTRIES INDICATE ABSENCE OF DATA

ORIGINAL PAGE IS
OF POOR QUALITY

TABLE A-V: P-ORDER STRESSES (±kPa), TWIN SCOOP FORWARD INLET

RUN NO.	INLET TYPE	INLET POS.	MASS FLOW RATIO	BLADE ANGLE DEG	POWER COEFF	PROP SPEED RPM	MACH NO.	BLADE GAGE	P ORDER COMPONENTS					
									1	2	3	4	5	6
381	TWIN	FWD	0.00	58.30	-0.056	4382.	0.600	BG1-1	1444.	10011.	951.	257.	271.	345.
								BG1-3	1082.	6884.	1100.	1363.	438.	517.
								BG1-4	321.	1310.	0.	0.	0.	0.
								BG1-6	1088.	3514.	796.	1323.	604.	732.
								BG3-1	2107.	10790.	1969.	216.	200.	369.
								BG3-3	1900.	7685.	2293.	1393.	368.	450.
								BG3-4	683.	1473.	0.	0.	0.	0.
								BG3-6	877.	4471.	1773.	1378.	533.	730.
401	TWIN	FWD	0.00	58.30	2.037	6927.	0.600	BG3-1	3408.	24315.	0.	1647.	0.	513.
								BG3-3	2951.	19791.	723.	2100.	0.	595.
								BG3-4	875.	1311.	0.	635.	0.	1167.
								BG3-6	1550.	13231.	800.	3962.	262.	1102.
402	TWIN	FWD	1.00	58.30	2.011	6927.	0.600	BG3-1	3391.	15374.	0.	801.	0.	498.
								BG3-3	3022.	12360.	735.	1064.	0.	581.
								BG3-4	927.	866.	191.	0.	0.	1145.
								BG3-6	1613.	8293.	836.	1843.	191.	1190.
403	TWIN	FWD	0.75	58.30	2.016	6927.	0.600	BG3-1	3410.	16440.	0.	609.	0.	455.
								BG3-3	3009.	13338.	652.	890.	0.	527.
								BG3-4	926.	915.	175.	188.	0.	1032.
								BG3-6	1622.	8954.	779.	1633.	272.	1017.
404	TWIN	FWD	0.57	58.30	2.009	6927.	0.600	BG3-1	3404.	17903.	0.	734.	0.	461.
								BG3-3	2981.	14565.	640.	1089.	0.	524.
								BG3-4	914.	986.	182.	266.	0.	1001.
								BG3-6	1592.	9782.	795.	1990.	275.	888.
405	TWIN	FWD	0.57	58.30	1.908	6721.	0.600	BG3-1	3456.	26120.	0.	868.	0.	304.
								BG3-3	3049.	21082.	501.	1259.	0.	313.
								BG3-4	979.	1379.	0.	401.	0.	647.
								BG3-6	1667.	14001.	614.	2273.	0.	549.
406	TWIN	FWD	0.75	58.30	1.901	6721.	0.600	BG3-1	3399.	23749.	0.	621.	0.	327.
								BG3-3	3019.	19142.	335.	954.	0.	367.
								BG3-4	977.	1255.	0.	301.	0.	728.
								BG3-6	1657.	12714.	408.	1739.	0.	633.
407	TWIN	FWD	1.00	58.30	1.898	6721.	0.600	BG3-1	3382.	21118.	0.	409.	0.	342.
								BG3-3	3029.	17007.	320.	706.	0.	404.
								BG3-4	968.	1113.	0.	233.	0.	794.
								BG3-6	1690.	11300.	392.	1304.	0.	735.
408	TWIN	FWD	1.00	58.30	1.807	6528.	0.600	BG3-1	2959.	27956.	0.	630.	0.	232.
								BG3-3	2684.	22292.	368.	906.	0.	280.
								BG3-4	880.	1531.	0.	317.	0.	602.
								BG3-6	1541.	14676.	445.	1623.	0.	820.
409	TWIN	FWD	0.75	58.30	1.813	6528.	0.600	BG3-1	2950.	31287.	0.	925.	0.	242.
								BG3-3	2647.	25013.	394.	1335.	0.	279.
								BG3-4	876.	1704.	0.	432.	0.	568.
								BG3-6	1516.	16464.	463.	2347.	0.	754.
4010	TWIN	FWD	0.57	58.30	1.815	6528.	0.600	BG3-1	2991.	33948.	0.	1141.	0.	252.
								BG3-3	2658.	27159.	447.	1671.	0.	290.
								BG3-4	884.	1835.	0.	529.	0.	570.
								BG3-6	1538.	17871.	524.	2933.	0.	705.

NOTE: ZERO-VALUE ENTRIES INDICATE ABSENCE OF DATA

TABLE A-V: P-ORDER STRESSES (±kPa), TWIN SCOOP FORWARD INLET

RUN NO.	INLET TYPE	INLET POS.	MASS FLOW RATIO	BLADE ANGLE DEG	POWER COEFF	PROP SPEED RPM	MACH NO.	BLADE GAGE	P ORDER COMPONENTS 1	2	3	4	5	6
411	TWIN	FWD	0.00	58.30	-0.044	5257.	0.700	BG3-1	2464.	26367.	1094.	560.	286.	196.
								BG3-3	2050.	19253.	1426.	2383.	200.	217.
								BG3-4	725.	3019.	0.	244.	0.	203.
								BG3-6	1224.	11751.	1119.	2994.	350.	250.
412	TWIN	FWD	0.00	58.30	1.811	7622.	0.700	BG3-1	3707.	18979.	487.	606.	0.	436.
								BG3-3	3113.	15604.	1290.	422.	0.	709.
								BG3-4	948.	2095.	341.	806.	572.	963.
								BG3-6	1916.	10429.	1658.	1027.	1625.	1277.
413	TWIN	FWD	1.00	58.30	1.792	7622.	0.700	BG3-1	3407.	12278.	472.	175.	0.	390.
								BG3-3	3030.	9728.	1167.	253.	0.	672.
								BG3-4	911.	1444.	369.	422.	299.	884.
								BG3-6	1828.	6395.	1577.	455.	847.	1134.
414	TWIN	FWD	0.75	58.30	1.767	7622.	0.700	BG3-1	3392.	13370.	492.	291.	0.	360.
								BG3-3	3024.	10671.	1088.	231.	0.	640.
								BG3-4	918.	1649.	353.	490.	308.	809.
								BG3-6	1841.	7025.	1464.	397.	935.	1071.
415	TWIN	FWD	0.57	58.30	1.762	7622.	0.700	BG3-1	3393.	13760.	439.	480.	0.	375.
								BG3-3	2989.	11114.	953.	260.	0.	663.
								BG3-4	907.	1725.	346.	467.	508.	882.
								BG3-6	1817.	7426.	1273.	379.	1655.	966.
416	TWIN	FWD	0.57	58.30	1.671	7430.	0.700	BG3-1	3138.	14786.	182.	578.	0.	460.
								BG3-3	2763.	12183.	808.	666.	0.	784.
								BG3-4	880.	1527.	333.	361.	0.	1160.
								BG3-6	1651.	8264.	1060.	1472.	441.	939.
417	TWIN	FWD	0.75	58.30	1.669	7430.	0.700	BG3-1	2970.	14155.	0.	428.	0.	423.
								BG3-3	2663.	11616.	774.	491.	0.	763.
								BG3-4	844.	1470.	351.	332.	0.	1108.
								BG3-6	1603.	7888.	1056.	1210.	388.	863.
418	TWIN	FWD	1.00	58.30	1.662	7430.	0.700	BG3-1	2935.	12528.	0.	329.	0.	479.
								BG3-3	2654.	10201.	733.	367.	0.	796.
								BG3-4	846.	1311.	362.	284.	174.	1168.
								BG3-6	1582.	6923.	1044.	988.	427.	959.
419	TWIN	FWD	1.00	58.30	1.567	7230.	0.700	BG3-1	2691.	15148.	0.	449.	0.	570.
								BG3-3	2474.	12374.	561.	474.	0.	923.
								BG3-4	777.	1324.	299.	353.	0.	1514.
								BG3-6	1482.	8389.	784.	692.	315.	1161.
4110	TWIN	FWD	0.75	58.30	1.572	7230.	0.700	BG3-1	2756.	16537.	0.	635.	0.	528.
								BG3-3	2477.	13562.	664.	696.	0.	847.
								BG3-4	809.	1438.	339.	317.	177.	1395.
								BG3-6	1461.	9196.	919.	1087.	339.	1062.
4111	TWIN	FWD	0.57	58.30	1.556	7230.	0.700	BG3-1	2703.	18522.	176.	685.	0.	516.
								BG3-3	2434.	15262.	679.	731.	0.	809.
								BG3-4	781.	1631.	304.	400.	0.	1316.
								BG3-6	1442.	10322.	864.	1212.	337.	1024.
421	TWIN	FWD	0.00	58.30	-0.034	6127.	0.800	BG3-1	1834.	173490.	521.	9350.	1275.	1227.
								BG3-3	1605.	134666.	1228.	13744.	878.	839.
								BG3-4	546.	15058.	686.	2972.	650.	1521.
								BG3-6	979.	84283.	1207.	22919.	820.	5272.

NOTE: ZERO-VALUE ENTRIES INDICATE ABSENCE OF DATA

TABLE A-V: P-ORDER STRESSES (±kPa), TWIN SCOOP FORWARD INLET

RUN NO.	INLET TYPE	INLET POS.	MASS FLOW RATIO	BLADE ANGLE DEG	POWER COEFF	PROP SPEED RPM	MACH NO.	BLADE GAGE	P ORDER COMPONENTS 1	2	3	4	5	6
432	TWIN	FWD	1.00	58.30	1.596	8505.	0.800	BG3-1	3009.	10366.	1093.	250.	0.	255.
								BG3-3	2625.	9417.	2391.	386.	0.	467.
								BG3-4	828.	1749.	765.	0.	0.	197.
								BG3-6	1196.	7186.	3513.	788.	192.	1471.
433	TWIN	FWD	0.75	58.30	1.592	8459.	0.800	BG3-1	2841.	12117.	849.	330.	207.	219.
								BG3-3	2415.	11056.	2075.	383.	0.	429.
								BG3-4	776.	2135.	674.	0.	0.	194.
								BG3-6	1124.	8293.	2962.	844.	403.	996.
424	TWIN	FWD	0.57	58.30	1.598	8442.	0.800	BG3-1	2784.	13959.	892.	291.	187.	241.
								BG3-3	2349.	12787.	2052.	465.	0.	332.
								BG3-4	765.	2382.	675.	199.	0.	180.
								BG3-6	1081.	9647.	2969.	1120.	339.	917.
425	TWIN	FWD	0.57	58.30	1.499	8246.	0.800	BG3-1	2993.	14478.	823.	273.	0.	240.
								BG3-3	2513.	13156.	1864.	397.	0.	396.
								BG3-4	893.	2224.	582.	378.	0.	232.
								BG3-6	1151.	9884.	2702.	1287.	293.	1159.
436	TWIN	FWD	0.75	58.30	1.497	8246.	0.800	BG3-1	2896.	12842.	863.	266.	0.	226.
								BG3-3	2508.	11708.	1902.	396.	0.	365.
								BG3-4	871.	1938.	619.	231.	0.	208.
								BG3-6	1152.	8821.	2787.	1115.	363.	1057.
437	TWIN	FWD	1.00	58.30	1.496	8246.	0.800	BG3-1	2976.	11464.	896.	266.	0.	213.
								BG3-3	2557.	10339.	1983.	412.	0.	367.
								BG3-4	874.	1698.	655.	0.	0.	210.
								BG3-6	1186.	7782.	2949.	962.	334.	1154.
438	TWIN	FWD	1.00	58.30	1.422	8058.	0.800	BG3-1	2865.	13440.	679.	206.	0.	226.
								BG3-3	2409.	11902.	1596.	286.	0.	362.
								BG3-4	966.	1895.	556.	196.	0.	322.
								BG3-6	1066.	8877.	2398.	777.	217.	1130.
439	TWIN	FWD	0.75	58.30	1.430	8058.	0.800	BG3-1	2869.	15127.	709.	226.	0.	230.
								BG3-3	2398.	13460.	1582.	296.	0.	364.
								BG3-4	856.	2148.	538.	300.	0.	321.
								BG3-6	1097.	9929.	2380.	882.	209.	1053.
4310	TWIN	FWD	0.57	58.30	1.430	8058.	0.800	BG3-1	2801.	16879.	668.	268.	0.	212.
								BG3-3	2319.	15175.	1451.	324.	0.	333.
								BG3-4	854.	2416.	502.	431.	0.	290.
								BG3-6	1081.	11163.	2166.	1025.	204.	1026.
431	TWIN	FWD	1.00	59.10	-0.037	5845.	0.800	BG3-1	1285.	63403.	414.	1162.	220.	0.
								BG3-3	1030.	48465.	822.	2366.	176.	227.
								BG3-4	186.	6098.	254.	384.	0.	545.
								BG3-6	1448.	30047.	670.	3384.	0.	496.
432	TWIN	FWD	1.00	59.10	1.749	8142.	0.800	BG3-1	1352.	14992.	770.	0.	0.	274.
								BG3-3	1143.	12975.	1995.	375.	0.	489.
								BG3-4	299.	2377.	573.	195.	0.	321.
								BG3-6	686.	9644.	2763.	922.	332.	1301.
433	TWIN	FWD	0.75	59.10	1.738	8142.	0.800	BG3-1	1538.	16308.	716.	187.	0.	218.
								BG3-3	1254.	14370.	1843.	317.	0.	502.
								BG3-4	357.	2502.	558.	311.	0.	323.
								BG3-6	740.	10582.	2525.	858.	295.	1338.

NOTE: ZERO-VALUE ENTRIES INDICATE ABSENCE OF DATA

TABLE A-V: P-ORDER STRESSES (±kPa), TWIN SCOOP FORWARD INLET

RUN NO.	INLET TYPE	INLET POS.	MASS FLOW RATIO	BLADE ANGLE DEG	POWER COEFF	PROP SPEED RPM	MACH NO.	BLADE GAGE	P ORDER COMPONENTS 1	2	3	4	5	6
434	TWIN	FWD	0.57	59.10	1.713	8142.	0.800	BG3-1	1781.	17903.	675.	254.	0.	208.
								BG3-3	1400.	15911.	1777.	317.	0.	507.
								BG3-4	382.	2783.	551.	449.	0.	307.
								BG3-6	720.	11731.	2415.	1019.	246.	1532.
435	TWIN	FWD	0.57	59.10	1.635	7938.	0.800	BG3-1	2014.	19203.	310.	210.	0.	273.
								BG3-3	1630.	16746.	1390.	328.	0.	495.
								BG3-4	405.	2646.	393.	404.	0.	509.
								BG3-6	905.	12099.	1787.	1001.	268.	1093.
436	TWIN	FWD	0.75	59.10	1.630	7938.	0.800	BG3-1	1925.	17973.	289.	0.	0.	240.
								BG3-3	1659.	15476.	1449.	332.	0.	461.
								BG3-4	402.	2521.	382.	303.	0.	447.
								BG3-6	799.	11273.	1835.	965.	302.	980.
437	TWIN	FWD	1.00	59.10	1.648	7938.	0.800	BG3-1	1857.	16732.	237.	0.	0.	267.
								BG3-3	1639.	14386.	1484.	330.	0.	479.
								BG3-4	429.	2270.	366.	218.	0.	462.
								BG3-6	865.	10430.	1868.	808.	493.	1156.
438	TWIN	FWD	1.00	59.10	1.579	7747.	0.800	BG3-1	1809.	15153.	0.	0.	0.	262.
								BG3-3	1632.	12602.	1214.	287.	0.	508.
								BG3-4	425.	2063.	310.	267.	0.	624.
								BG3-6	900.	8887.	1484.	688.	731.	1231.
439	TWIN	FWD	0.75	59.10	1.594	7747.	0.800	BG3-1	2019.	16816.	0.	0.	0.	305.
								BG3-3	1746.	14016.	1272.	306.	0.	546.
								BG3-4	426.	2276.	285.	391.	0.	664.
								BG3-6	931.	9873.	1555.	844.	604.	1306.
4310	TWIN	FWD	0.57	59.10	1.589	7747.	0.800	BG3-1	2195.	18150.	0.	0.	0.	375.
								BG3-3	1800.	15232.	1296.	353.	0.	490.
								BG3-4	445.	2419.	283.	509.	0.	646.
								BG3-6	910.	10754.	1581.	1045.	536.	1282.
441	TWIN	FWD	0.00	59.10	-0.052	4890.	0.700	BG3-1	2039.	19230.	1077.	440.	878.	211.
								BG3-3	1760.	13689.	1442.	2169.	1332.	195.
								BG3-4	557.	2359.	0.	249.	0.	0.
								BG3-6	1078.	8054.	1044.	2501.	2125.	287.
442	TWIN	FWD	0.00	59.10	1.950	7182.	0.700	BG3-1	3256.	29145.	763.	996.	337.	759.
								BG3-3	2687.	23393.	1291.	1362.	271.	738.
								BG3-4	538.	2672.	224.	829.	176.	1352.
								BG3-6	1508.	15194.	1554.	2750.	360.	1299.
443	TWIN	FWD	1.00	59.10	1.926	7182.	0.700	BG3-1	2657.	18707.	708.	643.	332.	658.
								BG3-3	2307.	14597.	1068.	465.	304.	712.
								BG3-4	429.	1986.	294.	443.	0.	1257.
								BG3-6	1389.	9407.	1349.	1029.	385.	1315.
444	TWIN	FWD	0.75	59.10	1.915	7182.	0.700	BG3-1	2751.	20309.	738.	569.	303.	778.
								BG3-3	2318.	15995.	1054.	512.	255.	821.
								BG3-4	473.	2057.	317.	631.	0.	1476.
								BG3-6	1348.	10351.	1353.	1004.	420.	1412.
445	TWIN	FWD	0.57	59.10	1.909	7182.	0.700	BG3-1	2790.	22163.	782.	680.	253.	746.
								BG3-3	2327.	17512.	1098.	820.	263.	834.
								BG3-4	482.	2215.	255.	654.	0.	1480.
								BG3-6	1359.	11314.	1355.	1394.	310.	1329.

NOTE: ZERO-VALUE ENTRIES INDICATE ABSENCE OF DATA

ORIGINAL PAGE IS
OF POOR QUALITY

TABLE A-V: P-ORDER STRESSES (±kPa), TWIN SCOOP FORWARD INLET

RUN NO.	INLET TYPE	INLET POS.	MASS FLOW RATIO	BLADE ANGLE DEG	POWER COEFF	PROP SPEED RPM	MACH NO.	BLADE GAGE	P ORDER COMPONENTS 1	2	3	4	5	6
446	TWIN	FWD	0.57	59.10	1.793	6984.	0.700	BG3-1	2679.	23180.	699.	1078.	188.	547.
								BG3-3	2279.	18405.	1133.	1729.	0.	597.
								BG3-4	506.	1946.	0.	431.	0.	1175.
								BG3-6	1290.	12065.	1247.	2801.	258.	1253.
447	TWIN	FWD	0.75	59.10	1.784	6984.	0.700	BG3-1	2533.	21052.	655.	1054.	236.	589.
								BG3-3	2184.	16655.	915.	1430.	209.	598.
								BG3-4	470.	1862.	0.	486.	0.	1208.
								BG3-6	1259.	10921.	1094.	2302.	355.	1257.
448	TWIN	FWD	1.00	59.10	1.776	6984.	0.700	BG3-1	2481.	18742.	591.	969.	261.	630.
								BG3-3	2154.	14789.	809.	1052.	225.	609.
								BG3-4	453.	1711.	235.	482.	0.	1248.
								BG3-6	1261.	9728.	1023.	1699.	312.	1286.
449	TWIN	FWD	1.00	59.10	1.674	6774.	0.700	BG3-1	2277.	25343.	667.	784.	193.	414.
								BG3-3	1991.	20302.	852.	999.	0.	364.
								BG3-4	504.	1927.	0.	387.	0.	841.
								BG3-6	981.	13318.	960.	1768.	0.	1158.
4410	TWIN	FWD	0.75	59.10	1.629	6774.	0.700	BG3-1	2348.	27280.	603.	1056.	180.	518.
								BG3-3	2048.	21905.	750.	1382.	231.	450.
								BG3-4	517.	2081.	179.	514.	0.	1011.
								BG3-6	999.	14400.	882.	2418.	317.	1167.
4411	TWIN	FWD	0.57	59.10	0.000	6774.	0.700	BG3-1	2489.	30577.	577.	1163.	217.	418.
								BG3-3	2115.	24772.	836.	1537.	186.	295.
								BG3-4	543.	2292.	0.	569.	0.	809.
								BG3-6	986.	16327.	961.	2772.	0.	1185.
451	TWIN	FWD	0.57	59.10	-0.071	4332.	0.600	BG3-1	1926.	8858.	555.	0.	230.	450.
								BG3-3	1809.	6117.	665.	824.	552.	602.
								BG3-4	599.	1120.	0.	0.	0.	191.
								BG3-6	975.	3456.	485.	848.	792.	1110.
452	TWIN	FWD	0.57	59.10	2.085	6668.	0.600	BG3-1	3082.	27641.	417.	940.	179.	263.
								BG3-3	2591.	22287.	828.	1194.	223.	196.
								BG3-4	744.	1721.	174.	514.	0.	387.
								BG3-6	1131.	14513.	934.	2143.	268.	357.
453	TWIN	FWD	0.75	59.10	2.075	6668.	0.600	BG3-1	2859.	26109.	405.	864.	190.	313.
								BG3-3	2455.	21054.	701.	912.	217.	230.
								BG3-4	698.	1672.	0.	511.	0.	456.
								BG3-6	1088.	13699.	808.	1714.	235.	571.
464	TWIN	FWD	1.00	59.10	0.000	6668.	0.600	BG3-1	2864.	23653.	428.	784.	209.	331.
								BG3-3	2490.	19036.	653.	607.	225.	219.
								BG3-4	705.	1554.	0.	464.	0.	462.
								BG3-6	1111.	12401.	755.	1257.	207.	641.
465	TWIN	FWD	1.00	59.10	0.000	6459.	0.600	BG3-1	2612.	29310.	510.	1036.	240.	287.
								BG3-3	2316.	23227.	1005.	1565.	234.	232.
								BG3-4	675.	1485.	0.	552.	0.	508.
								BG3-6	850.	15038.	988.	2718.	0.	709.
466	TWIN	FWD	0.75	59.10	0.000	6459.	0.600	BG3-1	2677.	34747.	511.	1237.	276.	304.
								BG3-3	2376.	27612.	967.	1910.	257.	254.
								BG3-4	699.	1749.	0.	652.	0.	562.
								BG3-6	843.	17921.	945.	3297.	0.	715.

NOTE: ZERO-VALUE ENTRIES INDICATE ABSENCE OF DATA

TABLE A-V: P-ORDER STRESSES (±kPa), TWIN SCOOP FORWARD INLET

RUN NO.	INLET TYPE	INLET POS.	MASS FLOW RATIO	BLADE ANGLE DEG	POWER COEFF	PROP SPEED RPM	MACH NO.	BLADE GAGE	P ORDER COMPONENTS 1	2	3	4	5	6
467	TWIN	FWD	0.57	59.10	0.000	6459.	0.600	BG3-1	2741.	38247.	510.	1521.	279.	285.
								BG3-3	2427.	30468.	1013.	2329.	265.	241.
								BG3-4	712.	1919.	0.	790.	0.	564.
								BG3-6	846.	19799.	990.	4028.	0.	688.
468	TWIN	FWD	0.57	59.10	0.000	6278.	0.600	BG3-1	2454.	54468.	541.	2473.	0.	244.
								BG3-3	2235.	43207.	834.	5277.	0.	483.
								BG3-4	683.	3083.	253.	1218.	0.	402.
								BG3-6	686.	27844.	741.	8390.	0.	1370.
469	TWIN	FWD	0.75	59.10	0.000	6278.	0.600	BG3-1	2436.	50038.	566.	2199.	0.	188.
								BG3-3	2235.	39613.	879.	4397.	0.	443.
								BG3-4	682.	2831.	239.	1086.	0.	395.
								BG3-6	688.	25507.	832.	7014.	0.	1562.
4610	TWIN	FWD	1.00	59.10	0.000	6278.	0.600	BG3-1	2420.	44236.	584.	1916.	0.	0.
								BG3-3	2232.	34950.	961.	3395.	0.	409.
								BG3-4	687.	2495.	231.	933.	0.	451.
								BG3-6	676.	22471.	915.	5491.	0.	1755.

*** END DATA ***

NOTE: ZERO-VALUE ENTRIES INDICATE ABSENCE OF DATA

TABLE A-VI: P-ORDER STRESSES (±kPa), ANNULAR FORWARD INLET

RUN NO.	INLET TYPE	INLET POS.	MASS FLOW RATIO	BLADE ANGLE DEG	POWER COEFF	PROP SPEED RPM	MACH NO.	BLADE GAGE	P ORDER COMPONENTS 1	2	3	4	5	6
2151	ANNULAR	FWD	0.86	59.00	-0.064	4212.	0.610	BG1-1	1614.	1186.	1652.	0.	0.	557.
								BG1-3	1383.	670.	1882.	0.	0.	801.
								BG1-4	354.	0.	0.	0.	0.	0.
								BG1-6	369.	375.	1470.	0.	0.	1283.
								BG3-1	1449.	716.	884.	0.	0.	363.
								BG3-3	1224.	830.	980.	0.	0.	543.
								BG3-4	619.	0.	0.	0.	0.	0.
								BG3-6	1110.	497.	717.	0.	0.	689.
2152	ANNULAR	FWD	0.86	59.00	2.123	6632.	0.610	BG1-1	0.	0.	418.	289.	0.	224.
								BG1-3	0.	0.	343.	287.	0.	235.
								BG1-4	0.	0.	0.	0.	0.	332.
								BG1-6	0.	0.	501.	421.	0.	678.
								BG3-1	0.	415.	304.	218.	0.	272.
								BG3-3	0.	322.	695.	459.	0.	253.
								BG3-4	0.	0.	0.	0.	0.	340.
								BG3-6	0.	186.	816.	756.	0.	473.
2153	ANNULAR	FWD	0.86	59.00	2.021	6432.	0.600	BG1-1	3508.	8716.	369.	803.	0.	231.
								BG1-3	2780.	6830.	234.	1090.	0.	202.
								BG1-4	792.	268.	0.	292.	0.	249.
								BG1-6	851.	4496.	364.	1797.	0.	299.
								BG3-1	3692.	6335.	314.	422.	0.	226.
								BG3-3	2792.	5122.	632.	841.	0.	0.
								BG3-4	1055.	383.	0.	0.	0.	384.
								BG3-6	1407.	2994.	635.	1297.	0.	1473.
2154	ANNULAR	FWD	0.86	59.00	1.887	6234.	0.610	BG1-1	2843.	12050.	287.	816.	0.	0.
								BG1-3	2310.	9643.	295.	1360.	0.	276.
								BG1-4	732.	469.	0.	237.	0.	955.
								BG1-6	729.	6336.	389.	2182.	0.	3180.
								BG3-1	3127.	9176.	208.	795.	0.	0.
								BG3-3	2364.	7514.	628.	1227.	0.	284.
								BG3-4	944.	716.	0.	239.	0.	927.
								BG3-6	1155.	4404.	620.	1824.	0.	3471.
2161	ANNULAR	FWD	0.86	59.00	-0.048	5007.	0.710	BG1-1	1784.	1851.	876.	0.	181.	0.
								BG1-3	1490.	1736.	849.	0.	365.	185.
								BG1-4	381.	364.	0.	0.	0.	212.
								BG1-6	321.	1080.	719.	0.	582.	223.
								BG3-1	1689.	3140.	891.	0.	172.	0.
								BG3-3	1292.	2642.	958.	0.	282.	274.
								BG3-4	460.	356.	0.	0.	0.	250.
								BG3-6	639.	1466.	595.	0.	411.	191.
2162	ANNULAR	FWD	0.86	59.00	1.871	7258.	0.710	BG1-1	2446.	1732.	0.	210.	196.	458.
								BG1-3	1975.	1308.	798.	280.	0.	591.
								BG1-4	794.	205.	328.	0.	0.	1531.
								BG1-6	562.	692.	1298.	299.	212.	978.
								BG3-1	3176.	1591.	275.	216.	283.	727.
								BG3-3	2342.	1350.	789.	312.	0.	813.
								BG3-4	984.	195.	338.	0.	186.	1104.
								BG3-6	1593.	680.	915.	426.	535.	1554.

NOTE: ZERO-VALUE ENTRIES INDICATE ABSENCE OF DATA

TABLE A-VI: P-ORDER STRESSES (±kPa), ANNULAR FORWARD INLET

RUN NO.	INLET TYPE	INLET POS.	MASS FLOW RATIO	BLADE ANGLE DEG	POWER COEFF	PROP SPEED RPM	MACH NO.	BLADE GAGE	P ORDER COMPONENTS 1	2	3	4	5	6
2163	ANNULAR	FWD	0.86	59.00	1.801	7145.	0.710	BG1-1	2151.	2057.	0.	267.	179.	508.
								BG1-3	1741.	1603.	796.	189.	0.	626.
								BG1-4	747.	245.	314.	0.	0.	3314.
								BG1-6	496.	934.	1197.	310.	0.	1542.
								BG3-1	2918.	1993.	245.	324.	187.	1456.
								BG3-3	2064.	1682.	915.	0.	0.	1868.
								BG3-4	987.	227.	313.	174.	0.	1195.
								BG3-6	1240.	914.	1010.	313.	247.	2606.
2164	ANNULAR	FWD	0.86	59.00	1.684	6954.	0.710	BG1-1	1824.	2657.	180.	305.	235.	432.
								BG1-3	1515.	2079.	767.	525.	0.	649.
								BG1-4	692.	236.	283.	185.	0.	1792.
								BG1-6	504.	1276.	1120.	695.	239.	1372.
								BG3-1	2676.	2565.	302.	434.	216.	684.
								BG3-3	1923.	2184.	948.	445.	0.	1046.
								BG3-4	898.	242.	274.	0.	0.	1260.
								BG3-6	1107.	1184.	1004.	763.	298.	1222.
2171	ANNULAR	FWD	0.86	59.00	-0.049	5794.	0.810	BG1-1	1037.	6460.	855.	240.	0.	0.
								BG1-3	961.	5106.	1023.	399.	184.	0.
								BG1-4	344.	884.	0.	0.	0.	493.
								BG1-6	228.	3233.	1010.	765.	380.	589.
								BG3-1	1418.	8397.	714.	282.	0.	175.
								BG3-3	1125.	6562.	795.	340.	188.	0.
								BG3-4	491.	652.	263.	210.	0.	551.
								BG3-6	991.	3666.	569.	485.	294.	511.
2172	ANNULAR	FWD	0.86	59.00	1.707	7964.	0.800	BG1-1	1435.	1948.	0.	0.	254.	228.
								BG1-3	1071.	1445.	1258.	0.	173.	422.
								BG1-4	774.	238.	390.	0.	0.	375.
								BG1-6	678.	873.	1758.	307.	380.	731.
								BG3-1	2416.	768.	354.	267.	251.	231.
								BG3-3	1548.	729.	1389.	0.	0.	353.
								BG3-4	964.	245.	463.	0.	0.	472.
								BG3-6	1415.	449.	1621.	248.	433.	916.
2173	ANNULAR	FWD	0.86	59.00	1.598	7758.	0.810	BG1-1	1253.	1960.	0.	0.	279.	0.
								BG1-3	949.	1352.	1181.	315.	191.	352.
								BG1-4	722.	256.	373.	0.	235.	526.
								BG1-6	634.	851.	1544.	496.	322.	917.
								BG3-1	2230.	1492.	315.	265.	279.	257.
								BG3-3	1450.	1269.	1208.	0.	0.	415.
								BG3-4	893.	274.	380.	0.	0.	410.
								BG3-6	1334.	699.	1315.	207.	505.	881.
2174	ANNULAR	FWD	0.86	59.00	1.515	7565.	0.800	BG1-1	1031.	2137.	217.	0.	253.	191.
								BG1-3	792.	1431.	1003.	196.	0.	425.
								BG1-4	578.	226.	348.	0.	211.	954.
								BG1-6	582.	938.	1249.	227.	345.	825.
								BG3-1	0.	207.	0.	247.	0.	0.
								BG3-3	0.	191.	0.	926.	0.	0.
								BG3-4	0.	0.	0.	283.	0.	0.
								BG3-6	0.	173.	0.	1008.	0.	0.

NOTE: ZERO-VALUE ENTRIES INDICATE ABSENCE OF DATA

TABLE A-VI: P-ORDER STRESSES (±kPa), ANNULAR FORWARD INLET

RUN NO.	INLET TYPE	INLET POS.	MASS FLOW RATIO	BLADE ANGLE DEG	POWER COEFF	PROP SPEED RPM	MACH NO.	BLADE GAGE	P ORDER COMPONENTS 1	2	3	4	5	6
2181	ANNULAR	FWD	0.70	59.00	-0.057	4311.	0.610	BG1-1	0.	808.	1537.	221.	191.	345.
								BG1-3	0.	743.	1740.	0.	313.	599.
								BG1-4	0.	290.	0.	0.	0.	0.
								BG1-6	0.	446.	1146.	0.	402.	946.
								BG3-1	0.	2308.	1053.	0.	325.	209.
								BG3-3	0.	1984.	1200.	0.	295.	341.
								BG3-4	0.	0.	230.	0.	0.	0.
								BG3-6	0.	1110.	994.	0.	428.	356.
2182	ANNULAR	FWD	0.70	59.00	2.073	6671.	0.610	BG1-1	2126.	5060.	248.	327.	0.	248.
								BG1-3	1850.	3937.	513.	279.	0.	374.
								BG1-4	772.	268.	0.	0.	0.	473.
								BG1-6	935.	2565.	619.	471.	190.	647.
								BG3-1	2971.	3824.	297.	252.	0.	343.
								BG3-3	2223.	3148.	507.	433.	0.	473.
								BG3-4	867.	313.	0.	0.	0.	413.
								BG3-6	771.	1761.	476.	699.	0.	211.
2183	ANNULAR	FWD	0.70	59.00	1.978	6473.	0.610	BG1-1	2202.	7349.	279.	623.	0.	0.
								BG1-3	1956.	5785.	487.	596.	0.	297.
								BG1-4	830.	313.	0.	0.	0.	0.
								BG1-6	996.	3786.	580.	1092.	267.	762.
								BG3-1	3196.	5395.	251.	275.	0.	192.
								BG3-3	2384.	4445.	443.	514.	0.	224.
								BG3-4	930.	407.	0.	0.	0.	496.
								BG3-6	838.	2589.	376.	737.	222.	1169.
2184	ANNULAR	FWD	0.70	59.00	1.868	6269.	0.610	BG1-1	2005.	11041.	395.	617.	0.	282.
								BG1-3	1827.	8745.	435.	937.	0.	173.
								BG1-4	826.	510.	0.	0.	0.	878.
								BG1-6	952.	5705.	483.	1482.	256.	3514.
								BG3-1	3034.	8080.	256.	435.	0.	251.
								BG3-3	2255.	6657.	396.	663.	0.	0.
								BG3-4	898.	746.	0.	0.	0.	775.
								BG3-6	765.	3882.	303.	912.	257.	3274.
2191	ANNULAR	FWD	0.70	59.00	-0.042	5056.	0.710	BG1-1	1655.	2514.	823.	0.	361.	195.
								BG1-3	1382.	1973.	892.	259.	457.	0.
								BG1-4	433.	427.	0.	0.	0.	249.
								BG1-6	592.	1257.	693.	269.	831.	260.
								BG3-1	2021.	2913.	822.	193.	275.	211.
								BG3-3	1449.	2250.	862.	0.	241.	230.
								BG3-4	457.	420.	0.	0.	0.	241.
								BG3-6	354.	1236.	627.	0.	350.	189.
2192	ANNULAR	FWD	0.70	59.00	1.851	7277.	0.710	BG1-1	1569.	2834.	443.	220.	433.	633.
								BG1-3	1516.	1990.	862.	360.	0.	215.
								BG1-4	797.	184.	265.	0.	0.	2018.
								BG1-6	898.	1320.	995.	604.	205.	857.
								BG3-1	2629.	3135.	460.	391.	360.	1025.
								BG3-3	1891.	2358.	790.	0.	189.	1284.
								BG3-4	895.	194.	322.	0.	0.	853.
								BG3-6	1019.	1400.	887.	206.	285.	2059.

NOTE: ZERO-VALUE ENTRIES INDICATE ABSENCE OF DATA

TABLE A-VI: P-ORDER STRESSES (±kPa), ANNULAR FORWARD INLET

RUN NO.	INLET TYPE	INLET POS.	MASS FLOW RATIO	BLADE ANGLE DEG	POWER COEFF	PROP SPEED RPM	MACH NO.	BLADE GAGE	P ORDER COMPONENTS 1	2	3	4	5	6
2193	ANNULAR	FWD	0.70	59.00	1.765	7082.	0.710	BG1-1	1448.	2641.	454.	204.	330.	530.
								BG1-3	1446.	1954.	905.	508.	197.	462.
								BG1-4	883.	195.	354.	190.	175.	2725.
								BG1-6	819.	1261.	1103.	704.	263.	1424.
								BG3-1	2698.	2709.	440.	443.	358.	1392.
								BG3-3	1896.	2087.	920.	0.	0.	1410.
								BG3-4	959.	194.	392.	0.	0.	1058.
								BG3-6	1043.	1232.	1043.	269.	320.	2231.
2194	ANNULAR	FWD	0.70	59.00	1.640	6878.	0.710	BG1-1	1468.	3773.	360.	503.	243.	517.
								BG1-3	1465.	2805.	853.	543.	0.	468.
								BG1-4	866.	213.	285.	0.	0.	1169.
								BG1-6	916.	1783.	934.	734.	174.	1129.
								BG3-1	2719.	3781.	377.	309.	219.	671.
								BG3-3	1955.	2984.	775.	484.	0.	528.
								BG3-4	955.	226.	254.	195.	0.	1093.
								BG3-6	959.	1723.	873.	555.	0.	935.
2201	ANNULAR	FWD	0.70	59.00	-0.043	5777.	0.810	BG1-1	1013.	6968.	838.	361.	0.	0.
								BG1-3	941.	5313.	925.	503.	0.	0.
								BG1-4	345.	870.	0.	0.	0.	413.
								BG1-6	527.	3352.	857.	856.	333.	450.
								BG3-1	1648.	8821.	663.	377.	0.	198.
								BG3-3	1221.	6752.	691.	670.	0.	0.
								BG3-4	474.	651.	262.	183.	0.	489.
								BG3-6	648.	3795.	522.	976.	200.	453.
2202	ANNULAR	FWD	0.70	59.00	1.671	7041.	0.800	BG1-1	1120.	2429.	470.	243.	578.	530.
								BG1-3	1051.	1738.	1594.	187.	291.	337.
								BG1-4	873.	222.	367.	0.	0.	501.
								BG1-6	964.	1212.	1967.	528.	623.	1109.
								BG3-1	2493.	1338.	589.	301.	480.	422.
								BG3-3	1533.	1030.	1069.	264.	271.	396.
								BG3-4	971.	215.	496.	0.	240.	530.
								BG3-6	1189.	732.	1399.	475.	360.	877.
2203	ANNULAR	FWD	0.70	59.00	1.597	7736.	0.800	BG1-1	827.	2525.	427.	303.	485.	405.
								BG1-3	790.	1627.	1350.	180.	207.	270.
								BG1-4	771.	223.	333.	0.	186.	580.
								BG1-6	901.	1119.	1624.	443.	300.	1002.
								BG3-1	2195.	2027.	528.	257.	488.	383.
								BG3-3	1390.	1683.	921.	181.	270.	381.
								BG3-4	860.	222.	428.	0.	0.	440.
								BG3-6	1115.	1015.	1151.	224.	463.	958.
2204	ANNULAR	FWD	0.70	59.00	1.486	7540.	0.800	BG1-1	787.	2358.	597.	237.	456.	535.
								BG1-3	801.	1541.	1118.	189.	196.	291.
								BG1-4	712.	224.	375.	0.	213.	1025.
								BG1-6	890.	1168.	1246.	296.	307.	1055.
								BG3-1	2132.	2328.	516.	348.	391.	532.
								BG3-3	1374.	1888.	1054.	0.	236.	658.
								BG3-4	849.	215.	351.	0.	0.	691.
								BG3-6	1044.	1207.	1270.	0.	606.	1352.

NOTE: ZERO-VALUE ENTRIES INDICATE ABSENCE OF DATA

ORIGINAL PAGE IS OF POOR QUALITY

TABLE A-VI: P-ORDER STRESSES (±kPa), ANNULAR FORWARD INLET

RUN NO.	INLET TYPE	INLET POS.	MASS FLOW RATIO	BLADE ANGLE DEG	POWER COEFF	PROP SPEED RPM	MACH NO.	BLADE GAGE	P ORDER COMPONENTS 1	2	3	4	5	6
2211	ANNULAR	FWD	0.70	58.10	-0.046	4470.	0.610	BG1-1	603.	1883.	1539.	209.	0.	324.
								BG1-3	709.	1699.	1471.	0.	380.	303.
								BG1-4	298.	265.	0.	0.	0.	193.
								BG1-6	1147.	1092.	1014.	0.	578.	402.
								BG3-1	1187.	3080.	1277.	217.	306.	201.
								BG3-3	1131.	2430.	1452.	202.	394.	423.
								BG3-4	0.	252.	0.	0.	0.	0.
								BG3-6	767.	1412.	936.	0.	561.	552.
2212	ANNULAR	FWD	0.70	58.10	1.977	6856.	0.610	BG1-1	2904.	3659.	320.	228.	178.	402.
								BG1-3	2267.	2773.	643.	0.	0.	406.
								BG1-4	658.	264.	193.	0.	0.	792.
								BG1-6	2511.	1837.	620.	260.	218.	636.
								BG3-1	1882.	3002.	413.	393.	0.	518.
								BG3-3	1816.	2411.	535.	0.	0.	494.
								BG3-4	0.	196.	183.	0.	0.	721.
								BG3-6	1663.	1383.	694.	316.	184.	489.
2213	ANNULAR	FWD	0.70	58.10	1.871	6660.	0.610	BG1-1	2577.	5302.	315.	450.	173.	395.
								BG1-3	2004.	4167.	573.	276.	0.	219.
								BG1-4	562.	253.	201.	0.	0.	564.
								BG1-6	2237.	2694.	575.	531.	250.	837.
								BG3-1	1520.	4326.	336.	232.	183.	481.
								BG3-3	1542.	3512.	445.	361.	0.	243.
								BG3-4	0.	290.	0.	0.	0.	543.
								BG3-6	1494.	2027.	588.	542.	0.	260.
2214	ANNULAR	FWD	0.70	58.10	1.764	6455.	0.610	BG1-1	2656.	8244.	341.	577.	0.	365.
								BG1-3	2030.	6534.	582.	584.	0.	188.
								BG1-4	570.	330.	224.	0.	0.	0.
								BG1-6	2326.	4181.	595.	1023.	252.	810.
								BG3-1	1566.	5574.	285.	202.	180.	350.
								BG3-3	1602.	4615.	436.	583.	0.	0.
								BG3-4	226.	444.	0.	0.	0.	571.
								BG3-6	1642.	2655.	571.	848.	191.	1229.
2221	ANNULAR	FWD	0.70	58.10	-0.034	5253.	0.710	BG1-1	1310.	3220.	638.	177.	279.	0.
								BG1-3	1126.	2689.	690.	0.	292.	0.
								BG1-4	352.	456.	211.	0.	0.	294.
								BG1-6	1544.	1630.	661.	0.	568.	0.
								BG3-1	629.	3205.	788.	0.	248.	183.
								BG3-3	788.	2561.	749.	198.	0.	0.
								BG3-4	0.	452.	0.	0.	0.	286.
								BG3-6	1021.	1338.	628.	197.	222.	0.
2222	ANNULAR	FWD	0.70	58.10	1.761	7518.	0.710	BG1-1	3108.	1996.	359.	268.	176.	433.
								BG1-3	2260.	1505.	547.	175.	0.	684.
								BG1-4	601.	232.	310.	181.	354.	766.
								BG1-6	2792.	892.	893.	282.	346.	919.
								BG3-1	1785.	1951.	431.	190.	0.	516.
								BG3-3	1613.	1711.	745.	0.	194.	527.
								BG3-4	212.	214.	238.	0.	0.	798.
								BG3-6	2182.	1014.	1087.	249.	1301.	1106.

NOTE: ZERO-VALUE ENTRIES INDICATE ABSENCE OF DATA

ORIGINAL PAGE IS OF POOR QUALITY

TABLE A-VI: P-ORDER STRESSES (±kPa), ANNULAR FORWARD INLET

RUN NO.	INLET TYPE	INLET POS.	MASS FLOW RATIO	BLADE ANGLE DEG	POWER COEFF	PROP SPEED RPM	MACH NO.	BLADE GAGE	P ORDER COMPONENTS 1	2	3	4	5	6
2233	ANNULAR	FWD	0.70	58.10	1.664	7315.	0.710	BG1-1	2945.	2178.	253.	212.	206.	324.
								BG1-3	2206.	1706.	548.	194.	0.	589.
								BG1-4	560.	207.	342.	0.	0.	1961.
								BG1-6	2688.	1124.	892.	345.	209.	904.
								BG3-1	1545.	2267.	338.	218.	0.	949.
								BG3-3	1469.	1877.	677.	211.	172.	1185.
								BG3-4	213.	199.	264.	0.	180.	928.
								BG3-6	2056.	1094.	1015.	276.	318.	1937.
2224	ANNULAR	FWD	0.70	58.10	1.571	7119.	0.710	BG1-1	2617.	2900.	308.	290.	0.	393.
								BG1-3	1891.	2339.	417.	315.	0.	658.
								BG1-4	426.	198.	270.	0.	0.	3666.
								BG1-6	2155.	1511.	667.	514.	0.	1553.
								BG3-1	1348.	2876.	269.	260.	0.	1468.
								BG3-3	1201.	2397.	620.	214.	0.	1965.
								BG3-4	189.	177.	197.	0.	0.	1189.
								BG3-6	1621.	1401.	872.	291.	0.	2652.
2231	ANNULAR	FWD	0.70	58.10	-0.035	6014.	0.810	BG1-1	1372.	11129.	549.	331.	189.	0.
								BG1-3	1027.	8794.	655.	1049.	0.	184.
								BG1-4	437.	1292.	198.	0.	0.	647.
								BG1-6	1663.	5691.	732.	1531.	0.	959.
								BG3-1	335.	17185.	438.	692.	0.	0.
								BG3-3	535.	13592.	723.	722.	0.	278.
								BG3-4	227.	872.	261.	0.	0.	657.
								BG3-6	1101.	7738.	606.	1124.	218.	1596.
2232	ANNULAR	FWD	0.70	58.10	1.589	8210.	0.800	BG1-1	2634.	2108.	735.	0.	0.	342.
								BG1-3	1785.	1818.	1451.	0.	0.	418.
								BG1-4	581.	359.	525.	0.	0.	217.
								BG1-6	2305.	1379.	2221.	377.	415.	885.
								BG3-1	1231.	1087.	252.	0.	0.	244.
								BG3-3	1078.	905.	1267.	0.	0.	369.
								BG3-4	351.	265.	510.	0.	0.	364.
								BG3-6	1888.	693.	1902.	239.	306.	890.
2233	ANNULAR	FWD	0.70	58.10	1.482	8001.	0.810	BG1-1	2416.	1691.	573.	0.	0.	242.
								BG1-3	1616.	1456.	1141.	0.	0.	363.
								BG1-4	537.	262.	504.	0.	0.	448.
								BG1-6	2033.	1085.	1768.	257.	545.	923.
								BG3-1	1138.	1278.	310.	0.	0.	243.
								BG3-3	1002.	1245.	1061.	0.	0.	391.
								BG3-4	304.	248.	396.	0.	178.	406.
								BG3-6	1737.	815.	1568.	330.	394.	818.
2234	ANNULAR	FWD	0.70	58.10	1.405	7801.	0.810	BG1-1	2439.	2252.	456.	0.	0.	202.
								BG1-3	1595.	1788.	1007.	242.	0.	295.
								BG1-4	525.	205.	481.	0.	287.	646.
								BG1-6	2103.	1243.	1521.	520.	480.	827.
								BG3-1	1232.	1751.	295.	0.	0.	297.
								BG3-3	991.	1616.	1132.	320.	0.	505.
								BG3-4	410.	205.	360.	0.	220.	351.
								BG3-6	1806.	1002.	1519.	588.	894.	903.

*** END DATA ***

NOTE: ZERO-VALUE ENTRIES INDICATE ABSENCE OF DATA

TABLE A-VII: P-ORDER STRESSES (±kPa), NO-INLET

RUN NO.	INLET TYPE	INLET POS.	MASS FLOW RATIO	BLADE ANGLE DEG	POWER COEFF	PROP SPEED RPM	MACH NO.	BLADE GAGE	P ORDER COMPONENTS 1	2	3	4	5	6
191	AXI-SYM	BARE	0.00	59.00	-0.060	4244.	0.600	BG1-1	1424.	2122.	1514.	0.	248.	472.
								BG1-3	1318.	1843.	1442.	0.	194.	680.
								BG1-4	467.	197.	0.	0.	0.	0.
								BG1-6	698.	925.	877.	0.	309.	886.
								BG3-1	1249.	2101.	1244.	0.	0.	376.
								BG3-3	1304.	1581.	1311.	176.	198.	546.
								BG3-4	458.	181.	0.	0.	0.	0.
								BG3-6	348.	1118.	993.	0.	228.	870.
192	AXI-SYM	BARE	0.00	59.00	2.094	6684.	0.600	BG1-1	2290.	2352.	248.	410.	280.	307.
								BG1-3	2083.	1992.	462.	415.	249.	470.
								BG1-4	647.	199.	0.	0.	0.	582.
								BG1-6	964.	1079.	459.	674.	215.	419.
								BG3-1	1992.	2316.	0.	349.	343.	261.
								BG3-3	1727.	1902.	553.	615.	214.	437.
								BG3-4	572.	214.	0.	0.	0.	541.
								BG3-6	426.	1123.	625.	1061.	0.	654.
193	AXI-SYM	BARE	0.00	59.00	1.984	6484.	0.600	BG1-1	2091.	2955.	216.	289.	265.	235.
								BG1-3	1967.	2500.	425.	374.	179.	379.
								BG1-4	651.	205.	0.	0.	0.	408.
								BG1-6	995.	1355.	428.	590.	0.	508.
								BG3-1	1711.	2934.	201.	183.	289.	228.
								BG3-3	1512.	2460.	642.	195.	0.	354.
								BG3-4	531.	241.	0.	0.	0.	415.
								BG3-6	331.	1458.	649.	375.	0.	706.
194	AXI-SYM	BARE	0.00	59.00	1.854	6285.	0.600	BG1-1	2079.	4420.	214.	270.	270.	245.
								BG1-3	2017.	3759.	508.	443.	191.	295.
								BG1-4	687.	258.	0.	0.	0.	294.
								BG1-6	1106.	1989.	512.	652.	199.	1776.
								BG3-1	1631.	5334.	0.	180.	311.	219.
								BG3-3	1475.	4407.	611.	447.	0.	174.
								BG3-4	545.	358.	0.	0.	0.	620.
								BG3-6	272.	2676.	570.	750.	0.	2303.
201	AXI-SYM	BARE	0.00	59.00	-0.057	5159.	0.700	BG1-1	0.	2803.	611.	181.	329.	260.
								BG1-3	0.	2297.	796.	244.	0.	365.
								BG1-4	0.	341.	0.	0.	0.	288.
								BG1-6	0.	1294.	561.	297.	190.	281.
								BG3-1	0.	1867.	760.	213.	197.	191.
								BG3-3	0.	1555.	929.	0.	304.	282.
								BG3-4	0.	277.	0.	0.	0.	287.
								BG3-6	0.	1062.	632.	210.	579.	310.
202	AXI-SYM	BARE	0.00	59.00	1.860	7352.	0.700	BG1-1	1857.	1165.	0.	245.	0.	604.
								BG1-3	1910.	875.	998.	427.	0.	755.
								BG1-4	503.	287.	246.	0.	202.	1330.
								BG1-6	1196.	714.	1255.	574.	378.	1473.
								BG3-1	1562.	1060.	231.	387.	0.	491.
								BG3-3	1572.	673.	1017.	253.	0.	881.
								BG3-4	485.	301.	313.	0.	0.	1412.
								BG3-6	0.	582.	1204.	514.	257.	1173.

NOTE: ZERO-VALUE ENTRIES INDICATE ABSENCE OF DATA

TABLE A-VII: P-ORDER STRESSES (±kPa), NO-INLET

RUN NO.	INLET TYPE	INLET POS.	MASS FLOW RATIO	BLADE ANGLE DEG	POWER COEFF	PROP SPEED RPM	MACH NO.	BLADE GAGE	P ORDER COMPONENTS 1	2	3	4	5	6
203	AXI-SYM	BARE	0.00	59.00	1.738	7149.	0.700	BG1-1	1819.	1382.	229.	271.	249.	1078.
								BG1-3	1735.	973.	986.	260.	0.	1410.
								BG1-4	485.	280.	322.	0.	0.	3056.
								BG1-6	1196.	721.	1206.	318.	292.	2278.
								BG3-1	1559.	1108.	0.	465.	207.	623.
								BG3-3	1435.	711.	903.	204.	0.	892.
								BG3-4	425.	273.	320.	187.	0.	1882.
								BG3-6	0.	549.	1088.	519.	234.	1375.
204	AXI-SYM	BARE	0.00	59.00	1.624	6948.	0.700	BG1-1	1544.	1634.	0.	784.	215.	950.
								BG1-3	1615.	1294.	920.	444.	0.	1199.
								BG1-4	482.	249.	275.	0.	0.	2539.
								BG1-6	1072.	724.	1220.	643.	174.	1745.
								BG3-1	1380.	1319.	0.	337.	0.	642.
								BG3-3	1331.	970.	855.	969.	0.	842.
								BG3-4	455.	244.	226.	249.	0.	1789.
								BG3-6	0.	539.	953.	1207.	0.	1490.
211	AXI-SYM	BARE	0.00	59.00	-0.057	5981.	0.800	BG1-1	1395.	9960.	559.	1276.	0.	221.
								BG1-3	1490.	8105.	1006.	2436.	0.	193.
								BG1-4	368.	877.	192.	338.	0.	755.
								BG1-6	1260.	4573.	858.	3551.	335.	1249.
								BG3-1	1306.	4434.	624.	681.	0.	227.
								BG3-3	1485.	3612.	1076.	856.	0.	190.
								BG3-4	468.	472.	255.	190.	0.	792.
								BG3-6	376.	2255.	921.	1251.	320.	1113.
212	AXI-SYM	BARE	0.00	59.00	1.615	8165.	0.800	BG1-1	1636.	784.	409.	459.	202.	331.
								BG1-3	1718.	660.	2591.	455.	242.	650.
								BG1-4	365.	386.	516.	0.	228.	410.
								BG1-6	1223.	769.	3409.	591.	0.	1435.
								BG3-1	1609.	664.	1034.	503.	269.	355.
								BG3-3	1579.	578.	2159.	515.	292.	674.
								BG3-4	467.	394.	695.	349.	175.	381.
								BG3-6	408.	702.	2823.	352.	312.	1633.
213	AXI-SYM	BARE	0.00	59.00	1.510	7961.	0.800	BG1-1	1615.	624.	289.	598.	323.	310.
								BG1-3	1621.	643.	1655.	492.	238.	748.
								BG1-4	345.	375.	380.	0.	0.	665.
								BG1-6	1293.	616.	2057.	640.	271.	1430.
								BG3-1	1476.	915.	840.	559.	327.	243.
								BG3-3	1451.	775.	2111.	448.	362.	662.
								BG3-4	408.	359.	516.	252.	262.	569.
								BG3-6	398.	885.	2679.	572.	387.	1374.
214	AXI-SYM	BARE	0.00	59.00	1.423	7770.	0.800	BG1-1	1611.	614.	203.	534.	342.	233.
								BG1-3	1727.	566.	1753.	615.	308.	747.
								BG1-4	359.	397.	351.	0.	200.	755.
								BG1-6	1377.	672.	2221.	798.	300.	1134.
								BG3-1	1477.	670.	531.	534.	318.	252.
								BG3-3	1441.	678.	1627.	553.	458.	701.
								BG3-4	411.	366.	433.	250.	296.	568.
								BG3-6	383.	523.	1972.	755.	809.	1004.

NOTE: ZERO-VALUE ENTRIES INDICATE ABSENCE OF DATA

TABLE A-VII: P-ORDER STRESSES (±kPa), NO-INLET

RUN NO.	INLET TYPE	INLET POS.	MASS FLOW RATIO	BLADE ANGLE DEG	POWER COEFF	PROP SPEED RPM	MACH NO.	BLADE GAGE	P ORDER COMPONENTS 1	2	3	4	5	6
221	AXI-SYM	BARE	0.00	58.00	-0.046	4596.	0.600	BG1-1	0.	2530.	602.	0.	786.	0.
								BG1-3	0.	1960.	659.	0.	1397.	468.
								BG1-4	0.	232.	0.	0.	0.	220.
								BG1-6	0.	1116.	593.	0.	1860.	444.
								BG3-1	0.	1951.	818.	0.	367.	185.
								BG3-3	0.	1449.	958.	0.	631.	525.
								BG3-4	0.	0.	0.	0.	0.	206.
								BG3-6	0.	883.	732.	0.	926.	767.
222	AXI-SYM	BARE	0.00	58.00	1.954	6972.	0.600	BG1-1	1596.	2002.	361.	233.	0.	682.
								BG1-3	1063.	1976.	656.	409.	0.	737.
								BG1-4	323.	307.	215.	196.	0.	1566.
								BG1-6	1079.	1177.	932.	499.	0.	1250.
								BG3-1	2333.	2812.	0.	348.	0.	564.
								BG3-3	2228.	2543.	528.	247.	0.	563.
								BG3-4	722.	365.	0.	0.	0.	1166.
								BG3-6	897.	1634.	705.	580.	185.	929.
223	AXI-SYM	BARE	0.00	58.00	1.875	6774.	0.600	BG1-1	1648.	2330.	224.	637.	0.	472.
								BG1-3	1155.	2171.	426.	506.	0.	259.
								BG1-4	380.	317.	191.	259.	0.	738.
								BG1-6	996.	1316.	651.	1119.	0.	632.
								BG3-1	2468.	2781.	0.	284.	0.	466.
								BG3-3	2365.	2436.	488.	914.	0.	250.
								BG3-4	804.	351.	0.	0.	0.	682.
								BG3-6	935.	1616.	604.	1313.	0.	784.
224	AXI-SYM	BARE	0.00	58.00	1.748	6567.	0.600	BG1-1	1556.	3633.	0.	286.	0.	336.
								BG1-3	1144.	3219.	373.	271.	0.	234.
								BG1-4	433.	369.	200.	190.	0.	502.
								BG1-6	921.	1891.	596.	497.	0.	526.
								BG3-1	2518.	3712.	0.	0.	0.	317.
								BG3-3	2366.	3187.	556.	395.	0.	203.
								BG3-4	863.	388.	0.	0.	0.	513.
								BG3-6	881.	2073.	631.	565.	0.	817.
231	AXI-SYM	BARE	0.00	58.00	-0.033	5470.	0.700	BG1-1	719.	3017.	524.	0.	199.	220.
								BG1-3	619.	2320.	616.	453.	219.	173.
								BG1-4	235.	228.	182.	0.	0.	333.
								BG1-6	742.	1410.	583.	514.	324.	243.
								BG3-1	1393.	2145.	446.	259.	0.	298.
								BG3-3	1382.	1673.	642.	0.	0.	187.
								BG3-4	487.	0.	0.	0.	0.	338.
								BG3-6	538.	1160.	560.	228.	214.	180.
232	AXI-SYM	BARE	0.00	58.00	1.726	7655.	0.700	BG3-1	2526.	1949.	331.	227.	338.	414.
								BG3-3	2443.	1885.	1062.	453.	310.	523.
								BG3-4	700.	297.	427.	0.	354.	739.
								BG3-6	1135.	1325.	1574.	715.	793.	1104.
233	AXI-SYM	BARE	0.00	58.00	1.623	7455.	0.700	BG1-1	1280.	1551.	177.	299.	366.	362.
								BG1-3	1118.	1421.	1209.	306.	285.	587.
								BG1-4	318.	380.	352.	196.	382.	948.
								BG1-6	1208.	934.	1595.	508.	1268.	1129.

NOTE: ZERO-VALUE ENTRIES INDICATE ABSENCE OF DATA

TABLE A-VII: P-ORDER STRESSES (±kPa), NO-INLET

RUN NO.	INLET TYPE	INLET POS.	MASS FLOW RATIO	BLADE ANGLE DEG	POWER COEFF	PROP SPEED RPM	MACH NO.	BLADE GAGE	P ORDER COMPONENTS 1	2	3	4	5	6
234	AXI-SYM	BARE	0.00	58.00	1.534	7256.	0.700	BG1-1	1155.	2201.	0.	0.	201.	1100.
								BG1-3	951.	2029.	1211.	0.	290.	1412.
								BG1-4	287.	378.	354.	0.	0.	2911.
								BG1-6	931.	1272.	1566.	242.	251.	2317.
								BG3-1	2024.	2687.	213.	0.	230.	675.
								BG3-3	1997.	2239.	783.	0.	313.	576.
								BG3-4	592.	395.	332.	0.	0.	1447.
								BG3-6	919.	1507.	1102.	294.	202.	1342.
242	AXI-SYM	BARE	0.00	58.00	1.534	8454.	0.800	BG1-1	689.	2069.	1389.	406.	403.	312.
								BG1-3	658.	1876.	4200.	368.	299.	488.
								BG1-4	298.	478.	1030.	0.	202.	262.
								BG1-6	861.	1315.	5578.	545.	300.	1964.
								BG3-1	1663.	1579.	719.	413.	433.	345.
								BG3-3	1796.	1467.	2802.	239.	380.	629.
								BG3-4	458.	429.	597.	179.	220.	188.
								BG3-6	737.	1143.	3864.	276.	275.	2770.
243	AXI-SYM	BARE	0.00	58.00	1.415	8276.	0.800	BG1-1	443.	947.	1483.	0.	0.	288.
								BG1-3	494.	836.	3186.	0.	0.	482.
								BG1-4	401.	273.	1095.	0.	0.	363.
								BG1-6	787.	692.	4567.	270.	185.	1621.
								BG3-1	1789.	640.	1333.	0.	0.	270.
								BG3-3	1783.	537.	2869.	0.	0.	488.
								BG3-4	540.	260.	817.	0.	0.	211.
								BG3-6	447.	605.	4197.	0.	0.	1952.
244	AXI-SYM	BARE	0.00	58.00	1.327	8070.	0.800	BG1-1	670.	838.	818.	0.	0.	290.
								BG1-3	656.	809.	1832.	0.	0.	472.
								BG1-4	400.	255.	690.	0.	0.	538.
								BG1-6	962.	630.	2646.	258.	214.	1319.
								BG3-1	1854.	959.	1001.	0.	0.	233.
								BG3-3	1912.	815.	2325.	0.	0.	412.
								BG3-4	525.	239.	696.	0.	0.	299.
								BG3-6	318.	667.	3427.	243.	211.	1666.

*** END DATA ***

NOTE: ZERO-VALUE ENTRIES INDICATE ABSENCE OF DATA